THE UNIVERSITY OF QUEENSLAND

AUSTRALIA

Mechanisms underlying inhibition of muscle disuse atrophy during aestivation in the green-striped burrowing frog, *Cyclorana alboguttata*

Beau Daniel Reilly

Bachelor of Marine Studies (Hons.)

A thesis submitted for the degree of Doctor of Philosophy at

The University of Queensland in 2014

School of Biological Sciences

Abstract

In most mammals, extended inactivity or immobilisation of skeletal muscle (e.g. bed-rest, limb-casting or hindlimb unloading) results in muscle disuse atrophy, a process which is characterised by the loss of skeletal muscle mass and function. In stark contrast, animals that experience natural bouts of prolonged muscle inactivity, such as hibernating mammals and aestivating frogs, consistently exhibit limited or no change in either skeletal muscle size or contractile performance. While many of the factors regulating skeletal muscle mass are known, little information exists as to what mechanisms protect against muscle atrophy in some species.

Green-striped burrowing frogs (*Cyclorana alboguttata*) survive in arid environments by burrowing underground and entering into a deep, prolonged metabolic depression known as aestivation. Throughout aestivation, *C. alboguttata* is immobilised within a cast-like cocoon of shed skin and ceases feeding and moving. Remarkably, these frogs exhibit very little muscle atrophy despite extended disuse and fasting. The overall aim of the current research study was to gain a better understanding of the physiological, cellular and molecular basis underlying resistance to muscle disuse atrophy in *C. alboguttata.*

The first aim of this study was to develop a genomic resource for *C. alboguttata* by sequencing and functionally characterising its skeletal muscle transcriptome, and to conduct gene expression profiling to identify transcriptional pathways associated with metabolic depression and maintenance of muscle function in aestivating burrowing frogs. A transcriptome was assembled using next-generation short read sequencing followed by a comparison of gene expression patterns between active and four-month aestivating *C. alboguttata*. This identified a complex suite of gene expression changes that occur in muscle during aestivation and provides evidence that aestivation in burrowing frogs involves transcriptional regulation of genes associated with cytoskeletal remodelling, avoidance of oxidative stress, energy metabolism, the cell stress response, cell death and survival and epigenetic modification. In particular, the expression levels of genes encoding cell cycle regulatory-, pro-survival and chromatin remodelling proteins, such as serine/threonine-protein kinase Chk1, cell division protein kinase 2, survivin, vesicular overexpressed in cancer prosurvival protein 1 and histone-binding protein RBBP4, were upregulated in aestivators.

The second aim of this study was to examine the potential role of mitochondrial ROS in the regulation of muscle mass and function during aestivation in *C. alboguttata*. In

mammals, muscle disuse atrophy has been associated with oxidative damage due to increased mitochondrial ROS production. *C. alboguttata* reduced skeletal muscle mitochondrial respiration by approximately 50% following four months of aestivation, while mitochondrial ROS production was more than 80% lower in aestivating skeletal muscle relative to controls when mitochondrial substrates were present at physiologically-relevant concentrations. In contrast to skeletal muscle, cardiac muscle of aestivating frogs must remain relatively active to still maintain adequate perfusion of organs. Aestivating frogs maintained cardiac mitochondrial respiration and ROS production at levels similar to those of control animals.

Accelerated protein degradation in mammalian skeletal muscle has been linked to increased mitochondrial ROS production and oxidative stress. When ROS are in excess, a number of proteolytic pathways appear to play a pivotal role in the development of atrophy in inactive muscle fibres including the cytosolic calcium-dependent calpains. The aim of the final chapter was to determine if aestivating *C. alboguttata* are able to resist disuse-induced atrophy as a consequence of the downregulation of calpain proteases in skeletal muscle. The enzyme activity, protein abundance and gene expression levels of calpain isoforms were examined in skeletal muscle of aestivating and control *C. alboguttata*. There was no decrease in the protein abundances of calpain 1 or calpain 2 in aestivating *C. alboguttata* muscle relative to controls. Similarly, gene expression and enzyme activity levels of calpain 1 and 2 were unaffected by aestivation. The protein abundance of 'muscle-specific' calpain 3, which is consistently downregulated during atrophic conditions, was also examined in aestivating muscle. Western blotting indicated that calpain 3 may be autolysed (and hence activated) in skeletal muscle of both active and aestivating frogs.

Results from the current study suggest that the relative inhibition of muscle atrophy in aestivating *C. alboguttata* is multifactorial in origin. ATP-dependent chromatin remodelling appears to be an important mechanism to actively regulate gene expression throughout aestivation, while elevated expression of anti-apoptotic genes is likely to be critical in preventing premature apoptotic muscle fibre degradation. In addition, decreased rates of skeletal muscle mitochondrial respiration during aestivation allows energy savings to be maximised. Low levels of hydrogen peroxide production suggests that ROS can be suppressed in immobilised skeletal muscles of aestivating frogs, which in combination with bolstering antioxidant defences may protect against potential oxidative stress and preserve skeletal muscle structure during aestivation and during arousal. While it is difficult to

determine the specific function of calpain 3 in *C. alboguttata* muscle, the maintenance (rather than an increase) of pre-aestivation enzyme activity, protein and mRNA abundances of calpains is consistent with the protection of muscle against uncontrolled proteolysis throughout aestivation.

Declaration by author

This thesis is composed of my original work, and contains no material previously published or written by another person except where due reference has been made in the text. I have clearly stated the contribution by others to jointly-authored works that I have included in my thesis.

I have clearly stated the contribution of others to my thesis as a whole, including statistical assistance, survey design, data analysis, significant technical procedures, professional editorial advice, and any other original research work used or reported in my thesis. The content of my thesis is the result of work I have carried out since the commencement of my research higher degree candidature and does not include a substantial part of work that has been submitted to qualify for the award of any other degree or diploma in any university or other tertiary institution. I have clearly stated which parts of my thesis, if any, have been submitted to qualify for another award.

I acknowledge that an electronic copy of my thesis must be lodged with the University Library and, subject to the policy and procedures of The University of Queensland, the thesis be made available for research and study in accordance with the Copyright Act 1968 unless a period of embargo has been approved by the Dean of the Graduate School.

I acknowledge that copyright of all material contained in my thesis resides with the copyright holder(s) of that material. Where appropriate I have obtained copyright permission from the copyright holder to reproduce material in this thesis.

Publications during candidature

Reilly, B.D., Schlipalius, D.I., Cramp, R.L., Ebert, P.R. and Franklin, C.E. (2013). Frogs and estivation: transcriptional insights into metabolism and cell survival in a natural model of extended muscle disuse. *Physiological Genomics* 45, 377-388.

Reilly, B.D., Hickey, A.J.R., Cramp, R.L. and Franklin, C.E. (2013). Decreased hydrogen peroxide production and mitochondrial respiration in skeletal muscle but not cardiac muscle of the green-striped burrowing frog, a natural model of muscle disuse. *The Journal of Experimental Biology* 217, 1087-1093.

Reilly, B.D., Cramp, R.L. and Franklin, C.E. (2014). Activity, abundance and expression of Ca^{2+}-activated proteases in skeletal muscle of the aestivating frog, *Cyclorana alboguttata*. *Journal of Comparative Physiology B – Biochemical, Systemic and Environmental Physiology* 185, 243-255.

Publications included in this thesis

Reilly, B.D., Schlipalius, D.I., Cramp, R.L., Ebert, P.R. and Franklin, C.E. (2013). Frogs and estivation: transcriptional insights into metabolism and cell survival in a natural model of extended muscle disuse. *Physiological Genomics* 45, 377-388 – Incorporated as Chapter 2.

Contributor	Statement of contribution
Reilly, B.D.	Conception and design (50%), data collection (100%), analysis (90%), interpretation (80%), writing and drafting (60%).
Schlipalius, D.I.	Conception and design (5%), analysis (5%), interpretation (5%), writing and drafting (10%).
Cramp, R.L.	Conception and design (20%), writing and drafting (10%).
Ebert, P.R.	Conception and design (5%), analysis (5%), interpretation (5%), writing and drafting (10%).
Franklin, C.E.	Conception and design (20%), interpretation (10%), writing and drafting (10%).

Reilly, B.D., Hickey, A.J.R., Cramp, R.L. and Franklin, C.E. (2013). Decreased hydrogen peroxide production and mitochondrial respiration in skeletal muscle but not cardiac muscle of the green-striped burrowing frog, a natural model of muscle disuse. *The Journal of Experimental Biology* 217, 1087-1093 – Incorporated as Chapter 3.

Contributor	Statement of contribution
Reilly, B.D.	Conception and design (50%), data collection (80%), analysis (80%), interpretation (70%), writing and drafting (70%).
Hickey, A.J.R.	Conception and design (50%), data collection (20%), analysis (20%), interpretation (20%), writing and drafting (10%).
Cramp, R.L.	Interpretation (5%), writing and drafting (10%).
Franklin, C.E.	Interpretation (5%), writing and drafting (10%).

Reilly, B.D., Cramp, R.L. and Franklin, C.E. (2014). Activity, abundance and expression of Ca^{2+}-activated proteases in skeletal muscle of the aestivating frog, *Cyclorana alboguttata*. *Journal of Comparative Physiology B – Biochemical, Systemic and Environmental Physiology* 185, 243-255 – Incorporated as Chapter 4.

Contributor	Statement of contribution
Reilly, B.D.	Conception and design (60%), data collection (100%), analysis (90%), interpretation (80%), writing and drafting (80%).
Cramp, R.L.	Conception and design (20%), interpretation (5%), analysis (10%), interpretation (10%), writing and drafting (10%).
Franklin, C.E.	Conception and design (20%), interpretation (10%), writing and drafting (10%).

Contributions by others to the thesis

Contributions by others to the thesis as a whole:

Craig Franklin and Rebecca Cramp, through discussions with myself, contributed significantly to the conception and design of this research overall. David Schlipalius and Paul Ebert provided significant technical and analytical assistance in chapter 2. Anthony Hickey aided in the conception and design of chapter 3, and provided important resources to carry out the work. Bradley Launikonis at the Laboratory for Muscle Research (School of Biomedical Sciences, The University of Queensland) provided tissues for use in experiments in chapter 4. Craig Franklin and Rebecca Cramp critically reviewed the final draft of this thesis.

Statement of parts of the thesis submitted to qualify for the award of another degree

None.

Acknowledgements

Well somehow I've managed to condense the last three and a half years of my life into approximately 100 pages. What an experience a PhD is. I've certainly learnt a lot during the PhD experience (time management, planning ahead, communication etc.) but also discovered a few things about my personal strengths and weaknesses. In the theses I've perused to help me during my own studies, I remember reading the acknowledgements and wondered what I would write when the time came for me. Well, here I am and of course I would like to thank a number of important people. First and foremost, thank you to my principal supervisor, Craig Franklin. I remember first approaching you at an undergraduate conference in 2008 and we chatted enthusiastically about sharks and sawfish living in freshwater. Well, that was the start of some exciting projects for the both of us. Thank you for the opportunities in your lab, the scientific discussions and the constant encouragement and support. Thanks for the support to attend national and international conferences (one of the best bits of science!), to visit a wild part of Cape York Peninsula and thank you for your ability to restore motivation in me! Thank you for making sure I didn't leave prematurely last year with a Masters under my belt! Many thanks for passing on your scientific knowledge.

Thank you to my co-supervisor, Rebecca Cramp. You are a wealth of knowledge and like Craig you were always available for discussions and general assistance when I needed it. You've taught me many laboratory skills, helped me to improve my writing and challenged me with alternative views or new ideas during my PhD project. I've always thought you did a tonne of work for all of us in the lab (teaching, administrative, research), but you insisted it was never too much a request. You also do an amazing job at keeping a good work-life balance!

I must thank Paul Ebert and David Schlipalius for their help with all things to do with bioinformatics. Your provision of resources and input into building a transcriptome for these unusual frogs was invaluable. I never imagined so much information could be generated in a few short months. A big thank you to Tony Hickey across the ditch in Auckland. You have an amazing knowledge of mitochondrial physiology and it was a pleasure to work together in the lab. You have an infectious enthusiasm and a constant flow of ideas for new experiments that could be performed! Thanks for the beers and the laughs as well, it was great to have you visit. I would also like to thank Craig White, who was always available to provide assistance whether it was related to statistics, metabolic physiology, or general feedback on my work.

Of course I have a number of good friends from the university that I would like to acknowledge. You've all made a contribution in helping me get to this stage. Lesley Alton, Hamish Campbell, Mariana Campbell, Ross Dwyer, Pippa Kern, Julian Beaman, Michel Ohmer, Anna Weier, Ben Yuen, Essie Rogers, Cassie Taylor, Adam Reddiex thank you all very much. All of you have made a significant impact during my PhD experience!

I need to thank my friends outside of the uni setting who have seen me get through this academic escapade. Cheers to Laurence Katsaras, Bree Wilson, Piri Tekanawa, Nick Yorsten and Will O'Brien. Whether it was drinking a beer (or more than several beers), having a surf, snowboarding, or general banter, these 'time-out' sessions from the PhD were always fantastic (and necessary).

Thanks Mum, Dad and Angie for the support throughout not only the PhD, but from that time I was working as a bartender in Dublin and decided it might be a good idea to come back to Australia and study some science for the remainder of my 20's! Thank you to my beautiful girlfriend, Raenuka Menon. Thank you for the great times spent together, in and around Brisbane and in Europe, and thank you for pushing me to finish off the PhD!

Where to now? Must be time to start a new experiment.....

Keywords

RNA sequencing, gene expression analysis, transcriptome, mitochondria, antioxidant, oxidative stress, atrophy, apoptosis, proteolysis, anuran.

Australian and New Zealand Standard Research Classifications (ANZSRC)

ANZSRC code: 060602, Animal Physiology – Cell, 50%

ANZSRC code: 060405, Gene Expression, 25%

ANZSRC code: 060102, Bioinformatics, 25%

Fields of Research (FoR) Classification

FoR code: 0606, Physiology, 60%

FoR code: 0601, Biochemistry and Cell Biology, 20%

FoR code: 0604, Genetics, 20%

TABLE OF CONTENTS

LIST OF FIGURES

LIST OF TABLES

Chapter 1

General Introduction

Basic skeletal muscle physiology and anatomy

Animal movement is dependent on the activity of voluntary skeletal muscle. Skeletal muscle is comprised of individual myocytes, otherwise known as 'muscle fibres' or myofibres. Muscle fibres are in turn composed of a large number of myofibrils, which vary in size (thick or thin filaments) but average about 1 μm in diameter, making up approximately 80% of the volume of a muscle fibre (Jones, 2004). Myofibrils largely consist of two contractile proteins, actin and myosin, which are repeated as a string of sarcomeres, the basic functional unit of muscle fibres (Jones, 2004). Actin and myosin constitute a large portion of the total protein in skeletal muscle, and their highly ordered arrangement in muscle fibres allows the controlled production of force and movement.

Muscle contraction is dependent upon a neural activation signal in a process known as excitation-contraction coupling (Lieber, 2010). Peripheral nerves at neuromuscular junctions contain packets of the neurotransmitter acetylcholine, which when released causes muscle fibre excitation. When fibres are stimulated, calcium ions bind to troponin, an actin regulatory protein, allowing interaction between actin and myosin. Muscle contraction takes place when myosin heads bond to actin and rotate to draw the thick and thin filaments past one another, and thus force generation and movement (Lieber, 2010). Muscle force is proportional to cross-sectional area of the muscle, and the speed at which muscle contracts is proportional to muscle fibre length.

Mammalian skeletal muscle fibres can be broadly divided into three main categories: fast glycolytic fibres, fast oxidative fibres, and slow oxidative fibres (Table 1.1). Generally, slow oxidative fibres use oxygen more efficiently to produce ATP for continuous muscle contraction over prolonged periods, whereas fast glycolytic fibres contract very quickly and with great force in the absence of oxygen (Lieber, 2010). Fast oxidative fibres are a combination of slow oxidative and fast glycolytic fibres and use both aerobic and anaerobic metabolism to generate ATP.

Table 1.1 Characteristics of each of the three categories of slow and fast muscle fibre types

Fibre type designation	Characteristics	Number of mitochondria	Myosin ATPase Activity	SDH Activity	α–GPDH Activity
Slow oxidative	Contract and fatigue slowest, with least force	High	Low	High	Low
Fast glycolytic	Contract and fatigue fast, with great force	Low	High	Low	High
Fast oxidative	Contract moderately fast, fatigue slowly	High	High	High	High

*Myosin ATPase activity is used to distinguish between fast- and slow-contracting muscle fibres; succinate dehydrogenase (SDH) activity is used to differentiate between oxidative and non-oxidative fibres; α-glycerophosphate dehydrogenase (α-GPDH) is used to distinguish among fibres based on their relative glycolytic potential. Table modified from (Lieber, 2010; Mantle, 2007).

Like mammalian muscle, early studies categorised amphibian muscles into different fibre types, each with distinct contractile properties (see Gans and de Gueldre, 1992 for a review). The motor units (i.e. motor neuron and its innervated fibre) of amphibian hindlimb muscle are generally referred to as being 'twitch' (phasic, fast) or 'tonic' (slow). Frogs usually have four or five different categories of muscle fibres, comprised of three twitch (Types 1, 2, and 3) and one or two tonic (Types 4 and 5) types. The proportions of twitch and tonic fibres differ among the skeletal muscles of amphibians with distinctions in physiological properties having also been documented between the fibre types (e.g. contraction velocities). Studies of *Rana* and *Xenopus* fibre types indicated that Type 1 myofibres exhibit the lowest oxidative activity (inferred from succinate dehydrogenase (SDH) staining) whereas Type 3 has the highest SDH activity. Furthermore, twitch Types 2 and 3 exhibited higher glycolytic activity than did Type 1 myofibres whereas tonic fibres showed low oxidative and glycolytic potential. The characterisation of amphibian muscle fibre types are roughly similar to the twitch type muscles of mammals (e.g. fast (Type II) and slow (Type I)). However, there are important differences between mammalian and frog fibres, such as the rarity of tonic fibres in mammals compared with anurans. Nevertheless, in the majority of hindlimb muscles of a

number of frog species, more than 80% of the muscle cross section is comprised of large twitch fibres, whereas tonic fibres rarely make up more than 10%. A recent comparison of hindlimb muscles of frogs with different locomotory behaviours suggested that the range of functional diversity within fibre types might be very broad, so that different species or muscles may achieve different functions using exactly the same fibre types (Crockett and Peters, 2008).

Muscle disuse atrophy

Skeletal muscle is one of the most plastic (i.e. changeable) tissues in an animal. Many structural aspects of skeletal muscle tissue have been shown to demonstrate plasticity, including fibre type distribution, fibre diameter, tendon length, mitochondrial distribution and myosin heavy chain profile (Lieber, 2010). The size of skeletal muscle is dependent on the pattern of muscular activity. Increased work by a muscle can lead to a large increase in size, such as during compensatory hypertrophy. In rodents, if the workload on a particular muscle is suddenly increased by surgical intervention on a synergistic muscle, the wet and dry mass of the loaded muscle may increase by 30-50% in less than a week (Goldberg, 1967). In contrast, long periods of disuse, such as lack of physical exercise, cast immobilisation, removal of weight bearing (unloading) or extended bed-rest lead to degenerative changes in skeletal muscle and the atrophy or 'wasting' of muscle tissue (Bloomfield, 1997; Musacchia et al., 1988). On a gross level these changes culminate in a loss of muscle mass and a reduction in the cross-sectional area of muscle fibres. Because the force production of muscle is related to its fibre cross-sectional area, atrophied muscles exhibit both decreased force production and fatigue resistance (Bruce et al., 1997). The degree of muscle disuse atrophy is variable and dependent on several factors such as age, physiological function of the muscle, the extent of unloading/inactivity, and muscle fibre type composition (Bodine, 2013a). For example, in dog quadriceps muscles immobilised for ten weeks, the magnitude of atrophy of distinct fibre types was shown to be muscle-specific (Lieber et al., 1988). Muscle types that are most susceptible to disuse atrophy include leg and postural muscles that are composed of a relatively large proportion of slow oxidative muscle fibres and cross a single joint (e.g. the soleus) (Leblanc et al., 1992; Lieber et al., 1988). In contrast, muscles least vulnerable to atrophy are those that are not used as postural muscles (i.e. phasic), that cross multiple joints and that are predominantly composed of fast fibres (e.g. extensor digitorum longus) (Lieber et al., 1988; Loughna et al., 1986).

The physiological stimuli that initiates muscle disuse atrophy includes an absence of weight bearing on muscle (unloading) combined with an absence of muscle contraction. The effects of prolonged muscle disuse appear to be common to the majority of vertebrates studied, and both human and laboratory animal models have been used to examine the physiology and mechanisms underpinning muscle disuse atrophy (Bodine, 2013a; Hudson and Franklin, 2002b; Powers et al., 2011). For example, human models of extended bed rest, limb immobilisation (casting) and unilateral lower limb suspension (e.g. immobilising a leg and using crutches to walk) studies have been performed to study disuse-induced skeletal muscle atrophy in humans (Brocca et al., 2012; Chen et al., 2007; Dalla Libera et al., 2009; Hather et al., 1992). Often these studies are complicated because of the invasive nature of muscle biopsy sampling, and as a result several rodent models have been designed to mimic the different forms of human muscle disuse atrophy. Mouse and rat models of limb immobilisation have been used to study the effect of muscle disuse on muscle fibre properties and cell signalling pathways (Sakakima et al., 2004; Talbert et al., 2013a; Vazeille et al., 2008) whereas a tail suspension protocol, which effectively unloads hindlimb muscles of rodents, is usually employed to mimic human skeletal muscle atrophy that results from prolonged bed rest or microgravity (Alford et al., 1987; Leeuwenburgh et al., 2005). Comparative studies of muscle disuse atrophy in humans and rodents indicates that while there are many similarities, the major difference that has been observed is the rate of atrophy, with the loss of muscle mass in rodents occurring much more rapidly than in humans (Phillips et al., 2009).

Apart from a reduction in cross-sectional area, atrophied muscle fibres as a result of disuse exhibit other structural changes including sarcomere dissolution and an increase in connective tissues around the muscle fibres (Lieber et al., 1988; Oki et al., 1995). Metabolic alterations that occur during muscle disuse atrophy include decreased capacity for fatty acid metabolism and a greater reliance on glucose as an energy source, while lipid appears to accumulate in disused muscle regardless of whether test subjects are in a positive or negative energy state (Stein and Wade, 2005). The maintenance of skeletal muscle mass is dependent on the balance between the rates of both protein synthesis and degradation. In rodents, it has been well established that muscle disuse due to an absence of weight bearing leads to an early reduction in protein synthesis rates and an increase in the rate of protein degradation (Goldspink et al., 1986; Loughna et al., 1986; Thomason et al., 1989). However, there is continued debate as to the importance of protein degradation in human studies of muscle

disuse atrophy. It has been suggested that during muscle disuse the major process that changes leading to the loss of muscle mass is protein synthesis, with no elevation in the extent of protein degradation (Phillips et al., 2009). However, others have demonstrated an increase in the abundance of mRNA for proteases of the ubiquitin-proteasome system (UPS) (Jones et al., 2004), which has been associated with muscle atrophy in various clinical settings (Price, 2003). Despite the apparent disparities among experimental disuse models, clearly there is an apparent shift in the balance of protein synthesis and/or degradation so that there is a net loss of muscle proteins.

Although there is a decrease in total muscle protein during muscle disuse atrophy, less is known about the initiating triggers or the signalling proteins underlying the net loss of muscle protein during the atrophic process. Thus, the molecular and cellular pathways regulating muscle loss during disuse remain an active area of research.

Molecular and cellular mechanisms involved in muscle disuse atrophy

An array of triggers and signals are hypothesised to be important in the events leading to muscle disuse atrophy (Bodine, 2013a; Jackman and Kandarian, 2004; Pellegrino et al., 2011; Powers et al., 2011). Numerous protein degradation pathways contribute to the proteolysis of muscle proteins, and evidence suggests that interactions among major protein degradation pathways (ubiquitin-proteasome system, Ca^{2+}-dependent proteases (calpains), the autophagy-lysosome system and cysteine-aspartic proteases (caspases)) are involved in proteolysis during disuse atrophy (Talbert et al., 2013b). Reactive oxygen species (ROS) have been implicated as potential triggers leading to skeletal muscle atrophy under various disuse conditions (Jackman and Kandarian, 2004; Powers et al., 2011), while gene expression profiling of disused muscle has demonstrated both increases and decreases of numerous genes over time, indicating that a complex suite of biochemical changes act simultaneously to induce muscle atrophy (Chen et al., 2007; Stevenson et al., 2003). For example, genes encoding myostatin and insulin-like growth factor 1 (IGF-1) (important mediators of muscle growth and size in adult mammals) have been shown to change during prolonged muscle disuse (Awede et al., 1999; Reardon et al., 2001; Wehling et al., 2000), but their relative contributions to disuse-induced muscle atrophy remain poorly defined. The following sections provide a summary of the molecular triggers and signals hypothesised to play prominent roles in muscle disuse atrophy.

Reactive oxygen species and oxidative damage

A large body of evidence suggests that ROS and oxidative stress are important in the events leading to muscle disuse atrophy (Powers et al., 2011). ROS or 'free radicals' refers to a number of chemically reactive species that are generated during normal aerobic metabolism, namely superoxide anion ($O_2^{\cdot-}$), hydrogen peroxide (H_2O_2) and hydroxyl radicals ($^{\bullet}OH$). The mitochondrion is known to be a major site of ROS production (Figure 1.1). Specifically, the electron transport chain (ETC) within mitochondria comprises a series of enzymes or complexes which participate in electron transfer via oxidation-reduction reactions. The final step of the ETC usually involves the reduction of oxygen to water; however, a small proportion of electrons leak out of the pathway to directly produce $O_2^{\cdot-}$ (Turrens, 2003). Within the ETC, respiratory complex I (NADH: ubiquinone oxidoreductase) and respiratory complex III (cytochrome bc_1) are deemed the two most significant sources of $O_2^{\cdot-}$ production (Turrens, 2003). Although $O_2^{\cdot-}$ is not in itself a powerful oxidant, it is the antecedent of other major ROS (H_2O_2, $^{\cdot}OH$) and is involved in the production of oxidative chain reactions (Turrens, 2003). Whereas minor fluctuations in ROS levels can promote positive intracellular signalling and regulate physiological processes (Barbieri and Sestili, 2012), large increases in ROS concentrations can attack the structure and function of nucleic acids, lipids and proteins which may lead to cell injury or death. However, the harmful effects of excessive ROS production are, to a large extent, limited by numerous antioxidants (e.g. superoxide dismutases, glutathione peroxidase).

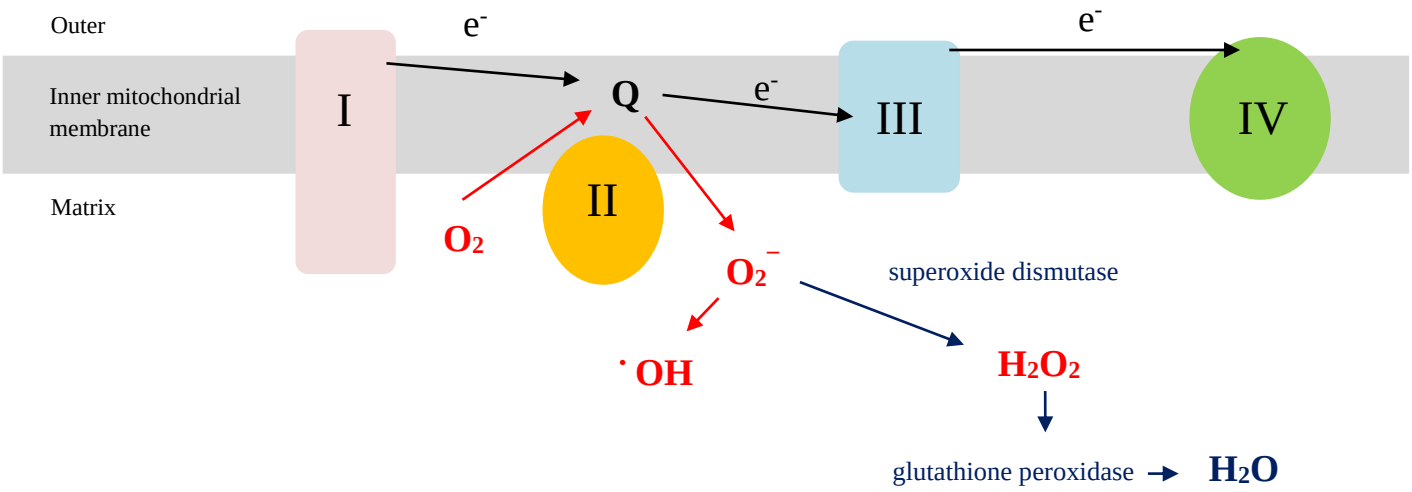

Figure 1.1. Premature electron (e^-) leakage occurs when the rate of electron entry into the mitochondrial electron transport chain does not equal the rate of electron transfer through the chain. As a result, superoxide ($O_2^{\cdot-}$) production increases at complexes I and III as ubiquinone (Q) donates an electron to oxygen (O_2). The formation of $O_2^{\cdot-}$ leads to production of hydroxyl free radical ($^{\cdot}OH$) or alternatively undergoes dismutation (via superoxide dismutase) to form hydrogen peroxide (H_2O_2). H_2O_2 is in turn rendered harmless by the action of glutathione peroxidase by reducing it to water (H_2O).

The link between oxidative stress and muscle disuse atrophy was suggested following observations that prolonged bed rest in humans, and both hindlimb immobilisation and hindlimb unloading in rats results in increased levels of a number of markers of oxidative damage (e.g. thiobarbituric acid-reactive substances, (TBARS), dichlorohydrofluorescein diacetate (DCFH-DA) oxidation and protein carbonylation (Dalla Libera et al., 2009; Kondo et al., 1991; Lawler et al., 2003). Oxidative stress in skeletal muscle during disuse appears to be related to an imbalance in cellular antioxidant defence systems, including suppression of superoxide dismutases, antioxidant scavenger status and thioredoxin-related proteins (Brocca et al., 2012; Lawler et al., 2003; Matsushima et al., 2006). Prolonged periods of muscle disuse have also been reported to induce higher production of mitochondrial ROS (e.g. $O_2^{\cdot-}$, H_2O_2) in skeletal muscle fibres (Min et al., 2011, Talbert et al., 2013, Xu et al., 2010). Thus, it appears that oxidative stress occurs when the production of harmful mitochondrial ROS overwhelms the antioxidant capacity of the cell, leading to oxidative injury and the fibre damage that is characteristic of muscle disuse atrophy.

Reactive oxygen species: key regulators of protein degradation pathways

Several protein degradation pathways are active during atrophy in skeletal muscle, including: 1) the ubiquitin-proteasome system (UPS) 2) the Ca^{2+}-dependent proteases (calpains) 3) the autophagy-lysosome system , and 4) caspase-3 (a protease involved in apoptosis) (Jackman and Kandarian, 2004; Powers et al., 2007). The relative importance of each system in the progression of muscle disuse atrophy continues to be debated. Nevertheless, the UPS and the calpains have received the most experimental attention. The highly conserved UPS tags proteins for degradation via the protein ubiquitin. The process of tagging a protein with ubiquitin (ubiquitylation) involves multiple, complex steps resulting in a polyubiquitin chain, which provides a recognition signal for the 26S proteasome to degrade the tagged protein (Myung et al., 2001). Studies have indicated that the UPS is the predominant proteolytic pathway during disuse-induced atrophy as the UPS catabolises most sarcomeric proteins (e.g. myosin, actin, troponin) (Mitch and Goldberg, 1996). However, the UPS is unable to degrade myofibrils or multicomponent complexes of actin and myosin due to specific interactions between these proteins within muscle sarcomeres (Solomon and Goldberg, 1996). Thus, the UPS might not be the rate-limiting step during muscle disuse atrophy because myofilament release may be required before the UPS can degrade both actin and myosin. It has been suggested that the calpain proteases might assist the UPS in this process. Calpains can catabolise several muscle structural proteins which could lead to the release of myofilaments making them accessible to the UPS (Talbert et al., 2013a).

Calpains are proteolytic enzymes found in all vertebrate cells and function in diverse cellular processes including cytoskeletal organisation, proteolysis of cell cycle proteins, signal transduction and apoptosis (Goll et al., 2003). Calpains are activated by a sustained increase in cytosolic Ca^{2+} concentrations and/or deactivated by the endogenous calpain inhibitor, calpastatin (Bartoli and Richard, 2005). Of the many existing calpain isoforms, calpain-1 and calpain-2 (the ubiquitous calpains) are the best-characterised in skeletal muscle (Goll et al., 2003). Emerging evidence suggests that the production of ROS appears to be a necessary signal for both the UPS and calpains to participate in protein degradation during muscle disuse atrophy.

Exposure of mouse myoblasts to ROS (H_2O_2) has been shown to increase the activity and expression of major elements of the UPS, including proteasome subunits (20S proteasome), ubiquitin-conjugating enzymes (E2 proteins) and ubiquitin ligases (specifically, the ligases MAFbx/atrogin-1 and MuRF1, two ‘atrogenes’ which are consistently upregulated

in different muscle atrophy models) (Gomes-Marcondes and Tisdale, 2002; Li et al., 2003). More recently, one week of hindlimb-casting in rats was shown to increase mitochondrial emission of ROS and correlate with significant increases in the mRNA abundance of both MAFbx/atrogin-1 and MuRF1 (Talbert et al., 2013b). Importantly, the disuse-induced activation of both MAFbx/atrogin-1 and MuRF1 in skeletal muscle was inhibited by treatment with a mitochondrial-targeted antioxidant (SS-31), suggesting that activation of the UPS during immobilisation-induced atrophy requires mitochondrial ROS production.

Evidence that calpains 1 and 2 are important contributors to skeletal muscle disuse atrophy is largely based on examinations of gene expression, protein abundance or enzyme activity (Enns et al., 2007; Haddad et al., 2003; Min et al., 2011; Taillandier et al., 1996). However, it has been demonstrated that overexpression of calpastatin in 10-day unloaded mouse skeletal muscle eliminates calpain activity and decreases muscle atrophy by 30%, confirming that calpains are involved in muscle disuse atrophy (Tidball and Spencer, 2002). With respect to ROS, *in vitro* oxidation of myofibrillar proteins has been shown to increase their susceptibility to degradation by both calpain-1 and calpain-2 (Smuder et al., 2010). Exposure of human skeletal muscle satellite cells to H_2O_2 has been shown to lead to calcium imbalance and an upregulation of calpain gene expression and activity (and subsequent protein oxidation and programmed cell death) (Dargelos et al., 2010), while H_2O_2-induced skeletal muscle myotube oxidative damage and atrophy was shown to be dependent upon calpain 1 expression (McClung et al., 2009). Recently, fourteen days of hindlimb immobilisation in rodents was shown to increase mitochondrial ROS production and calpain 1 activation (Min et al., 2011). Similar to the study of Talbert et al. (Talbert et al., 2013b), application of SS-31 abolished the disuse-induced activation of skeletal muscle calpain 1. These recent experiments provide strong evidence of a potential mechanistic link that connects oxidative stress with calpains and muscle disuse atrophy.

Mitochondrial signalling and apoptosis

It has become apparent that dysfunctional mitochondria and subsequent acceleration of apoptosis may be involved in muscle disuse atrophy (Marzetti et al., 2010; Powers et al., 2012). Apoptosis, or programmed cell death, is a physiological mechanism involved in morphogenesis, changes in cell number, the eradication of abnormal cells, and can play a key role in pathophysiological muscle cell loss (Marzetti et al., 2010; Rossi and Gaidano, 2003). Apoptosis may be initiated via extracellular (extrinsic) or intracellular (intrinsic) pathways.

The extrinsic pathway is activated by specific death receptors (such as ligand-mediated activation via tumour necrosis factor α), while the intrinsic pathway originates within mitochondria (Rossi and Gaidano, 2003). However, mitochondria can be considered the major centre for the integration of apoptotic signalling and induction of apoptosis, because many of the extrinsic apoptotic stimuli activate pathways that also converge on the mitochondria to initiate cell death (Marzetti et al., 2010).

Limb immobilisation has been shown to induce a reduction in muscle fibre size but not the number of myocytes (Nicks et al., 1989). However, myonuclear apoptosis has been reported during muscle disuse atrophy following measurements of terminal deoxynucleotidyl transferase dUTP nick end-labelling (TUNEL) (Dupont-Versteegden et al., 2006). Sixteen days of muscle disuse in rats leads to a reduction in myonuclear number and domain size, as well as a decrease in satellite cell activity in muscle fibres, suggesting apoptosis is active during muscle disuse atrophy (Wang et al., 2006). Two recent studies promoted skeletal muscle atrophy by two weeks of hindlimb suspension in the soleus (Leeuwenburgh et al., 2005) and the gastrocnemius (Siu et al., 2005) muscles of rats, and demonstrated that apoptosis was occurring in both types of the atrophied muscles (Leeuwenburgh et al., 2005; Siu et al., 2005). Mechanistically, elevated cytosolic levels of both apoptosis-inducing factor (an intrinsic regulator of apoptosis) and cytochrome c (often released from mitochondria during the early phase of apoptosis) also develop in the gastrocnemius muscle following hindlimb suspension (Siu et al., 2005), while caspase-3 proteolytic activity is key in the elimination of cells undergoing apoptosis in the disused soleus muscle of rats (Leeuwenburgh et al., 2005).

Apoptotic signalling also occurs in the early phases of muscle disuse atrophy (Ferreira et al., 2008). Maximal apoptosis-inducing factor expression was found after one day of hindlimb suspension in the soleus muscle of mice, which overlapped temporally with the highest levels of apoptotic DNA fragmentation (Ferreira et al., 2008). Further confirmation for the role of mitochondria-mediated apoptosis during muscle disuse atrophy arises from a unilateral hindlimb immobilisation study (Vazeille et al., 2008). Signalling mechanisms within this pathway appear to be activated during atrophy, but are then decreased during the recovery period following immobilisation (Vazeille et al., 2008). Thus, muscle disuse atrophy in mammals appears to be associated with activation of the apoptotic program.

Hibernating mammals as models of muscle disuse atrophy

Although there appears to be multiple molecular mechanisms potentially involved in the events leading to muscle disuse atrophy, the gross loss of skeletal muscle tissue appears to hold true for the majority of vertebrates studied thus far. Generally this includes a relatively limited variety of mammalian model systems, such as rodents and humans (but also cats, dogs and guinea pigs), which have been artificially immobilised in a laboratory setting (Musacchia et al., 1988). The deleterious effects of muscle disuse atrophy may be reversed upon the return of normal weight bearing (i.e. reloading) of the limbs (Bodine, 2013a; Booth and Seider, 1979). However, currently there are no sound therapeutic options to treat muscle disuse atrophy, clearly due an incomplete understanding of the cellular and molecular mechanisms participating in the induction and maintenance of muscle wasting.

It is well known that negligible or no loss of skeletal muscle mass occurs in a variety of hibernating mammals despite the fact they experience repressed neural activity and natural periods of chronic muscle disuse (Bodine, 2013b; Harlow et al., 2001; Shavlakadze and Grounds, 2006). Hibernation is a survival strategy used by many mammals (e.g. bears, bats, squirrels, lemurs, hedgehogs and tenrecs) to cope with very low environmental temperatures and/or scarcity of food supplies. Winter hibernators typically retreat during cold, unfavourable conditions into sheltered sites called hibernacula, relying on lipid stores accumulated during a short pre-hibernation period to survive. The thirteen-lined ground squirrel (*Spermophilus tridecemlineatus*) hibernates for up to seven months during which time it enters into a deep torpor (days to weeks) interspersed with short arousal periods (less than 24 h). Six months of hibernation (i.e. immobility) in this species has been shown to have no effect on the muscle fibre size or morphology of the quadriceps or tibialis anterior (Andres-Mateos et al., 2013). However, the amount of muscle tissue loss can vary in hibernating squirrels depending on the type of muscle examined. James et al. (James et al., 2013) reported no loss of mass or tension in soleus muscle of *S. tridecemlineatus* following three months of hibernation, whereas a 14% loss was found in the gastrocnemius and 43% loss in the semitendinous muscles of the golden-mantled ground squirrel (*Spermophilus lateralis*) (Wickler et al., 1991). Muscle atrophy develops early on in hibernating *S. lateralis* but does not advance in the final 3 months (Nowell et al., 2011), a result which is similar to that which occurs during prolonged bed rest in humans (Adams et al., 2003; Phillips et al., 2009).

Hibernating bears also retain most of their muscle mass despite prolonged inactivity and food deprivation during winter. A recent study examined the biceps femoris muscle of

summer active and winter hibernating brown bears (*Ursus arctos*) (Hershey et al., 2008). After five months of hibernation, the average cross-sectional areas of fast and slow fibres remained unchanged from summer to winter, while muscle protein concentration decreased by only 8% (Hershey et al., 2008). Like squirrels, the magnitude of muscle wasting in bears is dependent on the type of muscle studied. In black bears (*U. americanus*), loss of muscle protein content is much greater in biceps femoris compared with the gastrocnemius (Tinker et al., 1998). The apparent retention of muscle integrity and locomotor function is not restricted to squirrels and bears, as other studies have shown that hibernating mammals such as prairie dogs (Harlow and Menkens, 1986), hamsters (Wickler et al., 1987), and bats (Yacoe, 1983) experience either limited losses in muscle size, protein, or strength.

Resistance to muscle disuse atrophy during hibernation does not appear to be associated with the degree to which core body temperature is reduced. Whereas hibernating *U. americanus* lower their body temperature by only 2-5°C (Lohuis et al., 2007b), ground squirrels in deep torpor reduce core temperature to near ambient (approximately 4°C), yet both species show minimal muscle atrophy despite months of inactivity. Furthermore, a study examining two species of prairie dogs found no difference in the extent of muscle or strength loss between the two despite differences in their hibernation strategies (one experiencing normal torpor cycles with very low core temperatures, the other being facultative hibernators that use sporadic, moderate-temperature torpor cycles) (Cotton and Harlow, 2010). Regardless of the muscle type, core body temperature or species studied the loss of muscle mass and strength in hibernators is significantly less than what occurs in humans and laboratory rodents during extended muscle disuse. For example, black bears lose 29% of their tibialis anterior muscle peak force production over 110 days of hibernation without food or water (Lohuis et al., 2007b). In comparison, humans subjected to bed rest for 3 months exhibit between 51-60% decrease in the maximum voluntary contraction of both knee extensors and plantar flexor muscles (Alkner and Tesch, 2004).

Investigations of the cellular and molecular mechanisms that may underpin inhibition of muscle atrophy in hibernators have been limited. Although mechanistic links between ROS and both proteolysis and protein synthesis have been demonstrated in clinical models of muscle disuse atrophy (Powers et al., 2011), almost nothing is known about the effects of ROS signalling during dormancy. However, one study did report an increase in antioxidant capacity in hibernating muscle which might protect cells by scavenging ROS (James et al., 2013). This is important given that throughout dormancy the capacity to replace ROS-

damaged molecules is compromised as a consequence of drastically reduced rates of transcription and translation (Storey et al., 2010). It has been shown that rates of both protein degradation and synthesis can be reduced by up to 70% in skeletal muscle of hibernating bears (Lohuis et al., 2007a). Curiously, a more recent study found increased gene expression of mRNAs largely involved in protein biosynthesis in muscles of hibernating *U. americanus* relative to summer active animals, suggesting that induction of translation could be enhanced during dormancy (Fedorov et al., 2009). These contradictory results may be explained by the fact that protein translation can be modulated by reversible phosphorylation of initiation and elongation factors (Storey et al., 2010).

In regard to programmed cell death, studies of differential gene expression in arctic ground squirrels (*Spermophilus parryii*) found that mRNA profiles of genes involved in apoptosis increased significantly in skeletal muscle during arousal phases of the torpor-arousal cycle (Yan et al., 2008). In skeletal muscle of *S. tridecemlineatus* however, the protein expression of X-linked inhibitor of apoptosis (belonging to the inhibitor of apoptosis family of proteins) increased significantly when animals were undergoing torpor (Rouble et al., 2013).

Due to its involvement in regulation of muscle growth and mass, myostatin has also received experimental attention in hibernators. Brooks and coworkers demonstrated that myostatin protein levels in mixed hindlimb muscle of *S. tridecemlineatus* were largely constant throughout torpor relative to controls, but increased significantly during arousal (Brooks et al., 2011) while in hibernating *S. lateralis*, a significant reduction in myostatin gene expression was found in soleus and diaphragm muscles, but not in limb muscles with fast-type fibres (Nowell et al., 2011). Many of the above molecular changes may represent key mechanisms for reducing atrophy during hibernation, although clearly there is still much to learn.

While hibernating mammals have been widely used as ‘natural analogs’ to which clinical disuse models such as bed rest and cast immobilisation may be compared, another group of organisms that experience extended muscle disuse during dormancy includes aestivating (burrowing) frogs. Aestivation in amphibians represents a relatively novel, natural model system to study mechanisms that increase the resistance of skeletal muscle to atrophy and dysfunction following prolonged periods of inactivity. Furthermore, because aestivation occurs at relatively higher ambient temperatures than hibernation, the inherent relationship between environmental temperature and rates of biochemical reactions in ectotherms means

that metabolic suppression might be more prone to perturbations. Temperature-induced elevations in metabolic rate during prolonged inactivity and fasting could therefore lead to accelerated losses in muscle mass and protein. Thus, studies on aestivating animals can expand our knowledge of how patterns of dormancy/arousal affect organismal and organ function.

Dormancy and metabolic depression

The common feature among animals that exhibit minimal muscle disuse atrophy relative to typical clinical models is that all undergo lengthy periods of dormancy. This is because these organisms inhabit extreme environments which are often incompatible with sustaining the fundamentals of life (e.g. feeding and reproduction). Dormancy is an advantageous strategy as it prolongs the amount of time an organism may survive on internal fuel stores. Substantial energy savings may be made simply by reducing both locomotor activity and digestion, however dormancy typically lasts for many months, if not years. Under such circumstances, animals undergo a strong metabolic depression in addition to inactivity (Carey et al., 2003; Storey and Storey, 1990). Since the metabolic rate of an animal converts directly into its energy requirements, metabolic depression, otherwise known as hypometabolism, allows animals to significantly decrease the rate of consumption of their endogenous fuel supplies (Guppy and Withers, 1999; Storey and Storey, 1990).

Dormancy is widespread among animal phyla and can occur in response to a range of conditions, including extreme environmental temperatures, food deprivation, desiccation, and anoxia (Carey et al., 2003; Guppy and Withers, 1999; Storey and Storey, 1990). The most well-known example of dormancy is hibernation, which entails a decrease in core body temperature (T_b), bradycardia, reduced blood flow and a metabolic rate that can be less than 5% of normal (Carey et al., 2003). The strategies adopted by hibernators are variable and range from regular, extended bouts of torpor with a low T_b near ambient levels, to irregular, brief torpor bouts with moderately reduced T_b (Geiser and Ruf, 1995). Nevertheless, torpor bouts are usually interrupted by periodic arousals where the animal returns to normothermia. By depressing whole-animal metabolic rate and letting T_b drop, animals can preserve almost 90% of the energy that would be required to sustain activity at a typical endothermic T_b (Wang, 1979). Other examples of dormancy coinciding with metabolic depression include diapause in insects, cryptobiosis in crustaceans and aestivation in molluscs, fish, reptiles and amphibians (Guppy and Withers, 1999).

Regardless of the type of metabolic depression, all share a common set of behavioural, physiological and biochemical characteristics. Before entering dormancy, animals either accrue body lipid stores or stockpile food (e.g. hibernators) (Brenner and Lyle, 1975; Buck and Barnes, 1999) before seeking shelter for physical protection from predators and to limit environmental perturbations, such as changes in temperature and humidity. Physiological adjustments accompanying metabolic depression include hypoventilation, bradycardia, hypophagia (cessation of feeding) and strongly suppressed renal function (Delaney et al., 1974; Rizzatti and Romero, 2001; Storey et al., 2010; Zatzman, 1984). Suppression of cell metabolism is achieved via the coordinated downregulation of the rate of cellular ATP turnover (e.g. decreasing ion pump activity, macromolecular synthesis and macromolecular turnover) (Ramnanan et al., 2009; Ramnanan and Storey, 2006), while there may also be declines in extra- and intracellular pH, changes in protein phosphorylation status, alterations in patterns of fuel use (lipid becomes the primary fuel) and changes in gene expression (Carey et al., 2003; Pedler et al., 1996; Storey and Storey, 2010; Van Beurden, 1980). Despite these common themes shared by dormant animals, there are numerous important differences between endothermic (e.g. hibernating mammals) and ectothermic (aestivating amphibians) dormancy. Firstly, endotherms undergoing metabolic depression may spend days or weeks with a core T_b that is often near to 0°C. This is followed by spontaneous rewarming against a large thermal gradient during episodic arousals without any external environmental cues (Cannon and Nedergaard, 2004). Another important feature of endothermic dormancy is the brown adipose tissue highly specialised for non-shivering thermogenesis and the elevation of T_b during arousal (Cannon and Nedergaard, 2004). In contrast, metabolic depression in ectotherms can occur at relatively high environmental temperatures, when for most ectotherms, metabolism is positively correlated with ambient temperature (Young et al., 2011).

The physiology of aestivating amphibians

Aestivation is usually defined as a dry season or summer dormancy. The common triggers for aestivation are food and water deprivation associated with arid conditions, which are often (but not always) accompanied by high environmental temperatures. Numerous species of amphibians inhabit arid and semi-arid regions of the world that are subject to sporadic and seasonal rainfall events, and dry periods may last from many months to several years. Such arid-zone amphibians normally avoid exposure to dry conditions and cease

activity throughout these periods because they rapidly lose water via evaporation through the integument. Consequently, aestivation in amphibians typically involves the excavation of a burrow, the adoption of a water-conserving posture, and in some species the formation of an impermeable cocoon around the body (Loveridge and Withers, 1981; Tracy et al., 2007; Withers, 1995). However, little is known about the conditions that cue burrow formation, the timing of emergence, cocoon formation, or microclimates of natural burrows (Seymour, 1973b). Burrow depth varies remarkably between species of aestivating amphibians, although cocoon-forming species appear to excavate shallower burrows than non-cocoon-forming species (Tracy et al., 2007).

The whole-animal metabolism of aestivating frogs is usually suppressed to 20-30% of their normal resting rate, and tends to occur four to five weeks after the onset of aestivation (Kayes et al., 2009a; Withers, 1993). In general, aestivation is considered a 'moderate' type of dormancy, as the physiological changes that occur can be quickly reversed to initiate arousal (Whitwam and Storey, 1990). The suppression of whole-animal metabolic rate in aestivating frogs is accompanied by a reduction in the metabolic rate of skeletal muscle. *In vitro* skeletal muscle preparations have shown metabolic rate to be reduced anywhere between 25-70%, and occur without the manipulation of external factors such as oxygen tension or temperature (Flanigan and Guppy, 1997; Flanigan et al., 1991; Kayes et al., 2009a). This indicates that the mechanisms underpinning metabolic depression are endogenous and must exist within the tissue itself (Flanigan et al., 1991).

The reduction in the metabolic rate of all tissues, but in particular that of muscle, can account for a major proportion of the metabolic depression seen at the whole-animal level in aestivating frogs (Flanigan and Guppy, 1997; Flanigan et al., 1991). This is because muscle mass constitutes a fairly large percentage of whole body mass in anurans. During aestivation the rate of energy expenditure determines the rate of depletion of endogenous fuel stores because there is no external food supply. Seymour (Seymour, 1973a) estimated on theoretical grounds that aestivating spadefoot toads (*Scaphiopus couchii*) could survive at least two years of drought on endogenous fat stores, thereby deferring the onset of starvation.

The reductions in both whole-animal and tissue metabolism during aestivation are also reflected at other levels of biological organisation. Given that mitochondrial function underpins not only cellular but also tissue and whole animal aerobic metabolic rate, a decrease in mitochondrial energy expenditure (oxygen consumption) would result in substantial energy savings during metabolic depression. Indeed, in the green-striped

burrowing frog (*Cyclorana alboguttata*) the rate of skeletal muscle mitochondrial oxygen consumption has been shown to be reduced by more than 80% following seven months of aestivation (Kayes et al., 2009b). Furthermore, aestivating *C. alboguttata* were shown to increase mitochondrial coupling efficiency (i.e. the ratio of ATP synthesis to proton leak) which is likely to be associated with an increase in energy savings (Kayes et al., 2009b). Consistent with the reduction in mitochondrial oxygen consumption, significant decreases in transcription of mitochondrial components including NADH ubiquinone oxidoreductase subunit 1 (71% downregulated) and ATP synthase (67% downregulated) occurred after six months in aestivating muscle (Hudson et al., 2006).

During aestivation it has been demonstrated that reversible protein phosphorylation is an important physiological process to change the activity states of enzymes and functional proteins (Storey and Storey, 2010). In particular, the phosphorylation of pyruvate kinase and phosphofructokinase appears to be important in controlling glycolysis throughout the aestivating period. Using isoelectric focusing, Cowan and Storey (Cowan and Storey, 1999) showed that the proportions of the high and low phosphate forms of these enzymes exhibited distinct kinetic properties in skeletal muscle of aestivating *S. couchii* toads. The quantities of low phosphate pyruvate kinase and phosphofructokinase were elevated during aestivation, while kinetic analysis indicated that these were the less active forms. Two months of aestivation in this species also results in reduced activity levels of enzymes involved in fatty acid synthesis and ketone body metabolism (Cowan et al., 2000). Activity levels of other metabolic enzymes change during aestivation (Mantle et al., 2010), including cytochrome *c* oxidase (CCO), lactate dehydrogenase (LDH) and citrate synthase (CS) which function in the ETC, anaerobic glycolysis and the citric acid cycle, respectively. In 9-month aestivating *C. alboguttata*, LDH and CS activities were significantly lower in both sartorius and iliofibularis muscles, whereas CCO was decreased in the gastrocnemius (Mantle et al., 2010). However, metabolic enzyme activities were maintained at control levels in the cruralis, a powerful muscle involved in jumping. The predominant metabolic substrate in aestivating amphibians is likely to be lipid, with large reserves of triglycerides deposited as ‘fat bodies’ within the abdomen (Van Beurden, 1980).

Because dehydration is a major threat for frogs inhabiting arid environments, frogs possess a sizeable bladder and can utilise their urine volume as a water reserve which can be released during aestivation. Indeed, the metabolic rate of the kidneys in aestivating frogs can increase following months of dormancy (Kayes et al., 2009a). In addition, in many species the

‘waterproof’ cocoon formed from shed skin surrounds the entire body surface except for the narial openings (Figure 1.2A). As the external environment dries, the cocoon becomes a thick, opaque and tough layer consisting of multiple sheets of epidermal cells (Withers, 1995).

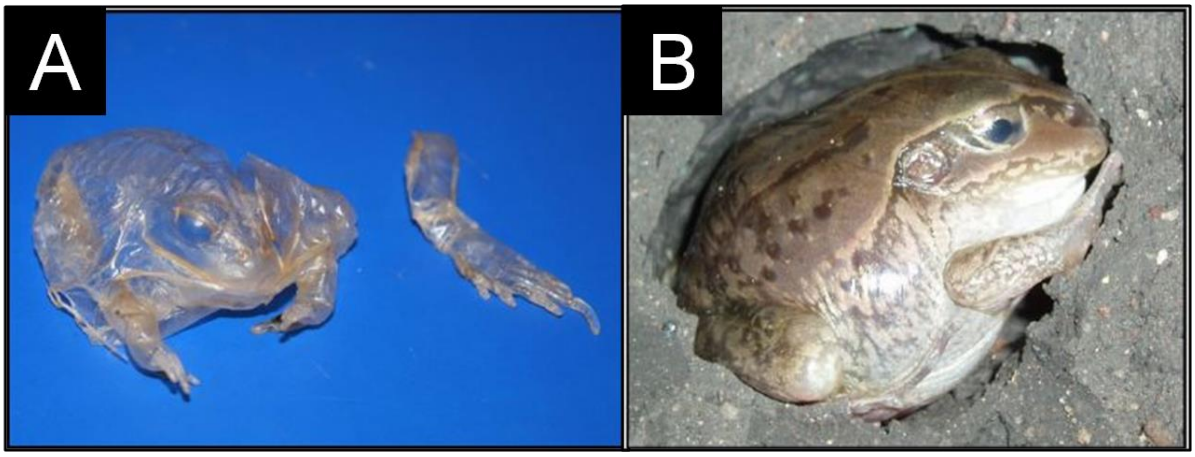

Figure 1.2. The ‘waterproof’ cocoon formed from shed epidermis of *C. alboguttata* after 1 year of aestivation (A) *Cyclorana alboguttata* encased within a clay soil chamber (B). Photographs by Doctor Sara Kayes.

Aestivating frogs as natural muscle disuse systems

The green striped burrowing frog (*Cyclorana alboguttata*) is an abundant species of burrowing frog inhabiting arid to semi-arid regions of Queensland, the Northern Territory and Northern New South Wales. *C. alboguttata* is both nocturnal and fossorial, spending most of its life in aestivation. Aestivating frogs remain inactive in their burrows and are encased within the cocoon for many months, and perhaps years (Figure 1.2B). As a consequence the hindlimb skeletal muscles are rendered immobile; a state which has been likened to the hindlimb casting seen in laboratory muscle disuse models (Hudson and Franklin, 2002b). The structural alterations associated with muscle wasting negatively affect skeletal muscle function and ultimately locomotor performance of the animal. For aestivating/hibernating animals any degenerative changes to skeletal muscle would be disadvantageous during the transition from a dormant to an active state. This is particularly true for aestivating frogs that only have a narrow window of opportunity to feed and breed before the highly ephemeral waters retreat.

The long period of skeletal muscle disuse typical of aestivating *C. alboguttata*, combined with the constricting effect of forming a cocoon, and ability to depress metabolism at relatively high temperatures, makes them one of the most remarkable muscle disuse models

among vertebrates. As a result *C. alboguttata* has become a model organism for studying the effects of aestivation on skeletal muscle and associated physiological processes which may confer resistance to muscle disuse atrophy. In regard to muscle morphology, 6-9 months of aestivation had no effect on muscle mass, water content, or myofibre number in gastrocnemius or cruralis muscles in *C. alboguttata* (Mantle et al., 2009). Similarly, six months of aestivation had no effect on the total cross-sectional area of cruralis muscle (Hudson et al., 2006; Mantle et al., 2009). However, aestivation had different effects on muscle fibre cross-sectional area in distinct muscles, with 6-9 months of aestivation leading to significant reductions in cross-sectional area of both oxidative and glycolytic fibres in cruralis and iliofibularis muscles (Hudson et al., 2006; Mantle et al., 2009; Symonds et al., 2007). Extended immobilisation during aestivation can lead to some atrophy of skeletal muscle in burrowing frogs, although this generally appears to be correlated with muscle locomotor function, with smaller non-jumping muscles (e.g. sartorius, iliofibularis) atrophying before larger jumping muscles (e.g. cruralis, gastrocnemius) (Mantle et al., 2009). The effect of aestivation on the properties of neuromuscular junctions has also been examined in *C. alboguttata*. Hudson et al. (Hudson et al., 2005) found there were no differences in neuromuscular junction structure, miniature endplate potential frequency and amplitude, or resting membrane potentials of iliofibularis fibres following six months of dormancy. Extended limb immobilisation in mammals may lead to loss of capillary tortuosity, resulting in haemorrhaging of skeletal muscle if rapid remobilisation occurs. Hudson and Franklin (Hudson and Franklin, 2003) reported no effect of aestivation on the three-dimensional capillary structure in the semimembranosus muscle of 4-month aestivating *C. alboguttata* compared with active frogs, indicating preservation of capillary tortuosity.

Prolonged aestivation has been shown to cause minimal changes to the *in vitro* skeletal muscle mechanics of burrowing frogs (Hudson and Franklin, 2002a; Hudson et al., 2006; Symonds et al., 2007). The isometric twitch (e.g. force production, rise and relaxation times, and latency period) and tetanic characteristics (maximal force production and tetanic-to-twitch ratio) of aestivating gastrocnemius muscle was shown to be maintained at control levels, despite the muscle disuse associated with extended aestivation (three or nine months) (Hudson and Franklin, 2002a; Hudson et al., 2006). However, following nine months of aestivation twitch activation and relaxation times were substantially slower in iliofibularis muscle when compared with controls (Symonds et al., 2007). Isometric assessment of muscular function has demonstrated that fatigue resistance of the gastrocnemius was

unaffected by three months of aestivation (Hudson and Franklin, 2002a). Indeed, frogs that had recently aroused from aestivation were shown to maintain burst swimming performance at a level similar to that of control frogs (Hudson and Franklin, 2002a). However, after nine months of aestivation a decrease in fatigue resistance of this muscle has been observed (Hudson et al., 2006). Overall, the relative maintenance of skeletal muscle mechanics throughout aestivation is clearly beneficial and allows *C. alboguttata* to rise from their burrows and immediately feed and breed.

Because muscle disuse atrophy in mammalian models has been linked to an accumulation of ROS, it has been proposed that hibernators and aestivators might regulate endogenous antioxidant levels in skeletal muscle as a potential means of inhibiting muscle wasting (Hudson and Franklin, 2002b). Consistent with this hypothesis is the finding that levels of antioxidants (catalase and glutathione peroxidase 4) were maintained at control levels in aestivating muscle of *C. alboguttata*, whilst the total antioxidant capacity increases (when standardised to the oxygen consumption rate of the animal or tissue) (Hudson et al., 2006; Mantle et al., 2009; Young et al., 2013). There is some evidence that oxidative damage occurs in muscle during aestivation, but this appears to be confined to the iliofibularis muscle (Young et al., 2013). The modulation of antioxidants is unlikely to constitute the entire 'strategy' by which *C. alboguttata* inhibits muscle disuse atrophy because other mechanisms (e.g. protein turnover), as yet not measured in this species, are probably regulated. For example, recent studies have emphasised the importance of maintaining protein synthesis in hibernating muscle via activation of the mammalian target of rapamycin (mTOR) signalling cascade (e.g. Andres-Mateos et al., 2013; Fedorov et al., 2014; Lee et al., 2010; Nowell et al., 2011). The mTOR is a major effector of cell growth and proliferation via the regulation of protein synthesis through a multitude of downstream targets. *S. lateralis* squirrels decrease myostatin expression (an mTOR inhibitor) in skeletal muscles that are resistant to winter atrophy, potentially facilitating mTOR signalling by suppressing this inhibition (Nowell et al., 2011), while periodic arousals from winter hibernation in bats appears to be associated with oscillations in the activation of mTOR (Lee et al., 2010).

The induction of heat shock proteins may also play an important role in countering muscle wasting during hibernation and aestivation (Lee et al., 2008; Young et al., 2013), especially given that heat shock protein overexpression improves structural and functional recovery of skeletal muscle following immobilisation-induced atrophy in mice (Miyabara et al., 2012). Despite such advances in understanding the biochemical regulation associated with

dormancy, overall little is known about the modulation of cell mechanisms (e.g. gene/protein expression changes) that could be responsible for inhibition of skeletal muscle atrophy and dysfunction following prolonged periods of inactivity in aestivating frogs. Preservation of muscle performance is paramount for reproductive success and survival upon arousal in dormant animals. Studying skeletal muscle adaptation in *C. alboguttata* will lead to a better understanding of both the common principles and the diversity of mechanisms that facilitate inhibition of muscle disuse atrophy in different hypometabolic systems. In addition, furthering our understanding of the regulation of muscle function that occurs in aestivating *C. alboguttata* may one day offer significant insights for understanding muscle disuse atrophy in other systems.

Aims of research

The aim of this study was to examine the cellular and molecular mechanisms that may inhibit muscle disuse atrophy in *C. alboguttata*. Specifically, the first aim of this study was to examine the effect of 4-months of aestivation (disuse) on global gene expression changes in skeletal muscle using next generation sequencing (RNA-Seq; Chapter 2). RNA-Seq is a relatively new technology that has a number of significant advantages in gene expression profiling experiments. For example, RNA-Seq does not require species- or transcript-specific probes, and is thus highly suitable for studies on non-model animals such as aestivating frogs. RNA Seq enables unbiased detection of novel transcripts and other changes, such as single nucleotide polymorphisms, while also offering a broader dynamic range by quantifying discrete, digital sequencing read counts. Additionally, deep sequencing coverage can allow detection of rare transcripts or weakly expressed genes. By measuring the expression levels of thousands of genes simultaneously, RNA-Seq could provide insights into novel functional pathways and regulatory mechanisms involved in muscle remodelling in aestivating *C. alboguttata*.

The modulation of ROS and antioxidants are important for cell homeostasis. In addition to generating ATP, mitochondria are also a major site of ROS production in cells. It follows then that mitochondrial metabolic suppression might have consequences for mitochondrial ROS production and oxidative stress. Suppression of mitochondrial respiration is a prominent feature of hibernating mammals and amphibians, and aestivating frogs. To date however, little work has been conducted to understand how changes in oxidative phosphorylation affect mitochondrial ROS production, particularly alterations resulting from

natural effectors, such as metabolic depression. This is because measurements of ROS themselves are usually not without significant analytical challenges, let alone simultaneous evaluations of changes in ROS production and oxidative phosphorylation. Consequently, most studies have concentrated on measurements of antioxidant levels and/or the severity of oxidative damage. The second aim of this study was to measure ROS production and mitochondrial respiration simultaneously in skeletal and cardiac muscles of *C. alboguttata*.

While protein turnover is substantially suppressed during metabolic depression, the mechanisms that reduce protein synthesis and degradation, and their relationship with regulation of muscle mass during dormancy are not entirely clear. The aim of the third experiment (Chapter 4) was to determine if downregulation of the calpain proteolytic pathway might contribute to inhibition of muscle disuse atrophy in 4-month aestivating *C. alboguttata*. This was achieved by measuring the enzyme activity, protein abundance and gene expression levels of calpain isoforms in gastrocnemius muscle of aestivating and control *C. alboguttata*.

The final chapter of this thesis (Chapter 5) concludes by integrating the data collected throughout all experimental chapters and broadly discussing the mechanisms and cellular pathways that may regulate muscle integrity during metabolic depression. Chapter 5 also raises important questions generated as a result of the current study and specific areas where future research should focus, and concludes with a discussion about how aestivating *C. alboguttata* may be utilised as a model organism in biomedical research.

Structure of thesis

This thesis is comprised of three experimental chapters, a general introduction and a general discussion. These chapters have been written in the format of papers which have been published in leading international journals. The first experimental chapter uses RNA Seq technology to generate a burrowing frog skeletal muscle transcriptome, and conduct comparative gene expression profiling between active and four-month aestivating *C. alboguttata*. The second experimental chapter investigates mitochondrial respiration and ROS production within permeabilised cardiac and skeletal muscle fibres of 4-month aestivating *C. alboguttata*. The third experimental chapter examines the potential of the calpain proteolytic pathway in modulating muscle protein degradation during aestivation. The final chapter of this thesis concludes by discussing the cellular mechanisms by which *C. alboguttata* may regulate skeletal muscle homeostasis during aestivation, and future directions for research.

Chapter 2

Frogs and aestivation: transcriptional insights into metabolism and cell survival in a natural model of extended muscle disuse

INTRODUCTION

Under adverse environmental conditions many organisms enter dormancy, a period of inactivity that prolongs the amount of time an animal can survive on endogenous fuel reserves. Dormancy involves strong suppression of both locomotor activity and metabolic rate, and is a common factor of various survival strategies including hibernation, torpor, anhydrobiosis and diapause (Storey and Storey, 1990). Under circumstances of food and water deprivation associated with xeric conditions, numerous animals (invertebrates, fish, frogs, reptiles) become dormant by entering into a metabolically depressed state known as aestivation. Whole animal metabolism during aestivation may be depressed by as much as 80% and can sustain viability for an entire dry season, if not years (Kayes et al., 2009a; Van Beurden, 1980).

Despite the adaptive value of the dormant phenotype, dormancy in vertebrates may expose cells to diverse stressors, including fluctuations in temperature or oxygen levels, acidosis and oxidative damage (van Breukelen et al., 2010). Moreover, because dormancy entails prolonged periods of inactivity and fasting, an expected outcome arising from organ and tissue disuse is cellular atrophy and the potential for compromised performance upon arousal. In typical models (humans, mice, rats), prolonged inactivity or immobilisation of skeletal muscle (e.g. cast immobilisation or extended bed-rest) results in muscle disuse atrophy, a condition which is characterized by the 'wasting' or loss of muscle mass and strength (Bloomfield, 1997). Such losses can often be accompanied by accelerated apoptosis (Marzetti et al., 2010), a genetically-programmed form of cell death that may be initiated by cell death receptors or via mitochondrial pathways (Rossi and Gaidano, 2003). In muscle tissue apoptosis may contribute to atrophy by leading to loss of myofibres (hypoplasia) or loss of myofibre segments (hypotrophy), and is likely to be related to dysfunction of mitochondria (Marzetti et al., 2010).

Research on muscle disuse atrophy has primarily focused on mammals, and the deleterious effects of atrophy appear to be common to most species studied (Hudson and Franklin, 2002b). However, recent investigations have examined the structure, function and plasticity of muscles in organisms that experience natural periods of muscle disuse or

immobilisation, such as aestivating frogs and hibernating mammals (Cotton and Harlow, 2010; Harlow et al., 2001; Hudson and Franklin, 2002a; Mantle et al., 2009; Nowell et al., 2011; Symonds et al., 2007; Young et al., 2011). These studies have shown that animals which undertake extended bouts of natural immobility (i.e. dormancy) consistently demonstrate less of an atrophic response than that experienced by the usual mammalian models immobilised for considerably less time. Dormancy is characterized by a complex suite of highly coordinated biochemical changes, however very little is known about the physiological or molecular underpinnings of processes to mitigate atrophy or apoptosis in dormant animals such as mammalian hibernators and aestivating frogs.

The green-striped burrowing frog (*Cyclorana alboguttata*) is found in hot, arid regions of eastern Australia and spends the majority of its life in aestivation. Studies have shown that throughout aestivation, burrowing frogs experience extended periods (up to 9 months) of inactivity and fasting without suffering any substantial skeletal muscle atrophy and are able to resume locomotor ability immediately upon arousal, indicating preservation of muscle functional capacity throughout the aestivation period (Hudson and Franklin, 2002a; Hudson et al., 2006; Mantle et al., 2009; Symonds et al., 2007). Thus, *C. alboguttata* is an intriguing model for investigating the physiological and molecular mechanisms underlying metabolic suppression, atrophy and apoptosis. The preservation of muscle in *C. alboguttata* is likely to be a complicated process involving multiple cellular pathways operating in parallel to mediate inhibition of muscle wastage. Such complexity requires a more global approach to investigating the biochemical changes that occur throughout aestivation to maintain cell viability.

The development of high throughput sequencing technologies has enabled the rapid generation of large-scale sequencing data at a level which was previously unfeasible. High throughput RNA sequencing (RNA Seq; sequencing of steady-state RNA in a sample) has proven to be an invaluable tool used in a variety of applications in non-model organisms that lack existing genomic information, for example transcriptome characterisation, gene expression profiling and detection of allele-specific expression (Ekblom and Galindo, 2011). The aim of this study was to use RNA Seq technology to generate a burrowing frog skeletal muscle transcriptome, and conduct comparative expression profiling between active and four-month aestivating *C. alboguttata* to gain insight into genes and pathways underlying the aestivating phenotype. In particular, we were interested in transcriptional pathways which may mediate inhibition of muscle atrophy in *C. alboguttata*.

MATERIALS AND METHODS

Experimental animals

Green-striped burrowing frogs, *Cyclorana alboguttata* (13-44 g body mass) were collected from the districts of Dalby and Theodore, Queensland, Australia (Scientific Purposes Permit WISP10060511). Frogs were transported back to the laboratory and were kept in plastic containers with wet paper towels and fed weekly on crickets. Frogs were randomly assigned to one of two treatment groups (4-month aestivators and controls) and all animals were fed six days before commencing the experiment. During experimentation control frogs were maintained under a 12:12 h light: dark regime to simulate conditions of active, awake frogs, whereas aestivating frogs were kept in 24 h darkness. All experiments were conducted with the approval of the University of Queensland Animal Ethics Committee (permit number: SBS/238/11/ARC).

Whole animal metabolic rate

Respirometry was conducted to verify metabolic depression during aestivation in burrowing frogs. Frogs required to aestivate were placed into 500 mL glass respirometry chambers with wet paper pellets (Breeders Choice Cat Litter, FibreCycle Pty Ltd, Yatala, Australia) and the water allowed to slowly dry out. Frogs rapidly burrowed into the paper and entered into aestivation. While aestivators remained in their chambers for the entire experimental period, control animals were weighed and placed into their chambers 24 h prior to sampling and removed immediately following final oxygen consumption measurements. Control frogs were then fed and placed into a 12:12 h light:dark regime. Respirometry chambers (both control and aestivating frogs) were kept in a dark, constant temperature (24.3 ± 0.2°C) room during the experimental period. During non-sampling periods chambers were covered with mesh to allow air flow. Rates of oxygen consumption ($\dot{V}O_2$) were measured using closed-system respirometry in frogs from each treatment group (controls N = 10; aestivators N = 9). At the start of a sampling period chambers were sealed with a rubber bung and a fiber optic oxygen transmitter with oxygen-sensitive spots (Precision Sensing GmbH, Regensburg, Germany) was used to measure the partial pressure of oxygen (as a percentage of air saturation) within the chamber. This method allows oxygen partial pressures to be measured non-invasively through the wall of the respirometer. Oxygen measurements were taken several hours later, depending on the treatment group (i.e. longer for aestivators), and on multiple occasions to calculate repeated rates of oxygen consumption. The lowest rate in

the analysis was used before oxygen consumption and CO_2 production were determined according to the formula of Vleck (Vleck, 1987).

Muscle sampling and morphometrics

In the current study the gastrocnemius muscle was selected for analysis because in anurans this muscle produces the force necessary for jumping. After four months of aestivation, frogs were removed from their chambers and immediately euthanized by cranial and spinal pithing. Control frogs were fasted for 5 days before euthanasia. Body mass and snout-vent length (SVL) were measured. The right gastrocnemius muscle was then rapidly excised, weighed and placed immediately into RNA*later*® (Ambion). Tissue samples were stored at 4°C overnight and then transferred to -80°C until processed. The contralateral gastrocnemius muscle was pinned to a small piece of dental wax while it was still attached to the bone to maintain muscle length. Once pinned, the muscle was then separated from the bone, weighed and placed into 10% neutral-buffered formalin (NBF) and kept at 4°C for subsequent morphometric analysis. Fixed gastrocnemius muscles were removed from NBF and cross-sectional slices of approximately 3-5 mm were taken from the midsection. Specimens were mounted in embedding medium (Tissue-Tek® OCT™ Compound, ProSciTech), frozen in isopentane cooled to the temperature of liquid nitrogen, and stored dry at -80°C for later sectioning. Frozen muscle blocks were sectioned into 16 µm thick slices with a Leica 3050n cryostat at - 20°C. The sections were melted onto glass slides and air dried before sections were viewed with an Olympus SZ61 stereomicroscope and images were captured with a Micropublisher 3.3 Real-Time Viewing camera (QImaging). For each animal, two cross-sections were selected and images were analyzed with SigmaScan (SPSS Inc.) to determine whole muscle cross-sectional area.

Total RNA isolation

Total RNA was isolated from approximately 80-100 mg of preserved gastrocnemius muscle tissue. Muscle samples were thawed in 1 mL of PureZOL (BioRad) and homogenized with stainless steel beads using a TissueLyser II (Qiagen). The homogenates were centrifuged at 12 000 *g*, at 4°C for 10 min to remove any insoluble cell debris. Cell lysates were combined with chloroform and centrifuged (12000 *g*, 4°C, 15 min) to separate aqueous and organic phases. The aqueous phase containing RNA was then isolated using a PureLink® RNA Mini Kit (Life Technologies). An on-column PureLink® DNase treatment protocol (Life Technologies) was conducted to obtain DNA-free total RNA before RNA quality assessment was performed using a RNA 6000 Nano Kit (Agilent Technologies) on an Agilent

Bioanalyser. Total RNA from eight male frogs (controls *N*=4; aestivators *N*=4; 13-26 g body mass) were prepared for subsequent high-throughput sequencing; all RNA samples had an RNA integrity number ≥ 8.5.

mRNA library preparation and Illumina sequencing

The following poly(A)+ selection, mRNA library construction, cluster generation and sequencing was conducted by Macrogen Inc., Seoul, Korea. RNA samples were prepared for sequencing using a TruSeq RNA Sample Preparation Kit (Illumina) according to the manufacturer's instructions. mRNA was purified from total RNA by way of poly (A)+ selection before samples were fragmented and reverse transcribed to cDNA using random hexamer priming. Following fragment end-repair, individual frog cDNA libraries were tagged by ligation of unique indexing adapters to cDNA ends in preparation for hybridization onto a flow cell. PCR was then used to enrich for adapter-containing cDNAs followed by quality control analysis of each sample library and quantification of the DNA library templates. Prior to sequencing, DNA templates were bridge-amplified to produce clonal clusters on the surface of the flow cell. Sequencing was then carried out using an Illumina HiSeq 2000.

Bioinformatics

De novo *assembly, annotation and RNA Seq*

To reconstruct *C. albogutatta* contiguous nucleotide sequences (contigs), paired-end reads up to 100 bp in length were assembled and aligned using CLC Genomics Workbench 5 (CLC Bio, Aarhus, Denmark). CLC Bio's *de novo* assembly algorithm works by using De Bruijn graphs. The minimum acceptable contig length was 200 bp, and scaffolding was performed by using paired-end read-information to ascertain both distances between, and orientation of the contigs. The contigs were then searched against the non-redundant NCBI protein database (BLASTx) with an expectation value of 0.001 using Blast2GO (B2G) (Conesa et al., 2005). B2G was then used to retrieve associated gene ontology (GO) terms describing biological processes, molecular functions, and cellular components. The following criteria were adopted when reads were mapped back against the *C. alboguttata* reference transcriptome, 1) at least 90% of a given read was required to have at least 80% identity with the reference in order to be included in the final mapping; and 2) up to 10 alignments to the reference were allowed for a given read.

Identifying differential gene expression

Putative transcripts from control (N = 4) and aestivating (N = 4) frog gastrocnemius samples were tested for differential expression using the Bioconductor (http://www.bioconductor.org/) package EdgeR (Robinson et al., 2010). EdgeR fits a negative binomial model to read count data and uses empirical Bayes methods to moderate the degree of overdispersion (i.e. large variability) across genes, which is typical of RNA Seq read counts. Furthermore, EdgeR uses a normalisation method (trimmed mean of M-values, see reference (Robinson and Oshlack, 2010)) which estimates scaling factors between libraries before being incorporated directly into the model used to test for differential expression. In the present study, genes with very low counts were removed before testing for changes in gene expression. Genes were retained only if they were expressed in at least one control or aestivating frog, and if they attained one count per million for at least four individual libraries. Following library normalisation and dispersion estimates of genes, exact tests were conducted to calculate differences in the means of each gene between control and aestivating frogs. Genes were selected for further analysis if they met a minimum fold change threshold of 1.5 on a log2 scale. The significance threshold was set at $P \leq 0.05$, and Benjamini and Hochberg's algorithm (Benjamini and Hochberg, 1995) was used to control the false discovery rate (< 0.05).

Ingenuity pathways analysis

To perform gene functional analysis differentially expressed *C. alboguttata* genes were analysed using Ingenuity Pathways Analysis (IPA) software (Ingenuity Systems, http://www.ingenuity.com). IPA uses a human-curated knowledge base to analyse expression data in the framework of known biological response pathways and regulatory networks. IPA analysis was used to identify canonical pathways and molecular/cellular functions that were most significantly overrepresented for the entire set of differentially expressed *C. alboguttata* genes, and also separately among the up- and downregulated genes. For all analyses, statistical significance of gene/pathway groups was determined using a Fisher's exact test.

Statistical analysis of whole animal metabolic rate and muscle data

A one-way covariance analysis (ANCOVA) was used with SVL as the covariate to examine the effect of aestivation on muscle mass and muscle cross-sectional area. Oxygen consumption and whole body mass were analysed using one-way ANOVA. All data were assessed for normality and constancy of variance and log transformed where appropriate.

RESULTS

Whole animal metabolic rate and muscle size

At the end of the 4-month treatment period, the mean rate of oxygen consumption ($\dot{V}O_2$) of control frogs was 57.3 $\mu l\ O_2 \cdot g^{-1} \cdot h^{-1}$ whereas in aestivating animals the mean $\dot{V}O_2$ was significantly lower at 17.2 $\mu l\ O_2 \cdot g^{-1} \cdot h^{-1}$ ($P<0.001$; Table 2.1). Thus, immediately prior to muscle tissue sampling, the $\dot{V}O_2$ of aestivating *C. alboguttata* was depressed by approximately 70% relative to control animals. Aestivation resulted in a decrease in whole body mass, by approximately 27% ($P<0.01$; Table 2.1). The wet mass of gastrocnemius muscle from aestivating frogs (mean = 244.9 mg; SD = 59.5) was approximately 23% less that of control animals (mean = 317.2 mg; SD = 109.5), although the effect of aestivation on gastrocnemius wet mass was not significant once adjusted for the difference in snout-vent length (SVL) between the groups (ANCOVA: full model, $P = 0.15$; treatment, $P = 0.78$; relationship to SVL, $P<0.001$). Similarly, whole cross-sectional area of gastrocnemius muscle was less in aestivators (~ 35%; mean = 14.8 mm^2; SD = 4.1) relative to controls (mean = 22.8 mm^2; SD = 5.8), but was not significant after accounting for SVL (ANCOVA: full model, $P = 0.92$; treatment, $P = 0.70$; relationship to SVL, $P<0.001$).

Table 2.1. Whole animal metabolic rates and body masses for control and four-month aestivating *Cyclorana alboguttata*

	$\dot{V}O_2$ ($\mu l\ O_2 \bullet g^{-1} \bullet h^{-1}$)	Body mass (g)	
		Initial	Final
Control	57.3 ± 38.0 (10)	22.6 ± 7.8 (10)	22.3 ± 7.0 (10)
Aestivation	17.2 ± 2.8 (9)*	23.2 ± 3.3 (9)	17.0 ± 3.6 (9)†

Values represent means ± SD; numbers in parentheses represent number of animals. *p= <0.001, significant difference between control and aestivating animals. †p= <0.01, significantly different from initial body mass.

Table 2.2. Summary of *Cyclorana alboguttata* transcriptome assembly

Total number of reads	400,032,568
Total number of contigs	68,947
Maximum contig length	37,233
Average contig length	861
N50	1,586
Total number of bases	59,345,855

De novo assembly and annotation

Eight separate cDNA libraries were generated from gastrocnemius muscle of male frogs. These libraries were tagged and sequenced simultaneously on a single lane of a flow cell by Illumina HiSeq technology to produce approximately 400 million reads (available at NCBI Sequence Read Archive (SRA) under Accession SRA061647, Bioproject: PRJNA177363). Sequenced samples from both control and aestivating frogs were used in the *de novo* transcriptome assembly to maximize representation of expressed genes. A summary of the *de novo* assembly is presented in Table 2.2. There was a large range in contig size and as expected, the overall quantity of contigs decreased with increasing contig length (Figure 2.1). The *C. alboguttata* contigs were annotated by searching the NCBI non-redundant protein databases using BLASTx. Approximately 33%, or 22,695 of the 68,947 total constructed contigs were related to proteins in NCBI's non-redundant database with an E value of $<1e^{-3}$.

Taxa with the most matches were the Western clawed frog (*Silurana tropicalis*) and African clawed frog (*Xenopus laevis*) (12,162 and 3,531 matches, respectively) where matches correspond to the BLAST top hit for each sequence (Figure 2.2A). The majority of the contigs showed ≥50% similarity with each sequences' respective closest BLAST match (Figure 2.2B). The functional classification based on biological process, molecular function and cellular component is shown in Figure 2.3. Among the biological process GO terms, a significant percentage of genes were categorized into cellular (23.5%) and metabolic (18.8%) processes, whereas many genes were assigned to protein binding (29.6%) and ion binding (18.0%) for the molecular functions class. Cell part (35.8%) and membrane-bounded organelle (21.8%) represented a large proportion of cellular components.

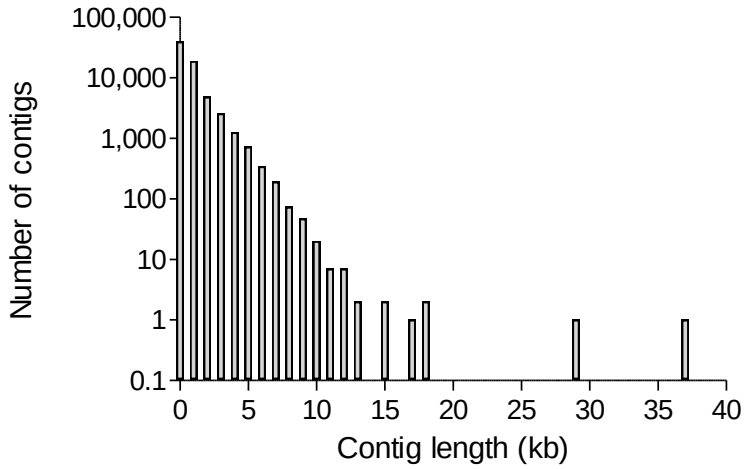

Figure 2.1. Summary of the lengths of *Cyclorana alboguttata* skeletal muscle contiguous nucleotide sequences (contigs). *De novo* assembly of RNA-seq data using CLC Genomics Workbench generated contigs between 200 and 37 250 bp in length.

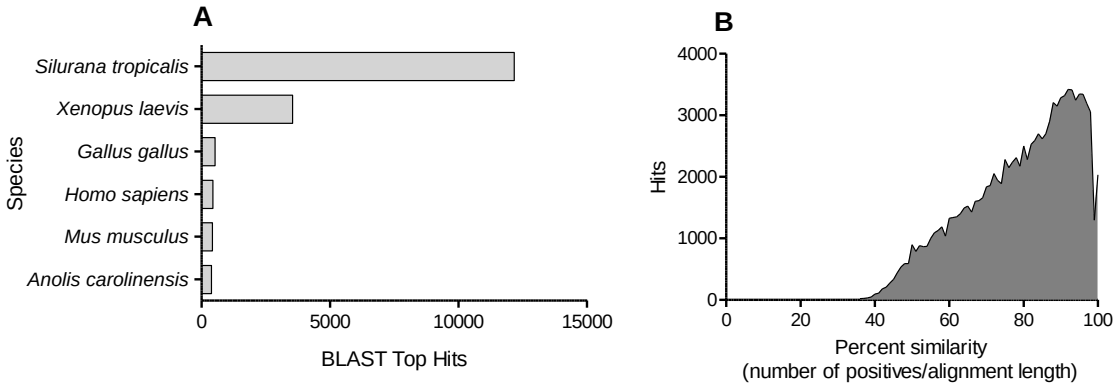

Figure 2.2. Summary of BLAST hit species distribution and similarity of *C. alboguttata* contigs using a cutoff E-value $<1e^{-3}$ *A*: *Silurana tropicalis* and *Xenopus laevis*, the two best-annotated amphibians, exhibited the most matches against *C. alboguttata* contigs, where matches correspond to the BLAST top hit for each sequence. *B*: summary of the percent sequence similarity of *C. alboguttata* contigs with NCBI nr protein database.

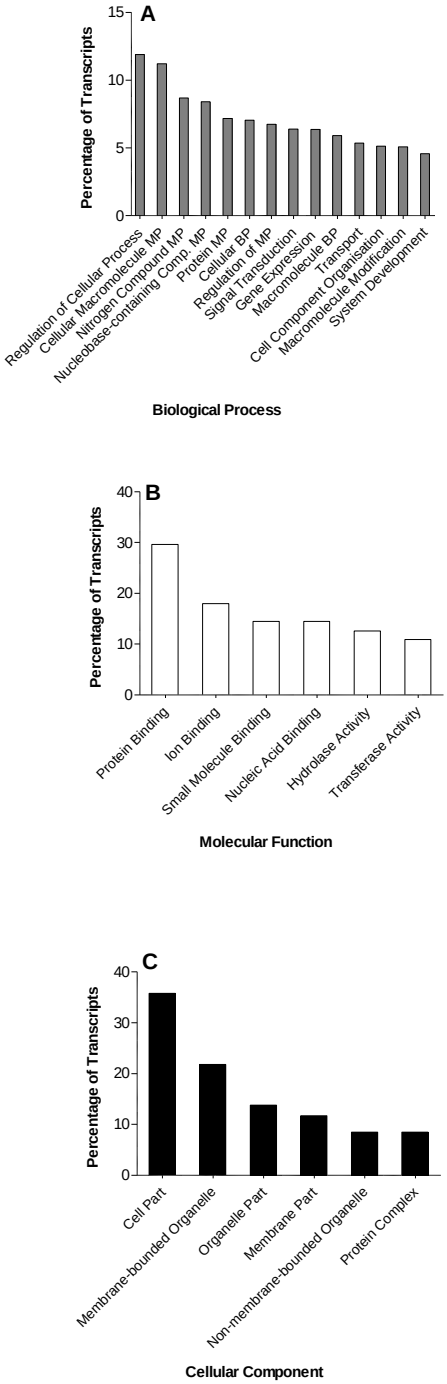

Figure 2.3. Distribution of the GO categories assigned to the *C. alboguttata* skeletal muscle transcriptome. The data from InterPro terms and enzyme classification codes were merged with GO terms using Blast2GO software. 22, 695 sequences were annotated into three categories: biological process *(GO level 4) (A)*, molecular functions *(GO level 3) (B)* and cellular components *(GO level 3) (C)*. MP, metabolic process; BP, biosynthetic process; Comp., compound.

RNA Seq Analysis and Differential Gene Expression

We used the CLC Genomics Workbench RNA Seq tool to map the short sequence reads to our *C. alboguttata* reference transcriptome assembly. Fifty-four percent of reads from control animals mapped back to the *C. alboguttata* reference transcriptome. In the aestivating frogs, 62% of reads mapped onto the reference transcriptome. Across all samples the mean percentage of reads that mapped non-uniquely was less than 0.2%. We compared expression patterns of the annotated contigs (genes) between 4-month aestivating frogs (N = 4) with those of control animals (N = 4).

Before conducting exact tests, read counts were normalised using scaling factors for the different library sizes in edgeR. Following normalisation, count distributions for the 8 libraries were similar in composition (Figure 2.4). With a false discovery rate-adjusted p-value of 0.05, we found that the expression levels of 533 genes changed significantly between aestivating and control frogs, the majority of which were downregulated in aestivators (342 genes). More than half (54%) of all the differentially-expressed genes demonstrated expression changes exceeding fourfold. When considering both p-value and fold change, the gene most upregulated in aestivating frogs was a sodium-dependent nucleoside cotransporter (*slc28a3*-like), which plays a role in maintaining cellular nucleoside homeostasis (increased 150-fold; p = 2.9E-23). Muscle-specific enolase (*eno3*), which functions in glycolysis and also muscle development, was the gene most downregulated (~ 200-fold; p = 3.8E-19). The full set of differentially expressed genes is provided in Supplemental Table S1 (http://physiolgenomics.physiology.org/content/45/10/377.figures-only).

To gain insight into the signalling pathways and molecular functions that may be activated/deactivated in skeletal muscle of *C. alboguttata* during aestivation, we used IPA to perform functional analysis of genes that were differentially expressed during aestivation as determined by EdgeR. Analysis of the entire set of these genes showed that the most significantly overrepresented canonical pathways were glycolysis/gluconeogenesis, adherens junction signalling and remodelling, and nuclear factor E2-related factor 2 (NRF2)- mediated oxidative stress response (Figure 2.5). A subset of these genes is presented in Table 2.3, and several of these have previously been shown to be differentially regulated during muscle remodelling. Skeletal muscle exhibits highly specialized subsarcolemmal adherens junctions, such as myotendinous and neuromuscular junctions, and also costameres which couple myofibrils with the sarcolemma. Genes coding for the muscle contractile proteins actin and myosin were suppressed during aestivation, as were vinculin and alpha actinin which bind to

and cross-link with actin filaments. In contrast, components of the microtubule cytoskeleton (tubulin isoforms) were upregulated. Nrf2 is a transcription factor which binds to the antioxidant response element to initiate transcription of target genes involved in antioxidant defence systems, including superoxide dismutase, catalase, peroxiredoxins, and genes participating in glutathione synthesis and function (Hur and Gray, 2011). Several genes associated with the Nrf2 oxidative stress response were induced in aestivating muscle, including MafK transcription factor and kelch-like ECH-associated protein 1, both of which directly interact with Nrf2 (Table 2.3). The regulatory subunit of glutamate cysteine ligase, glutathione S-transferase omega 2, peroxiredoxin 1, DnaJ/heat shock protein 40, transitional endoplasmic reticulum ATPase and ferritin showed increased expression. However, glutathione S-transferase P1 and another DnaJ/heat shock protein 40 (subfamily B, member 5) were found to be suppressed.

When IPA was used to solely analyse all the downregulated genes (Figure 2.6) the molecular functions significantly overrepresented during aestivation were amino acid metabolism, small molecule biochemistry, carbohydrate metabolism and lipid metabolism. Given the overrepresentation of the energy metabolism categories, all energy metabolism genes that were identified by IPA are shown in Table 2.4. Although not detected by IPA, we also identified two genes that were downregulated in aestivating muscle and are known to be involved in myogenesis and muscle growth. These were insulin-like growth factor binding protein-like 1 (*igfbpl1*) and myostatin (also known as growth-differentiation factor 8; *mstn*) (Table 2.4).

Among the upregulated genes detected using IPA (Figure 2.6) nucleic acid metabolism, small molecule biochemistry, cell death and survival and DNA replication, recombination and repair were found to be overrepresented. A summary of the genes implicated in these processes have been provided in Table 2.5. Genes associated with pro-apoptotic signalling included tumor necrosis factor receptor superfamily member 6 precursor (also known as Fas receptor; *fas*), ras association (RalGDS/AF-6) domain family member 1 (*rassf1*), apoptosis-inducing factor 2 (*aifm2*) and apoptosis-enhancing nuclease (*aen*). There was elevated expression of genes with cytoprotective functions, such as vesicular over-expressed in cancer prosurvival protein 1 (*vopp1*), survivin **(***birc5.2-b*), heat shock 70 kDa protein 5 (*hspa5*; aka 78 kDa glucose-regulated protein), heat shock protein 90kDa beta member 1 (*hsp90ab1*; 94 kDa glucose-regulated protein) and small heat shock protein (family B) member 11 (*hspb11*). Serine/threonine protein kinase Chk1 (*chek1*), which is chiefly

responsible for cell cycle arrest in response to DNA damage or replication stress, and *Cdk2*, another gene critical in controlling the cell cycle, were upregulated during aestivation. Also of interest was the increased expression of genes coding for DNA repair proteins, tonsoku-like protein (*tonsl*), DNA mismatch repair protein MSH6 (*msh6*), nei endonuclease VIII-like 3 (*neil3*), and genes that play a role in remodelling of chromatin (*rbbp4*; *smarca4*; *smarca5*).

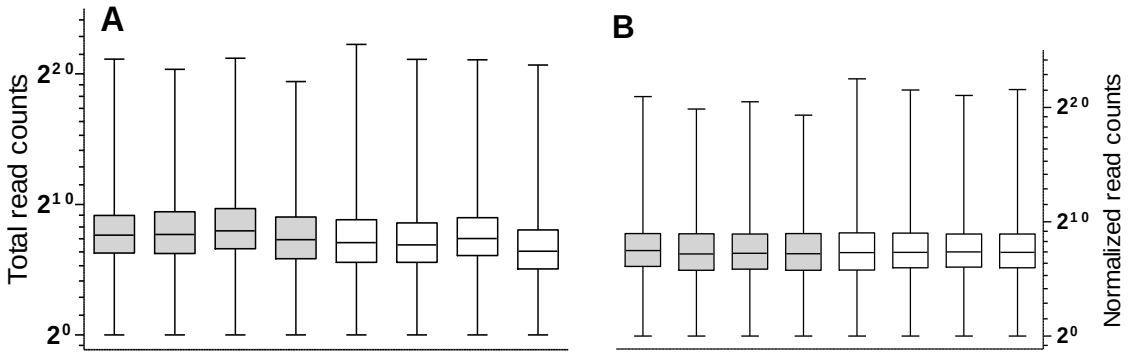

Figure 2.4. Boxplots of the number of RNA Seq reads obtained from each *C. alboguttata* cDNA library. *A:* The raw total number of read counts (on a log2 scale) before normalisation; *B:* number of read counts (on a log2 scale) following TMM normalisation in EdgeR. Shaded boxes are aestivating animals whereas open boxes represent control frogs.

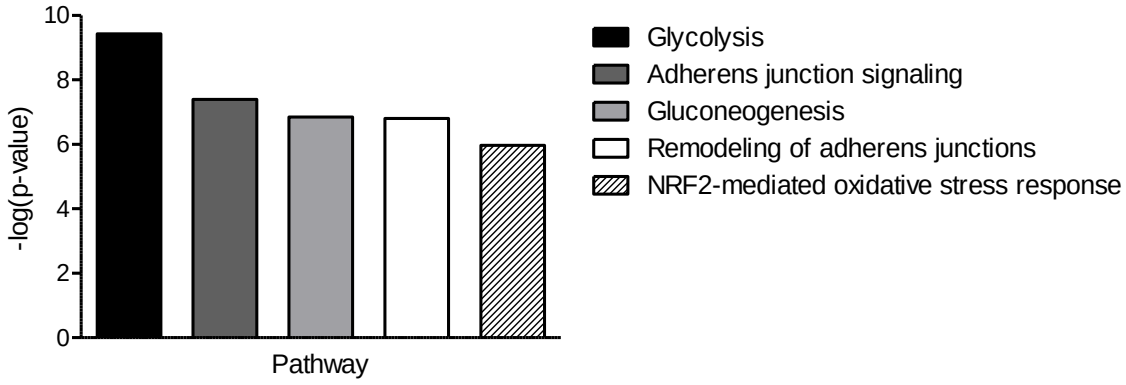

Figure 2.5. Canonical pathways found to be overrepresented in skeletal muscle in aestivating *C. alboguttata* as determined by Ingenuity Pathways Analysis (IPA). The y axis represents the –log of the *P* value given during the analysis; thus, larger values equate to more significant regulation of a pathway.

Table 2.3. Log2 fold-changes of differentially expressed genes associated with adherens junction signalling and remodelling, and the Nrf2-mediated oxidative stress response in gastrocnemius muscle of burrowing frogs (*C. alboguttata*).

	Symbol	Top Hit Accession No.	% Similarity	*P* value	Log2 fold change
Adherens junction signalling					
Actin, alpha cardiac muscle 1-like isoform 2	LOC100566451	XP_003228734	99	3.0E-07	-4.3
Actin, aortic smooth muscle isoform 2	*acta2*	XP_003363513	100	1.9E-06	-4.2
Alpha-muscle actin, partial	*actc1*	AAA29846	100	1.3E-06	-3.8
Beta-actin, partial	*actb*	ABK88258	97	7.6E-06	-2.8
Myosin heavy chain IIa	*myh3*	NP_001006915	94	1.0E-06	-5.1
Myosin 4-like	LOC100492956	XP_002937039	92	6.5E-07	-5.0
Myosin, light chain 1, alkali; skeletal, fast	*myl1*	NP_988954	98	1.4E-05	-3.7
Actinin, alpha 2	*actn2*	NP_001005053	96	6.3E-05	-2.1
Actinin, alpha 3	*actn3*	NP_001135513	98	6.1E-06	-2.7
Vinculin	*vcl*	Q04615	92	9.6E-04	-2.0
Tubulin alpha-1C chain-like, partial	LOC100701978	XP_003460440	100	3.7E-05	2.4
Tubulin subunit alpha	LOC100135051	AAW30622	100	5.8E-06	2.4
Tubulin beta-5 chain	*tubb6*	NP_001026183	99	2.3E-03	1.9
Nrf2 oxidative stress response					
Transcription factor MafK-like	LOC100488557	XP_002934281	97	1.6E-03	1.5
Kelch-like ECH-associated protein 1a	*keap1a*	NP_878284	78	4.9E-04	2.1
Glutamate-cysteine ligase regulatory subunit	*gclm*	ACO52032	89	1.2E-04	2.0
Glutathione S-transferase omega 2	*gsto2*	NP_001005086	77	5.0E-04	1.9
Similar to peroxiredoxin 1	*srxn1*	XP_002193267	88	4.2E-04	1.9

DnaJ (Hsp40) homolog, subfamily A, member 4, gene 1	*dnaja4.1*	NP_001072848	89	1.7E-04	2.3
Ferritin, heavy polypeptide 1	*fth1*	NP_989008	87	1.4E-05	2.9
Transitional endoplasmic reticulum ATPase	*vcp*	NP_001005677	99	2.8E-05	2.2
Glutathione S-transferase P 1	*gstp1*	P81942	91	1.0E-03	-1.7
DnaJ (Hsp40) homolog, subfamily B, member 5	*dnajb5*	NP_001088287	95	1.4E-03	-1.6

Negative fold changes indicate downregulation of genes in frogs aestivating for 4-month relative to controls, whereas positive fold changes indicate upregulation of genes.

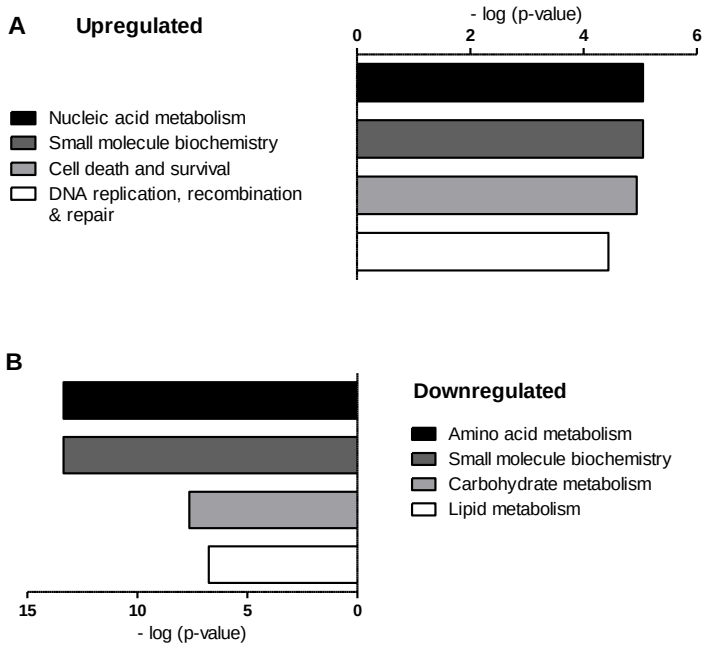

Figure 2.6. Molecular/cellular functions found to be significantly overrepresented during aestivation as determined by Ingenuity Pathways Analysis (IPA). *A*: Among the genes that were upregulated in muscle of aestivating frogs, those involved in nucleic acid metabolism, small molecule biochemistry, cell death and survival, and DNA replication, recombination and repair were overrepresented. *B*: Among the downregulated genes, those implicated in amino acid metabolism, small molecule biochemistry, carbohydrate metabolism and lipid metabolism were found to be overrepresented. Data are plotted as the –log of the *P* value given during the analysis, meaning larger values correspond to more significant activation/deactivation of a cellular functional group.

Table 2.4. Log2 fold-changes of differentially expressed genes involved in both energy metabolism and regulation of muscle size/growth in gastrocnemius muscle of burrowing frogs (*C. alboguttata*).

	Symbol	Top Hit Accession No.	% Similarity	P-value	Log2 fold change
Carbohydrate metabolism (glycolysis)					
Phosphoglucomutase 1	*pgm1*	NP_001080172	96	7.8E-09	-2.9
Glucose-6-phosphate isomerase-like	*gpi*	CAC83783	98	2.8E-07	-3.5
6-phosphofructokinase, muscle type	*pfkm*	AAI68800	95	4.1E-06	-2.3
Aldolase A, fructose-bisphosphate	*aldoa*	AAF60276	63	5.2E-06	-2.4
Fructose-1,6-bisphosphatase 2	*fbp2*	NP_001167494	97	2.6E-09	-3.2
Triosephosphate isomerase	*tpi1*	NP_001080476	96	6.5E-12	-4.4
Phosphoglycerate kinase 1	*pgk1*	NP_001016545	97	2.6E-04	-1.7
Phosphoglycerate mutase 2 (muscle)	*pgam2*	NP_001080086	96	3.1E-11	-4.1
Pyruvate kinase, muscle isoform 1	*pkm2*	NP_001016470	97	1.0E-07	-2.6
L-lactate dehydrogenase A chain	*ldhb-b*	NP_001081050	82	1.9E-07	-2.9
Enolase 3	*eno3*	NP_001080346	97	3.8E-19	-7.7
Lipid metabolism					
Peroxisome proliferator-activated receptor gamma coactivator 1-alpha-like	LOC100491667	XP_002936759	90	5.6E-05	-2.5
Peroxisome proliferator-activated receptor delta	*ppard*	NP_001081310	85	2.4E-03	-1.6
Protein kinase, AMP-activated, alpha 2 catalytic subunit	*prkaa2*	NP_001135554	96	5.8E-04	-1.9
Lipase, hormone-sensitive	*lipe*	NP_001124413	85	5.8E-04	-2.6
Adiponectin, C1Q and collagen domain containing precursor	*adipoq*	NP_001005793	83	3.7E-08	-2.8
Alcohol dehydrogenase 1	*adh1b*	P22797	93	1.8E-04	-2.6
Aldehyde dehydrogenase class 1	*aldh1a1*	BAA76411	93	5.5E-04	-1.8

Aldehyde oxidase-like	LOC100495429	XP_002937768	91	4.3E-06	-2.4
Aldo-keto reductase family 1, member C1	*akr1c1*	NP_001087453	87	3.6E-11	-4.0
Glutaryl-CoA dehydrogenase	*gcdh*	NP_001016289	94	6.3E-04	-1.5
		Amino acid metabolism			
Branched chain amino-acid transaminase, cytosolic-like	*bcat1*	XP_003202557	82	5.9E-06	-3.3
Branched chain amino-acid transaminase 2, mitochondrial	*bcat2*	NP_001006740	89	1.7E-07	-2.7
Branched chain keto acid dehydrogenase E1, beta polypeptide	*bckdhb*	NP_001108310	93	8.4E-04	-1.6
Isovaleryl-CoA dehydrogenase	*ivd*	NP_001011380	93	4.8E-04	-1.6
Methylcrotonoyl-CoA carboxylase 2 (beta)	*mccc2*	NP_001025656	96	7.8E-04	-1.5
3-hydroxyisobutyrate dehydrogenase	*hibadh*	NP_001025604	99	8.0E-05	-1.8
Aldehyde dehydrogenase 6 family, member A1	*aldh6a1*	NP_001089889	96	6.6E-04	-1.5
3-oxoacid CoA transferase 1	*oxct1*	NP_001083240	93	5.9E-04	-1.6
Aminoadipate-semialdehyde synthase	*aass*	NP_001011437	95	1.2E-06	-2.7
α-aminoadipic semialdehyde dehydrogenase	*aldh7a1*	NP_001087698	98	4.7E-04	-1.8
Proline dehydrogenase (oxidase) 1	*prodh*	NP_001089485	96	5.7E-09	-4.8
Delta-1-pyrroline-5-carboxylate dehydrogenase, mitochondrial	*aldh4a1*	NP_001096184	93	1.2E-05	-2.1
Ornithine aminotransferase	*oat*	NP_001086690	97	2.0E-08	-3.7
Betaine--homocysteine S-methyltransferase 1	*bhmt*	NP_001088416	97	1.2E-05	-2.9
Cystathionine-beta-synthase	*cbs*	NP_001008171	95	1.1E-03	-1.5
Dimethylglycine dehydrogenase, mitochondrial-like	*dmgdh*	XP_002940239	92	8.9E-07	-2.8
Uncharacterized protein LOC394486	MGC75760	NP_988891	82	1.9E-04	-2.2
Parvalbumin beta	*pvalb*	ACF23534	95	2.0E-06	-5.1

Muscle creatine kinase	*ckm*	NP_001080073	80	4.0E-05	-3.0
Glycine amidinotransferase, mitochondrial	*gatm*	NP_988971	98	2.0E-02	-2.1
Glutamine synthetase	*glul*	AAH64190	96	8.6E-07	-4.2
Aspartate aminotransferase 1	*got1*	BAM10994	98	3.5E-04	-2.2
Aspartate aminotransferase, mitochondrial precursor	*got2*	NP_001016933	96	6.2E-04	-1.6
		Amino acid transport			
Multidrug resistance-associated protein 1-like	LOC100493037	XP_002932264	89	4.1E-05	-2.3
Solute carrier family 3 (activators of dibasic and neutral amino acid transport), member 2	*slc3a2*	NP_001079446	72	2.3E-06	-3.3
Solute carrier family 7 (amino acid transporter light chain, L system), member 8	*slc7a8*	NP_988983	98	1.1E-04	-2.5
Solute carrier family 25 (mitochondrial carrier; adenine nucleotide translocator), member 4	*slc25a4*	NP_988909	96	9.6E-04	-1.6
Solute carrier family 25, member 12	*slc25a12*	NP_001016920	97	3.4E-04	-1.6
Large neutral amino acids transporter small subunit 3	*slc43a1*	NP_001186840	89	6.1E-06	-2.9
Low affinity cationic amino acid transporter 2-like	LOC100485546	XP_002940493	91	6.2E-09	-3.2
		***Regulation of muscle size/growth* (not detected by IPA)**			
Insulin-like growth factor binding protein-like 1	*igfbpl1*	ACO51872	90	7.5E-12	-4.7
Myostatin	*mstn*	XP_002931568	91	4.0E-06	-2.9

Negative fold changes indicate downregulation of genes in frogs aestivating for 4-month relative to controls.

Table 2.5. Log2 fold-changes of differentially expressed genes implicated in cell death and/or survival, and DNA replication, recombination and repair in gastrocnemius muscle of burrowing frogs (*C. alboguttata*).

	Symbol	Top Hit Accession No.	% Similarity	P-value	Log2 fold change
Cell death and survival					
Tumor necrosis factor receptor superfamily member 6 precursor	*fas*	NP_001009314	56	2.4E-04	1.9
Ras association (RalGDS/AF-6) domain family member 1	*rassf1*	NP_001090617	92	1.6E-04	2.0
Apoptosis-inducing factor 2	*aifm2*	NP_001135491	88	2.5E-05	2.6
Apoptosis-enhancing nuclease	*aen*	NP_001072399	70	6.2E-04	1.9
Baculoviral IAP repeat-containing protein 5.2-B	*birc5.2-b*	NP_001082412	56	8.7E-08	3.7
Vesicular overexpressed in cancer prosurvival protein 1	*vopp1*	NP_001088316	88	6.9E-05	2.5
78 kDa glucose-regulated protein-like	*hspa5*	XP_002941690	97	6.3E-05	2.0
Heat shock protein 90kDa beta (Grp94), member 1 precursor	*hsp90ab1*	NP_001039228	96	6.6E-05	1.9
Heat shock protein family B (small), member 11	*hspb11*	NP_001037976	85	1.5E-03	1.6
Heat shock 105kDa/110kDa protein 1	*hsph1*	ABE65386	89	1.9E-06	2.8
Fatty acid synthase	*fasn*	AAA82106	87	2.0E-05	3.0
HIV-1 Tat interactive protein 2, 30kDa	*htatip2*	NP_001089518	93	2.3E-04	1.9
Suppressor of cytokine signalling 3	*socs3*	NP_001005696	93	3.2E-02	1.6
DNA replication, recombination & repair					
Serine/threonine protein kinase Chk1	*chek1*	Q6DE87	92	1.1E-08	4.0
Cell division protein kinase 2	*cdk2*	ACO51934	98	1.2E-07	2.8
Tonsoku-like protein	*tonsl*	XP_002944768	76	8.2E-04	2.0
DNA mismatch repair protein Msh6	*msh6*	NP_001089247	94	2.6E-03	1.6
Nei endonuclease VIII-like 3	*neil3*	NP_001017201	75	9.3E-05	2.0

Remodelling of chromatin					
Similar to retinoblastoma-binding protein 4	RBBP4	AAH15123	79	9.1E-05	2.1
Smarca4 protein	*smarca4*	AAH23186	96	1.2E-04	2.3
Smarca5 protein	*smarca5*	AAH21922	98	2.3E-04	2.2

Positive fold changes indicate upregulation of genes in frogs aestivating for 4-month relative to controls.

DISCUSSION

Throughout aestivation *C. alboguttata* are immobilised within a cocoon of shed skin, and do not eat, drink or show any signs of activity. The inhibition of muscle atrophy in *C. alboguttata* is likely to be due to a number of factors including increased antioxidant defences relative to oxidant production (Hudson et al., 2006), maintenance of 'random' acetylcholine release at neuromuscular junctions (Hudson et al., 2005), and metabolic depression at the tissue and whole animal level (Hudson and Franklin, 2002b; Young et al., 2011). Despite the results of these and other studies, the molecular and cellular mechanisms responsible for the inhibition of skeletal muscle disuse atrophy in natural models have not been fully characterised. Transcriptome profiling of animals that experience natural periods of muscle immobilisation or inactivity (i.e. aestivators and hibernators) helps to provide a better molecular- and systems-level understanding of how these organisms resist cellular degenerative changes and retain locomotor performance upon arousal. In the following discussion, particular emphasis is placed on how the observed gene expression changes observed in our RNA Seq study pertain to the inhibition of skeletal muscle atrophy that is characteristic of aestivating *C. alboguttata*.

Adherens junction remodelling

We chose to analyse gene expression in gastrocnemius muscle of 4-month aestivating burrowing frogs, as previous analyses demonstrated a lack of muscle atrophy in the force-producing hindlimb muscles until 6-9 months of aestivation (Hudson et al., 2006; Mantle et al., 2009). In the current study genes encoding myosin and actin isoforms, as well as α-actinin and vinculin were significantly downregulated in muscle of aestivating animals. Myosin heavy chain and actin proteins are among the most important determinants of muscle force transduction, whereas α-actinin and vinculin regulate organization of the actin cytoskeleton.

Transcription of actin and myosin isoforms appears to not be required for the maintenance of muscle contractile function when *C. alboguttata* emerges from aestivation. It is conceivable that burrowing frogs might remodel and preserve existing muscle contractile proteins in the early stages of aestivation, precluding the requirement to transcribe actin and myosin genes in the middle and latter stages of dormancy. These findings are consistent with other studies of various species' of hibernating mammal which have shown that myosin heavy chain protein expression is often maintained despite prolonged muscle inactivity (Rourke et al., 2006; Rourke et al., 2004). While muscle contractile activity ceases during dormancy, skeletal muscle is also challenged to retain structural integrity despite disuse and starvation. Aestivating muscle exhibited increased expression of alpha and beta tubulin transcripts, suggesting that the reinforcement of cellular and organelle integrity is of increased importance in the gastrocnemius during aestivation. Upregulation of tubulin isoforms is in stark contrast to the situation during mammalian disuse remodelling (Sakurai et al., 2005), further supporting the unusual muscle inactivity response seen in *C. alboguttata*.

Nrf2-mediated oxidative defence

Muscle disuse atrophy in mammalian models has been linked to an accumulation of reactive oxygen species (ROS), which causes oxidative stress and damage to skeletal muscle tissue (Powers et al., 2007). The accrual of ROS-induced oxidation products is positively correlated with oxygen consumption in a range of species (Foksinski et al., 2004). As a result, the metabolic depression characteristic of dormant animals has been proposed to lead to a lower rate of ROS production and, in conjunction with a relative increase in antioxidant levels, protect the muscles of hypometabolic animals from significantly atrophying (Hudson and Franklin, 2002b). IPA analysis identified several differentially expressed genes related to the Nrf2-mediated oxidative stress response. Nrf2 activity is sensitive to the intracellular concentration of ROS and its induction is significant in protecting cells against oxidative stress. The upregulation of genes under Nrf2 control (*gclm*, *gsto2*, *srxn1*, *dnaja4.1*, *fth1*) suggests persistent bolstering of antioxidant defences in skeletal muscle of *C. alboguttata* throughout aestivation, which represents a potential means of reducing muscle wasting. Our expression data are supported by previous studies of *C. alboguttata* which have shown that transcription of antioxidant enzymes (catalase and glutathione peroxidase 4) and total antioxidant capacity are maintained at control levels in skeletal muscle during aestivation (Hudson et al., 2006; Mantle et al., 2009). Similar results have been found in aestivating toads (*Scaphiopus couchii*) indicating that endogenous regulation of antioxidants may reduce the

susceptibility of muscle tissue to the effects of oxidative damage (Grundy and Storey, 1998). In typical mammalian muscle disuse models the opposite trend has been observed, with a number of studies having documented skeletal muscle wasting despite the induction of defense mechanisms against oxidative stress (including increased Nrf2 trancription) (Brocca et al., 2012; Derbre et al., 2012; Lawler et al., 2003). However, a more definitive understanding of the role for the Nrf2-regulated antioxidant response in aestivating *C. alboguttata* will require additional research, as we found other cytoprotective genes (*gstp1*, *dnajb5*) regulated by Nrf2 to be suppressed. Moreover, *keap1a*, a negative regulator of Nrf2-dependent transcription, showed increased expression in aestivating muscle.

Energy metabolism

The pronounced depression of metabolism in muscle tissue of aestivating frogs (Flanigan et al., 1991; Kayes et al., 2009a) would necessitate suppression of both glycolytic and aerobic energy pathways. Our data indicate that downregulation of glycolysis in aestivating *C. alboguttata* is achieved via suppression of transcription. Previous studies on a variety of dormant animals have demonstrated that intrinsic control of carbohydrate metabolism is often coordinated via post-translational modification (Storey and Storey, 2010), and it is possible that such mechanisms are also at play in aestivating burrowing frogs. Several genes (*ppard, prkaa2, lipe, adipoq, adh1b, aldh1a1, akr1c1, gcdh, aox1*) implicated in the oxidation of lipids were found to be underexpressed in aestivators. The downregulation of peroxisome proliferator-activated receptor gamma coactivator 1-α (PGC-1*α*) is particularly noteworthy, as it plays a vital role in metabolic reprogramming in response to nutrient supply. PGC-1*α* regulates mitochondrial biogenesis, and its induction leads to enhanced capacity for fatty-acid β-oxidation and mitochondrial oxidative metabolism. Enhanced expression of PGC-1*α* also occurs during muscular exercise (Pilegaard et al., 2003). Although downregulation of PGC-1*α* might be expected during muscle disuse, the overall suppression of genes implicated in oxidation of lipids is somewhat surprising, as fatty acid β oxidation is enhanced in the skeletal muscle transcriptome and proteome of hibernating mammals (Hindle et al., 2011; Williams et al., 2005). Lipids are still likely to be an essential fuel source during periods of aestivation and/or fasting in *C. alboguttata*, although the liver and fat bodies are the most likely organs contributing to fatty acid metabolism, rather than skeletal muscle (Jones, 1980). Dramatic downregulation of energy metabolism pathways have been documented in clinical models of muscle disuse (Brocca et al., 2012; Chen et al., 2007). Evidence suggests there is a shift in fuel metabolism away from fat oxidation towards an increased reliance on glucose,

and that fat accumulates in atrophied muscles in place of muscle protein (Stein and Wade, 2005). In these models these changes are likely to negatively affect fatigue resistance, the recovery process and locomotor performance.

Transcriptional suppression of energy metabolism in muscle of aestivating *C. alboguttata* is clearly related to conservation of energy and body fuel, and appears to have no significant impact on locomotor condition (Hudson and Franklin, 2002a). Rather, metabolic depression at the whole-animal, tissue and molecular levels is beneficial for aestivating frogs, as hypometabolism extends endogenous lipid stores and postpones the need to catabolise muscle protein. Although skeletal muscle is a potential energy source, protein degradation must be avoided so that aestivating frogs can preserve skeletal muscle structure and strength in preparation for arousal. This is supported in our study by the downregulation of an abundance of genes functioning in amino acid metabolism (particularly catabolism) and transport, and in a previous examination which showed that skeletal muscle protein content is maintained in burrowing frogs despite prolonged aestivation (Mantle et al., 2010). These results are in agreement with previous work on black bears, which showed that both protein synthesis and degradation are reduced in the disused muscles of hibernating animals (Lohuis et al., 2007a). In contrast to aestivators and hibernators, the loss of muscle protein associated with typical models of muscle disuse atrophy is known to be due to a concurrent decline in the rate of protein synthesis and increase in the rate of protein degradation (Jackman and Kandarian, 2004).

Myogenesis and muscle growth

Throughout aestivation it is important that cells repress and reprioritise ATP-expensive processes, such as cell growth and proliferation (Storey and Storey, 2010), since burrowing frogs must sustain life for indefinite periods using endogenous fuel reserves alone. Although not detected by IPA, we noted that the gene for insulin-like growth factor binding protein-like 1 (*igfbpl1*) was significantly downregulated in aestivating frog muscle. In blood and tissues, IGF-binding proteins play an important role in the binding of IGF-1, a peptide which stimulates growth and target cell proliferation. Circulating levels of IGF-binding protein-1 are, in part, thought to regulate the bioavailability of IGF-1 (Lee et al., 1997). Furthermore, resistance exercise/increased loading in skeletal muscle stimulates the expression of IGF-1 (Devol et al., 1990). The signal transduction pathway induced by IGF-1 results in skeletal muscle growth and hypertrophy by activating the phosphatidylinositol 3-kinase/protein kinase-B pathway, which subsequently stimulates downstream signalling

pathways involved in translation and protein synthesis (Rommel et al., 2001). The downregulation of *igfbpl1* in muscle of *C. alboguttata* suggests that pathways promoting cell growth and proliferation are suppressed during aestivation. Though they have received little attention during aestivation, IGF-1 and IGF-binding proteins have been examined in sera of hibernating mammals throughout winter hibernation (Blumenthal et al., 2011; Schmidt and Kelley, 2001). Both studies demonstrated that serum levels of IGF-1 and IGF-binding protein 3 were substantially reduced in winter hibernating animals compared with euthermic controls. These investigations combined with our data indicate that the inhibition of pathways promoting tissue growth is a vital, conserved feature of dormancy.

Myostatin (also known as growth-differentiation factor 8; *mstn*), which is known to suppress muscle growth by inhibiting myocyte proliferation and differentiation (Elliott et al., 2012), was also downregulated during aestivation. Blocking of the myostatin pathway using various techniques has been shown to lead to muscle hyperplasia and hypertrophy (McPherron et al., 1997; Zhu et al., 2000). Myostatin is suspected as having a role in muscle atrophy during disuse with some studies demonstrating elevated myostatin mRNA and protein abundances in disused muscles (Reardon et al., 2001; Wehling et al., 2000). In addition, experimental inhibition of myostatin in 14-day unloaded mouse skeletal muscles significantly decreases the extent of muscle atrophy (Murphy et al., 2011). In the current study myostatin gene expression was decreased almost threefold in gastrocnemius of aestivating frogs and may be an important regulatory mechanism for preserving muscle mass, despite extended inactivity and fasting. In support of these findings, soleus and diaphragm muscles of hibernating ground squirrels were shown to be resistant to disuse atrophy, and coincided with a 50% reduction in myostatin gene expression (Nowell et al., 2011). However, additional work is required to define the actual role that myostatin plays in hibernating models of starvation and muscle disuse, since myostatin mRNA and protein abundance has been shown to increase, decrease, or remain unchanged depending on the species, muscle type and/or stage of dormancy examined (Brooks et al., 2011; Nowell et al., 2011).

Cell death and survival

The coordinated induction of genes associated with cell death and survival is a prominent feature of the transcriptome of aestivating *C. alboguttata*. Apoptosis, or programmed cell death, can be induced via extracellular (extrinsic) or intracellular (intrinsic) pathways. The extrinsic pathway is activated by specific death receptors, whereas the intrinsic pathway involves the release of cytochrome c from mitochondria in response to stressors

including DNA damage and nutrient or energy depletion (Rossi and Gaidano, 2003). Both the extrinsic and intrinsic pathways of apoptosis converge into a common pathway causing activation of the executioner proteases known as caspases. Caspases subsequently degrade various cell substrates, leading to DNA fragmentation, chromatin condensation, cell shrinkage and cell death (Rossi and Gaidano, 2003). Apart from their role in the intrinsic pathway of apoptosis, mitochondria also function in a pathway of caspase-independent apoptosis, which may be effected by apoptosis-inducing factor and related pro-apoptotic proteins (Susin et al., 1999; Wu et al., 2002; Xie et al., 2005). However, caspase-independent apoptosis *in vivo* has only been documented in neurons, for example during transient cerebral ischemia and traumatic brain injury (Cao et al., 2003; Zhang et al., 2002).

Increased expression of genes involved in both the intrinsic and extrinsic pro-apoptotic pathways in skeletal muscle of aestivating frogs suggests that the events leading to cell death are occurring, which would result in cellular degradation and ultimately manifest as atrophy. However, increased expression of pro-apoptotic genes during aestivation was paralleled by induction of a number of anti-apoptotic mechanisms. Two of these genes, survivin (*birc5*) and vesicular over-expressed in cancer prosurvival protein 1 (*vopp1*), are of particular interest as both are overexpressed in many human tumours and as a consequence are associated with conferring a prosurvival cellular phenotype (Baras and Moskaluk, 2010; Sah et al., 2006). Survivin belongs to the family of inhibitor of apoptosis proteins (IAP) and is widely expressed during embryonic development (when apoptosis is widespread) but has been reported to be low in most terminally differentiated tissues (Sah et al., 2006; Song et al., 2003). In human systems interference of both survivin and VOPP1 function results in an increase in apoptosis and suppression of tumour growth (Baras et al., 2011; Sah et al., 2006). Similar to our study, cellular actions that would suppress pro-apoptotic signalling have been demonstrated in dormant snails (Ramnanan et al., 2007). The Bcl-2-associated death promoter (BAD) is a pro-apoptotic protein in its dephosphorylated form, but when phosphorylated at serine 136 BAD is prevented from forming a pro-apoptotic interaction with another Bcl-2 family member, Bcl-X_L thereby promoting cell survival (Datta et al., 2000). Ramnanan et al. (Ramnanan et al., 2007) reported an almost two-fold increase in levels of phospho-BAD in foot muscle of the aestivating snails. A role of apoptosis in mammalian models of muscle disuse is evidenced by the observation that pro-apoptotic mechanisms are activated during hindlimb immobilisation in rats, but then subside during the muscle recovery period (Vazeille

et al., 2008). Thus, survivin and VOPP1 may represent key mechanisms that limit apoptosis and aid in the long term preservation of muscle tissue during aestivation in *C. alboguttata*.

Several stressors, including changes in redox status and glucose starvation, can result in the accrual of misfolded and/or unfolded proteins within cells. Cells respond via initiation of molecular chaperones (e.g., heat shock proteins) that assist in the reassembly and stabilization of macromolecular structures, thereby preventing aggregation of denatured proteins during cell stress (Malhotra and Kaufman, 2007). Aestivating muscle of *C. alboguttata* exhibited increased expression of a number of genes encoding various heat shock proteins. Consistent with our gene expression data, a recent study demonstrated an increase in levels of heat shock 70 kDa protein (HSP70) in the gastrocnemius of *C. alboguttata* during aestivation (Young et al., 2013). Interestingly, there is a decline in expression of various HSPs in atrophied muscles of rats subjected to hindlimb unloading, which is predicted to be associated with impairment of muscle mass recovery (Lawler et al., 2006; Sakurai et al., 2005; Stevenson et al., 2003). Furthermore, a recent study demonstrated that overexpression of HSP70 in mouse skeletal muscle immobilised for 7 days resulted in improved contractile performance during the recovery period relative to wild-type controls, indicating that HSP70 improved recovery of skeletal muscle following disuse atrophy (Miyabara et al., 2012). In *C. alboguttata* the upregulation of genes involved in refolding and stabilising proteins in gastrocnemius muscle may be important regulatory mechanisms contributing to the preservation of muscle contractile performance upon emergence from aestivation.

DNA replication, recombination and repair

DNA damage may occur during muscle atrophy, as levels of DNA fragmentation (a marker for apoptosis) were found to be elevated in skeletal muscles of rats subjected to hindlimb suspension (Leeuwenburgh et al., 2005). Cells exposed to DNA stressors induce defensive pathways by activating multiple genes involved in processes such as homologous recombination (HR), nucleotide excision repair (NER), nucleotide mismatch repair (MMR), and cell cycle checkpoint control. DNA damage and apoptosis are intimately linked, as widespread and irreversible DNA damage often leads to cell suicide. Very little research has been done on the mechanisms that may maintain genomic stability in hypometabolic animals. In the current study, we found increased expression of genes associated with the NER, MMR and cell cycle checkpoint control in muscle of aestivating frogs, which suggests that transcriptional regulation of DNA repair plays a critical role in the dormant state. Increased

tolerance to DNA damage during aestivation would presumably lead to increased rates of cell survival.

Chromatin influences access to DNA, and a number of genes implicated in chromatin remodelling showed increased mRNA levels in aestivating muscle. These results are in accordance with the requirement to tightly control transcription of specific genes during dormancy. In addition, recent evidence suggests that chromatin remodelling plays important roles during NER and HR (Lans et al., 2012). For example, chromatin frequently serves as a docking or signalling site for DNA repair and signalling proteins. The induction of genes functioning in cell cycle control and growth arrest, and DNA and chromatin remodelling and repair is consistent with the ubiquitously conserved cellular stress response (Kultz, 2005), and might be important for maintaining genome integrity during aestivation.

Conclusions

The green-striped burrowing frog, *C.alboguttata*, exhibits an atypical atrophic response to extended immobilisation and fasting during aestivation. In the present study we identified a number of transcriptional mechanisms that may contribute towards the relative inhibition of skeletal muscle atrophy in aestivating *C. alboguttata.* Our results suggest that cytoskeletal remodelling and induction of antioxidant defence genes are important for the maintenance of muscle integrity. The suppression of energy metabolism in immobilised muscle of aestivating frogs indicates utilisation of whole body, rather than local, fuel stores throughout aestivation. In particular, avoidance of amino acid catabolism is consistent with the preservation of muscle protein and function. Proapoptotic and antiapoptotic factors are coexpressed and would appear to compete for promotion or inhibition of apoptotic muscle fiber degradation. A novel finding of this study was the induction of prosurvival genes, *birc5.2-b* and *vopp1*. Such anti-apoptotic mechanisms are likely to be important in countering pro-apoptotic machinery and preventing muscle fibre apoptosis. Combined with upregulation of molecular chaperones and DNA repair mechanisms, aestivating burrowing frogs appear to possess the appropriate gene expression responses with which to inhibit atrophy and maintain tissue viability. Such modulation of gene expression is likely to be important in contributing to the preservation of muscle mass and integrity during aestivation, and the ability of *C. alboguttata* to quickly emerge from their subterranean burrows upon summer rainfall. The associations among various gene expression patterns shown here using RNA Seq will provide new directions for future studies of the regulation of atrophy in both natural and clinical models of muscle disuse.

Chapter 3

Decreased hydrogen peroxide production and mitochondrial respiration in skeletal muscle but not cardiac muscle of the green-striped burrowing frog, a natural model of muscle disuse

---

INTRODUCTION

Aestivation is a state of dormancy that enables numerous animals (invertebrates, fish, frogs and reptiles) to survive under desiccating conditions for extended periods of time. In arid and semi-arid environments where food and water are often limiting, aestivating animals promote survival by coordinately suppressing a suite of physiological and biochemical processes (e.g. hypophagia, hypoventilation, hypometabolism), decreasing locomotor activity, and persisting solely on endogenous energy stores (Storey and Storey, 1990). Green-striped burrowing frogs (*Cyclorana alboguttata*) survive in drought-affected areas of Australia by burrowing underground, shedding a waterproof cocoon, and aestivating for extended periods (months to years). Although the cocoon limits evaporative water loss, it also secondarily hinders skeletal muscle movement as the hindlimbs are completely immobilised. Despite this prolonged muscle inactivity, skeletal muscle atrophy has been shown to be minimal and muscle functional capacity maintained in frogs following aestivation (Hudson and Franklin, 2002a; Mantle et al., 2009; Symonds et al., 2007). *C. alboguttata* aestivating for nine months show no loss in myofibre cross-sectional area (CSA; a marker of muscle atrophy) in the gastrocnemius, an important muscle which produces power necessary for jumping (Mantle et al., 2009). In contrast, hindlimb immobilisation in conventional experimental models, such as rats, can result in a significant (up to 32%) loss in gastrocnemius myofibre CSA in as little as two weeks (Sakakima et al., 2004). Disuse-induced skeletal muscle atrophy has been linked to increased reactive oxygen species (ROS) production in muscle fibres, leading to oxidative stress and muscle tissue damage (Powers et al., 2011). For example, prolonged bed rest in humans can result in increased carbonylation of muscle proteins and an apparent weakening of antioxidant defence systems (Brocca et al., 2012; Dalla Libera et al., 2009).

ROS are formed as by-products of normal aerobic cellular metabolism. A number of comparative studies suggest that species with higher mass-specific metabolic rates have elevated ROS production (Adelman et al., 1988; Foksinski et al., 2004; Lopez-Torres et al., 1993). Consequently, it has been hypothesised that metabolic suppression during dormancy leads to a decrease in ROS production in muscle fibres, which may be a potential means of

reducing the effects of muscle disuse atrophy in natural models of muscle disuse (i.e. aestivating frogs and hibernating mammals) (Hudson and Franklin, 2002b). While skeletal muscle is effectively dormant throughout aestivation (Kayes et al., 2009a; Kayes et al., 2009b), cardiac muscle must remain active to ensure adequate perfusion of organs. For example, the mass of the heart and the number of apoptotic nuclei in cardiac muscle does not change between aestivating and awake conditions (Amelio et al., 2013; Secor and Lignot, 2010) while molecular mechanisms implicated in the control of redox balance and cardio-circulatory homeostasis (e.g. endothelial nitric oxide synthase; eNOS, which synthesises the free radical nitrc oxide) are also bolstered during aestivation (Amelio et al., 2013). In contrast, increased levels of apoptosis and phospho-eNOS/eNOS protein have been documented in aestivating skeletal muscle (Amelio et al., 2013).

The maintenance of cardiac muscle activity during aestivation would be particularly important for cocoon-forming aestivating frogs, such as *C. alboguttata*, which have an increased reliance on pulmonary gas exchange and pulmonary circulation relative to non-cocoon-forming species (Loveridge and Withers, 1981). In the mammalian heart ROS are an important determinant of cardiomyocyte homeostasis and proper contractile function. Whereas low concentrations can stimulate signal transduction processes, high concentrations may lead to cardiomyocyte injury (Seddon et al., 2007; Suzuki and Ford, 1999). Little is understood about ROS production and signalling during metabolic depression, therefore it is of interest to explore ROS in distinct tissues that respond differently throughout the dormant phase.

Oxidative stress occurs only when ROS overwhelm the detoxifying capacity of cells. One way cells can protect themselves from potentially lethal oxidative damage is to increase the synthesis and/or activity of intracellular antioxidant enzymes. Numerous studies have demonstrated the induction of antioxidant defences during dormancy (including aestivation), suggesting that enhanced oxidative stress resistance is an integral component of metabolic suppression (see Carey et al., 2003; Ferreira-Cravo et al., 2010 for reviews). In *C. alboguttata*, aestivation for four months resulted in the induction of mRNA transcripts associated with skeletal muscle nuclear factor erythroid 2-related factor 2 (Nrf2), a regulator of the oxidative stress response (Reilly et al., 2013) (Chapter 2). Furthermore, water-soluble and membrane-bound antioxidants and gene expression levels of muscle catalase and glutathione peroxidase were shown to be maintained at control levels in muscles of dormant frogs (Hudson et al., 2006). These studies indicate that modulation of antioxidants in

aestivating muscle might decrease the susceptibility of muscle fibres to the atrophic effects of oxidative stress. As direct measurements of ROS are complicated and often exposed to errors, redox balance during dormancy has been typically studied indirectly by examination of lipid peroxidation and/or protein carbonylation (Grundy and Storey, 1998; Young et al., 2013). In one of the few studies that measured ROS production directly, there was generally no difference observed in mitochondrial ROS production in skeletal muscle of dormant vs. interbout euthermic ground squirrels (Brown et al., 2012). However, this is perhaps unsurprising as measurements are typically conducted at saturating substrate concentrations (e.g. 5 -10 mM succinate), whereas substrate inputs to mitochondria are likely substantially depressed *in vivo*. Moreover, substrates used in assays are often chosen to maximise net ROS production and succinate (Armstrong and Staples, 2010; Bishop and Brand, 2000; Gallagher and Staples, 2013; St-Pierre et al., 2000), whereas *in vivo* substrates will be a composite of electron inputs to complexes I and II.

In the current study we examined mitochondrial respiration and ROS production within permeabilised cardiac and skeletal muscle fibres of 4-month aestivating *C. alboguttata*. A major aim in the present study was to add mitochondrial substrates together in proportions which are likely to reflect substrates present *in vivo*, and to understand the response of mitochondria in the aestivating condition when substrate supply and oxidation should be suppressed. Furthermore, we aimed to answer the following questions: 1) are ROS produced at a lower rate in skeletal and cardiac muscle of aestivating *C. alboguttata* compared with active awake animals? 2) how does substrate concentration reflect electron inputs and ROS leakage in different physiological states? We hypothesised that mitochondrial respiration in skeletal and cardiac muscle would be suppressed in aestivating *C. alboguttata*, and that they would generate less ROS during distinct respiratory states (e.g. without adenylates vs. during ATP production) with substrate inputs that reflect depressed blood glucose. To test our hypothesis, we used high resolution respirometry in conjunction with custom-made fluorometers that concurrently measured mitochondrial respiration and ROS production in permeabilised cardiac and skeletal muscle fibres.

MATERIALS AND METHODS

Experimental animals and whole animal metabolic rate

The following experiments were approved by the University of Queensland Animal Ethics Committee (Approval Number: SBS/238/11/ARC). Green-striped burrowing frogs (*Cyclorana alboguttata*) were collected after summer rainfall from roadsides in the Darling Downs region of Queensland, Australia under Scientific Purposes Permit WISP10060511. Frogs were housed in the laboratory in individual plastic boxes containing wet paper towelling and were watered and fed live crickets *ad libitum*. Frogs were allocated to their treatment groups (controls or 4-month aestivators), with treatments matched as closely as possible for body mass and sex. To induce aestivation, frogs were placed into individual 500 mL glass chambers filled with wet paper pellets (Breeders Choice Cat Litter) that was allowed to dry out naturally over a period of several weeks. Animals burrowed into the paper pellets as the chambers dried out and adopted a water-conserving posture. All frogs were maintained in a temperature-controlled room (23°C) with a 12:12 h light/dark regime. Aestivating frogs were kept in cardboard boxes to reduce the effects of light disturbance. Throughout the experiment, whole animal metabolism was measured in aestivating (N = 12) and control frogs (N = 10) as previously described (Reilly et al., 2013) (Chapter 2). Briefly, aestivators remained in their chambers for the entire experimental period whereas control animals were weighed and placed into their chambers 24 h prior to sampling and removed immediately following final oxygen consumption measurements. Control frogs were then fed. Rates of oxygen consumption ($\dot{V}O_2$) were measured using closed-system respirometry using a fibre optic oxygen transmitter with oxygen-sensitive spots (Precision Sensing GmbH, Regensburg, Germany), which measure the partial pressure of oxygen (as a percentage of air saturation) within the chamber. Oxygen measurements were taken several hours later, depending on the treatment group (i.e. longer for aestivators), and on multiple occasions to calculate repeated rates of oxygen consumption. After four months, all aestivating animals had formed thin cocoons around their bodies.

Preparation of permeabilised muscle fibres

The permeabilised skeletal and cardiac muscle fibre preparations were performed using methods following Hickey et al. (Hickey et al., 2012), which avoids problems associated with traditional mitochondrial isolation methods (Picard et al., 2011). All frogs were sacrificed by cranial and spinal pithing. Immediately following pithing, blood glucose of individual frogs was measured using an Accu-Chek® Performa Blood Glucose Meter and test

strips (Roche, Castle Hill, NSW, Australia). Both the heart and the left gastrocnemius muscle were dissected, weighed and placed immediately into ice cold muscle relaxant buffer containing 10 mM Ca-EGTA buffer, 20 mM imidazole, 20 mM taurine, 50 mM K-MES, 0.5 mM DTT, 6.56 mM $MgCl_2$, 5.77 mM ATP, 15 mM phosphocreatine and leupeptin at pH 6.8. Skeletal and cardiac muscle samples were then teased apart into individual fibre bundles using sharp forceps and placed into 1 ml of fresh relaxant buffer with 0.05 mg of saponin. Fibres were gently shaken at 4°C for 30 min and were then transferred into ice cold respiration assay medium (0.5 mM EGTA, 3 mM $MgCl_2$, 60 mM K-lactobionate, 700 mM sucrose, 20 mM taurine, 10 mM KH_2PO_4, and 1 mg mL^{-1} BSA in 20 mM HEPES, pH 7.1) and mixed gently at 4°C for 5 min (x 3) to wash out saponin and ATP. Muscle fibre preparations were then blotted dry on kimwipes (Kimtech) and weighed for use in mitochondrial respiration assays.

Mitochondrial respiration and ROS (H_2O_2) production

Mitochondrial respiration was measured in control (heart, N = 5; skeletal muscle, N = 5) and 4-month aestivating (heart, N = 7; skeletal muscle, N = 6) animals. Respiration rates of cardiac and skeletal muscle mitochondria were measured using two OROBOROS O2K Oxygraphs (Anton Paar, Graz, Austria) with custom-made fluorometers as previously described (Hickey et al., 2012). This method allows H_2O_2 signal amplification and integration with both oxygen concentration and flux signals in DATLAB 4.3 software. All respiratory measurements of permeabilised muscle fibres were conducted at 23°C in a 2 ml chamber containing respiration assay medium at air saturation. ROS production was determined by measuring H_2O_2 production using a horseradish peroxidase-linked Amplex Ultra Red fluorometric assay (Life Technologies, Mulgrave, Victoria, Australia). Superoxide dismutase (10 U), horseradish peroxidase (10 U), and Amplex Ultra Red (12.5 µM final concentration) were added to each chamber. To calibrate the fluorometer, 0.94 nmol of H_2O_2 was added to each chamber before each assay.

Substrates were titrated into each respiration chamber using an integrated controlled injection pump (TIP Oroboros Instruments, Schöpfstrasse, Innsbruck, Austria). A substrate cocktail was used to mimic the flow of substrates *in vivo*. However, we note that there are no data regarding mitochondrial substrate levels for *C. alboguttata* and we cannot rule out that a particular substrate/s are used preferentially as an energy source in aestivating skeletal muscle. Whereas respiratory quotient data suggest fatty acids are the preferred substrate for aestivating frogs (Van Beurden, 1980), other studies on aestivating animals show that energy

may be derived from other sources (carbohydrates, ketone bodies) (Frick et al., 2008a; Frick et al., 2008b).

The cocktail consisted of Complex I-NADH linked substrates (pyruvate 400 µM and malate 200 µM) which were added in conjunction with the complex II substrate succinate (400 µM). Substrates were titrated in stepwise additions of 5 x 0.5 µl, 5 x 1 µl and 5 x 3 µl injections with a 2 minute delay between injections (15 injections total). This initiated non-phosphorylating, 'resting' mitochondrial respiration ($LEAK_N$). Initial concentrations were 0.05 mM (malate) and 0.1 mM (pyruvate and succinate), while the final concentrations were 2.25 mM (malate) and 4.5 mM (pyruvate and succinate). Following the titration protocol with malate, pyruvate and succinate, excess ADP was then added to the chamber to initiate oxidative phosphorylation (OXPHOS). Finally, the complex III inhibitor antimycin A was added to the chamber to inhibit mitochondrial respiration and determine background respiratory flux. Rates of steady state H_2O_2 production were traced using DATLAB 4.3. The average background rate of H_2O_2 across experiments before introduction of tissue to the chamber was 0.04 nmol/s (± 0.01 s.e.m). Rates were corrected for tissue mass and background activity prior to analysis. We also divided the amount of H_2O_2 formed by O_2 to provide an indication of the % ROS of O_2 (i.e. % of efficiency).

Statistics

Snout-vent length (SVL), blood glucose concentration, whole animal metabolic rate and mitochondrial respiration during OXPHOS were analysed by one-way analysis of variance (ANOVA). The mass of gastrocnemius muscle was analysed using analysis of covariance (ANCOVA), with SVL as the covariate. Mitochondrial respiration was fitted with a Michaelis-Menten model in GraphPad Prism. Maximal respiratory flux (*V*max) and *K*m (the substrate concentration at which respiratory flux was half *V*max) values were compared between 4-month aestivating and control frogs using an extra sum-of-squares F test. Because H_2O_2 production did not closely follow a Michaelis-Menten model during $LEAK_N$, H_2O_2 production was tested for significance using individual *t*-tests at each separate mitochondrial substrate injection point (data sets were assessed for normality and constancy of variance). H_2O_2 production data during OXPHOS were non-normally distributed and analysed using a Wilcoxon Rank Sum Test. The % H_2O_2 of O_2 was also analysed using individual *t*-tests. All statistical tests were performed with the statistical programs R (www.r-project.org) and/or GraphPad Prism with $P = <0.05$ deemed statistically significant. Data are means ± s.e.m. unless stated otherwise.

RESULTS

Muscle mass and blood glucose

There was no significant difference in body size (SVL) of aestivating *C. alboguttata* (6.13 ± 0.93 cm) compared with controls (6.21 ± 1.32 cm; P = 0.66). Four months of aestivation resulted in an 8% reduction in the wet mass of gastrocnemius muscle of aestivating *C. alboguttata* (359.59 ± 17.35 mg) relative to control frogs (390.03 ± 21.34 mg). The effect of aestivation on gastrocnemius wet mass was not significant when the SVL of frogs was accounted for (ANCOVA: full model, P = 0.69; treatment, P = 0.34; relationship to SVL, P = <0.05). The blood glucose of aestivating frogs (0.96 ± 0.06 mM) was significantly lower compared with control frogs (1.66 ± 0.08 mM; P = <0.001).

Whole animal metabolic rate and muscle mitochondrial respiration

The whole animal O_2 consumption of *C. alboguttata* decreased by approximately 70%, from 66.2 ± 7.5 *u*l $O_2 \cdot g^{-1} \cdot h^{-1}$ for control individuals to 20.3 ± 3.2 *u*l $O_2 \cdot g^{-1} \cdot h^{-1}$ for individuals after 4 months of aestivation (P= <0.001; Figure 3.1). Given that substrates used to measure mitochondrial respiration were mixed we simplified the substrate concentrations to their respective electron inputs assuming that pyruvate (*in vitro*) oxidation results in 3 NADH + H^+, malate 1 NADH + H^+, and succinate 1 $FADH_2$. Multiplication of each substrate's concentration by the electron contribution and then by Avogadro's constant (6.02 x 10^{23}) provides an approximation of the number of electrons that can be donated to the electron transport system. Mitochondrial respiratory flux rates in both skeletal and cardiac muscles obeyed typical Michaelis–Menten kinetics with increasing substrate concentrations (i.e. $LEAK_N$; respiration without adenylates present; Figure 3.2A, C). In skeletal muscle the maximal respiratory flux (Vmax) decreased from 3.10 ± 0.10 pmols O_2 (s.mg wet mass)$^{-1}$ in controls to 1.79 ± 0.15 pmols O_2 (s.mg wet mass)$^{-1}$ in aestivators, equating to a 42% decrease in oxygen consumption (P= <0.0001; Table 3.1). By contrast, the apparent Km (the substrate concentration at which respiratory flux was half of Vmax) was not significantly different between control and aestivating frogs (P= 0.80; Table 3.1). Respiratory flux in skeletal muscle fibres during oxidative phosphorylation (OXPHOS) decreased by 46%, with a decrease from 9.86 ± 1.31 pmols O_2 (s.mg wet mass)$^{-1}$ in controls to 5.31 ± 0.94 pmols O_2 (s.mg wet mass)$^{-1}$ in aestivating frogs (P= <0.05, Figure 3.2B). Both the Vmax and Km of aestivating cardiac muscle were maintained at levels similar to that of control animals during $LEAK_N$ (P = 0.16 and 0.33, respectively; Table 3.1). Similarly, mitochondrial respiratory flux in the heart during OXPHOS was unaffected by aestivation (P = 0.63; Figure 3.2D).

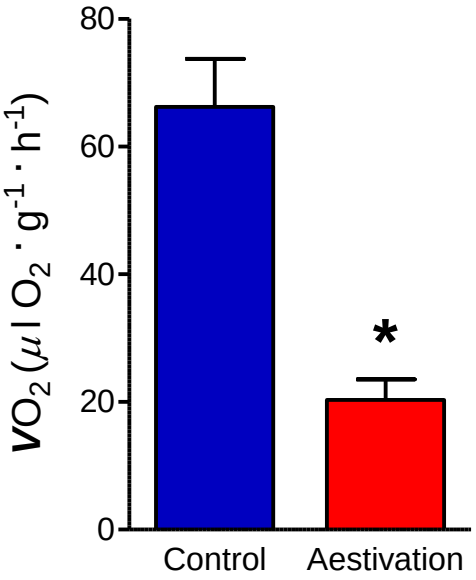

Figure 3.1. Whole-animal oxygen consumption ($\dot{V}O_2$, μl $O_2 \cdot g^{-1} \cdot h^{-1}$) of *Cyclorana alboguttata* at rest (Control, *N*= 10) and after 4 months of aestivation (*N*= 12). Data were analysed using one-way ANOVA and are presented as means ± s.e.m., **P* <0.001.

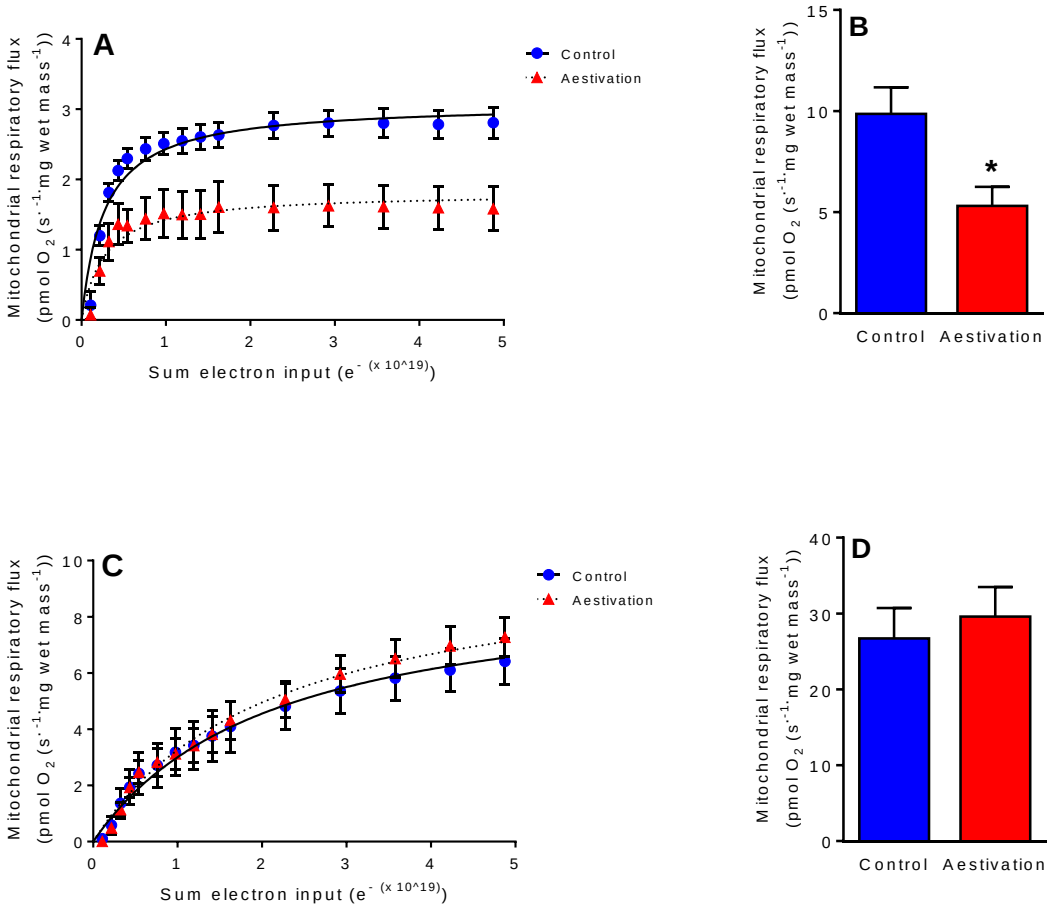

Figure 3.2. Mitochondrial respiratory flux (pmol $O_2 \cdot s^{-1} \cdot mg^{-1}$ wet mass) in permeabilised skeletal and cardiac muscle fibres of *C. alboguttata*. (A, B) Skeletal muscle: control, $N = 5$; aestivation, $N = 6$; (C, D) cardiac muscle: control, $N = 5$; aestivation, $N = 7$. Respiratory flux in muscle is shown in the presence of mitochondrial substrates malate, succinate and pyruvate only ($LEAK_N$; A, C), and the rate of respiratory flux in muscle is shown during maximum oxidative phosphorylation (OXPHOS; B, D). In A and C, the *x*-axis is presented as an approximation of the number of electrons that can be donated by malate, succinate and pyruvate to the electron transport system. *V*max and *K*m values during $LEAK_N$ were compared between 4-month aestivating and control frogs and tested for significance using an extra sum-of-squares F test. Mitochondrial respiration during OXPHOS was analysed by one-way ANOVA. Data are means ± s.e.m., $*P < 0.05$

Table 3.1. Mitochondrial respiratory flux followed a Michaelis-Menten model in permeabilised skeletal and cardiac muscle fibres of *C. alboguttata*

	Mitochondrial respiratory flux	
	*V*max	*K*m
	(pmol $O_2 \cdot s^{-1} \cdot mg^{-1}$)	($e^{-(x\ 10\text{^}19)}$)
Skeletal muscle		
Control (*N*=5)	3.10 ± 0.10	0.28 ± 0.04
Aestivation (*N*=6)	1.79 ± 0.15 ***	0.25 ± 0.10
Heart		
Control (*N*=5)	8.57 ± 1.11	1.71 ± 0.51
Aestivation (*N*=7)	10.89 ± 1.19	2.44 ± 0.54

Hydrogen peroxide production in permeabilised cardiac and skeletal muscle fibres

In skeletal and cardiac muscle H_2O_2 production could not be distinguished from background levels until the fifth cocktail injection, when cumulative substrate concentrations of pyruvate, succinate and malate were 0.5 mM, 0.5 mM and 0.25 mM, respectively. Because H_2O_2 production did not strictly follow a Michaelis-Menten model during $LEAK_N$ we determined whether H_2O_2 production differed between control and aestivating frogs at individual substrate concentrations. At low cumulative substrate concentrations H_2O_2 production was significantly lower in skeletal muscle of aestivating frogs (Figure 3.3A, P = 0.04 and P = 0.02, respectively), as was the amount of H_2O_2 formed per O_2 (an indication of the % ROS of O_2; Figure 3.4A, P = 0.04). H_2O_2 production was approximately 12% that of control frogs when cumulative substrate concentrations of pyruvate, succinate and malate were 1.3 mM, 1.3 mM and 0.65 mM, respectively, while H_2O_2 formed per O_2 was approximately 6% that of control frogs at similar concentrations. However, as mitochondrial substrate concentrations were increased in the medium H_2O_2 production did not differ significantly between aestivators and controls, due to a large variation among control animals (Figure 3.3A). Both H_2O_2 production and % ROS of O_2 from aestivating cardiac muscle fibres were similar to that of controls all throughout $LEAK_N$ (Figure 3.3C; 3.4C). During OXPHOS H_2O_2 production and % ROS of O_2 in skeletal and cardiac muscle were not significantly

different between aestivators and controls (H_2O_2 production wilcox tests, P = 0.18 and P = 0.76, respectively; % ROS of O_2, P = 0.07 and P = 0.49, respectively; Figure 3.3B, D; 3.4B, D). In general, ROS production was more tightly regulated (i.e. less variable) in aestivating frogs compared with control animals.

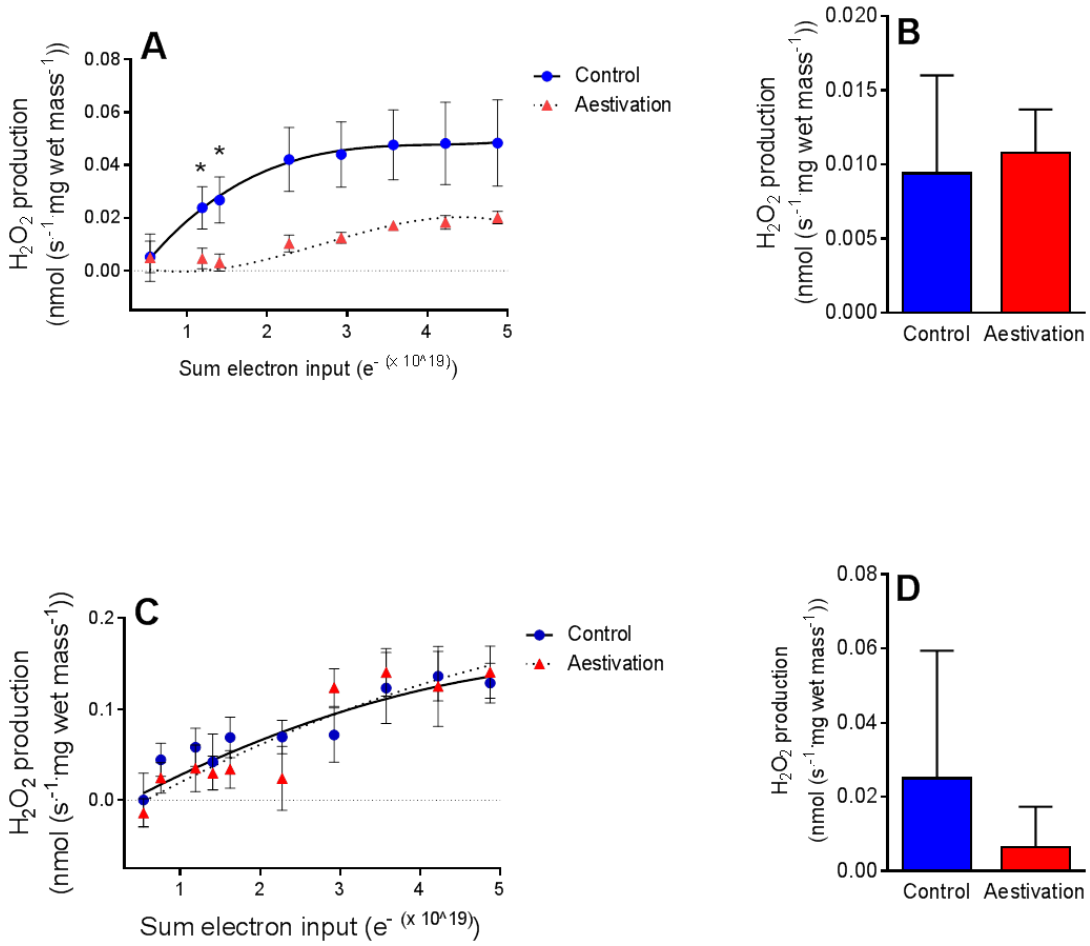

Figure 3.3. Hydrogen peroxide (H_2O_2) production (nmol $H_2O_2 \cdot s^{-1} \cdot mg^{-1}$) in permeabilised skeletal and cardiac muscle fibres of *C. alboguttata*. (A, B) Skeletal muscle: control, N = 5; aestivation, N = 6; (C, D) cardiac muscle: control, N = 5, aestivation, N = 7. H_2O_2 production was achieved by the addition of superoxide dismutase to the oxygraph chamber and determined in different respiration states ($LEAK_N$, A, C; and OXPHOS, B, D) as outlined in Materials and methods. In skeletal muscle, H_2O_2 production tended to be lower in aestivating animals during $LEAK_N$, whereas in cardiac muscle H_2O_2 production remained similar in control and aestivating frogs. There was no significant difference in skeletal or heart muscle H_2O_2 production between controls and aestivators during OXPHOS. In A and C the *x*-axis is presented as an approximation of the number of electrons that can be donated by malate, succinate and pyruvate to the electron transport system. During $LEAK_N$, H_2O_2 production was tested for significance using individual *t*-tests at each separate mitochondrial substrate injection point, whereas H_2O_2 production during OXPHOS were analysed using a Wilcoxon Rank Sum Test. Data are means ± s.e.m., *P <0.05

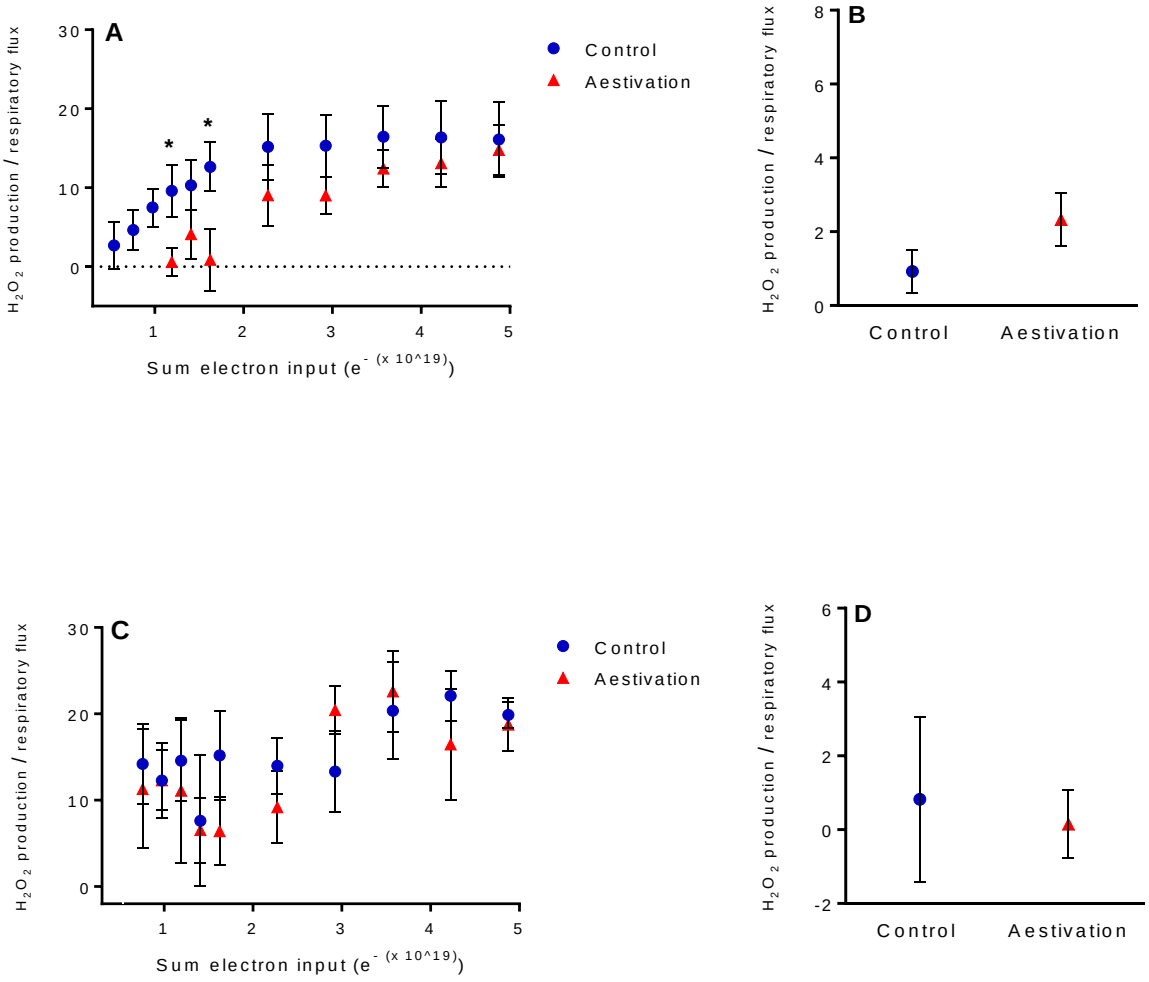

Figure 3.4. H_2O_2 production/mitochondrial respiratory flux in permeabilised skeletal and cardiac muscle fibres of *Cyclorana alboguttata*. (A, B) Skeletal muscle: control, N = 5; aestivation, N = 6; (C, D) cardiac muscle: control, N = 5; aestivation, N = 7. H_2O_2 production was divided by mitochondrial respiratory flux in different respiration states ($LEAK_N$, A, C; and OXPHOS, B, D) to provide an indication of H_2O_2 produced per O_2 turned over (%ROS of O_2). In skeletal muscle, %ROS of O_2 was significantly lower in aestivating animals during $LEAK_N$ at low substrate concentrations, whereas in cardiac muscle, %ROS of O_2 remained similar in control and aestivating frogs. There was no significant difference in skeletal or heart muscle %ROS of O_2 between controls and aestivators during OXPHOS. In A and C the *x*-axis is presented as an approximation of the number of electrons that can be donated by malate, succinate and pyruvate to the electron transport system. Individual *t*-tests were used to assess significance. Data are means ± s.e.m., **P* <0.05

DISCUSSION

In humans and most other mammals prolonged skeletal muscle disuse leads to a loss of muscle protein and fibre atrophy. It has been shown that long periods of limb immobilisation stimulate increased ROS production in disused fibres (Min et al., 2011). Though many studies have investigated muscle antioxidant levels during dormancy and/or arousal in aestivators and hibernators (Allan and Storey, 2012; Hudson et al., 2006; James et al., 2013; Ramos-Vasconcelos and Hermes-Lima, 2003; Young et al., 2013), little is known about changes in mitochondrial ROS production and this has only recently received experimental attention in natural models of muscle disuse (Brown et al., 2012). Additionally, relatively few physiological studies examine mitochondrial function using permeabilised fibres, tissues or cells. In the current study we have verified the use of saponin-permeabilised muscle fibres (Kuznetsov et al., 2008), an approach which is more likely to resemble conditions in living cells than analyses using isolated mitochondria preparations. We have shown that aestivating *C. alboguttata* are capable of selectively suppressing or maintaining rates of mitochondrial respiration within distinct muscle tissue types and our study is the first to measure net mitochondrial ROS production (i.e. the sum of H_2O_2 production that escapes the mitochondrial antioxidant system) during aestivation using a combination of mitochondrial substrates, which better reflects physiological conditions. We have also demonstrated that *C. alboguttata* are able to suppress ROS production in disused skeletal muscle at low substrate concentrations. Unlike skeletal muscle, ROS production in permeabilised cardiac muscle fibres appeared unaffected by aestivation. Overall, the current study enhances our understanding of the control of mitochondrial respiration and ROS production in aestivating animals.

Mitochondrial respiration

Mitochondria are the principal sites of skeletal muscle fuel metabolism and ATP production. It follows then that mitochondrial metabolism should be suppressed in disused skeletal muscles of aestivating or hibernating animals. Following four months of aestivation, *C. alboguttata* had depressed skeletal muscle mitochondrial respiratory flux by approximately 45% and whole-animal metabolic rate by almost 70%. The suppression of skeletal muscle mitochondrial- and whole-animal respiration clearly maximises energy savings for aestivating frogs. These results are in agreement with previous work on *C. alboguttata*, which demonstrated suppression of skeletal muscle mitochondrial and whole-animal respiration

during aestivation by more than 80% (Kayes et al., 2009b). The greater magnitude of metabolic depression in that study may be related to a longer period of aestivation and/or differences in the preparation of isolated mitochondria. Previous studies on aestivating frogs have recorded metabolic depression in tissues other than skeletal muscle, such as liver and skin (Flanigan et al., 1993; Kayes et al., 2009). In addition, the magnitude of metabolic rate depression of different skeletal muscle types has been shown to vary in aestivating muscle dependent on the size and/or type of muscle (Flanigan et al., 1993; Young et al., 2011). The gastrocnemius muscle has been estimated to account for only 8% of the entire muscle mass in *C. alboguttata* (Kayes et al., 2009), thus metabolic depression within other muscle types (and organs) would contribute to the 70% whole-animal metabolic suppression in frogs.

Whereas both resting and active mitochondrial respiration were significantly depressed in skeletal muscle of aestivators, cardiac muscle mitochondrial respiration remained similar between aestivating and control frogs across all respiratory states. In amphibians, the response of the heart during aestivation varies depending on the species. Heart rate has been shown to decrease (Gehlbach et al., 1973; Glass et al., 1997; Seymour, 1973b) or remain unchanged (Loveridge and Withers, 1981) in aestivators when compared with their awake conspecifics. While the coordinated downregulation of many organ and cell functions is a key priority during dormancy (e.g. transport across cell membranes, transcription, protein synthesis), aestivators must also reprioritise the use of ATP to support critical functions. The maintenance of mitochondrial respiration in aestivating *C. alboguttata* cardiac muscle at control levels suggests that aestivators continue to produce ATP in the heart for important functions such as contraction and relaxation, and membrane transport systems (e.g. Na^+/K^+ -ATPase). This is consistent with the requirement to continue adequate delivery of blood and oxygen to the tissues, whilst ensuring the cardiovascular system is ready to sustain sudden activity upon arousal from aestivation. Our heart data are supported by recent studies examining mitochondrial respiration of cardiac muscles in hamsters (*Phodopus sungorus*) and squirrels (*S. tridecemlineatus*) (Gallagher and Staples, 2013; Kutschke et al., 2013). In both these studies, torpid animals were shown to maintain their rate of cardiac mitochondrial oxygen consumption at levels similar to that of control (i.e. interbout euthermic) animals across a range of respiratory states.

ROS (H_2O_2) production

In the current study we hypothesised that aestivating *C. alboguttata* would produce less ROS from permeabilised muscle fibres relative to awake frogs. Skeletal muscle ROS production during $LEAK_N$ tended to be lower in aestivating animals, and was significantly decreased at sub-saturating substrate concentrations. Furthermore, aestivating frogs also produced less ROS per O_2 turned over (Fig. 4A), which suggests that aestivators can modulate the handling of electrons in the electron transport system independently of simply suppressing electron flow. We note there was particularly high variation in ROS production among control frogs at higher, saturating substrate concentrations, precluding a statistically-significant difference between aestivators and controls in this latter part of the experiment. In a recent study, Brown et al (Brown et al., 2013) suggested that sub-saturating mitochondrial substrate (succinate) concentrations are more physiologically-relevant *in vivo*. Indeed, the concentration of succinate in many mammalian tissues is considered to be low, in the 0.2–0.5 mM range (Starkov, 2008). Succinate (or malate or pyruvate) concentration data is not presented as these metabolites change rapidly (Zoccarato et al., 2009). However, blood glucose concentrations were much lower in aestivators than active *C. alboguttata* (this present study) and aestivators are likely to have a decreased reliance on carbohydrate metabolism in skeletal muscle (Reilly et al., 2013; Storey and Storey, 2010). While lipid-based substrates may dominate carbohydrates in aestivating animals, fatty acids can uncouple mitochondria, further suppressing ROS production in aestivators.

Previous studies have shown that aestivating *C. alboguttata* sustains hindlimb muscle mass until 6-9 months of aestivation (Hudson et al., 2006; Mantle et al., 2009). We suggest that decreased ROS production in four-month aestivating skeletal muscle may represent a mechanism by which dormant *C. alboguttata* limit muscle fibre atrophy. Indeed, a recent study found no evidence of lipid or protein oxidation (indices of ROS-induced oxidative damage) in the gastrocnemius muscle of *C. alboguttata* following 6 months aestivation (Young et al., 2013). Previous studies have also emphasised the protective effects of increased muscle antioxidant production in dormant burrowing frogs (Hudson and Franklin, 2002b; Hudson et al., 2006; Reilly et al., 2013). Together these experimental data suggest *C. alboguttata* maintain an appropriate ratio of antioxidants to pro-oxidants, and this should prevent oxidative stress and premature skeletal muscle fibre atrophy. Decreased production of ROS in *C. alboguttata* skeletal muscle is in contrast to what has been observed during immobilisation-induced muscle atrophy in mammalian models (Min et al., 2011). Two weeks

of cast immobilisation in mice resulted in both increased rates of mitochondrial H_2O_2 release from permeabilised skeletal muscle fibres and higher levels of muscle lipid peroxidation, while administration of a mitochondrial-targeted antioxidant to mice also inhibited the increase in muscle mitochondrial H_2O_2 production and attenuated myofibre atrophy.

Given that mitochondrial respiration in *C. alboguttata* permeabilised cardiac muscle fibres was not different between controls and aestivators, it is perhaps not surprising that mitochondrial ROS production from the heart was also unchanged. Due to its high energetic demand and abundance of mitochondria the heart is presumably very sensitive to oxidative damage. Data on the production of mitochondrial ROS from heart tissue and their role in cell signalling during dormancy are lacking in the literature. However, there is little evidence for oxidative damage occurring in cardiac muscle during aestivation, while protein and enzyme activity levels of antioxidants within heart have been shown to increase, decrease or remain unchanged depending on the species, duration of aestivation and specific antioxidant measured (Grundy and Storey, 1998; Page et al., 2010; Salway et al., 2010). It is difficult to draw conclusions about the effects of ROS production in aestivating *C. alboguttata* cardiac muscle. It is conceivable that aestivating *C. alboguttata* may modulate antioxidants in the heart to protect macromolecules from potentially lethal stress-induced damage. On the other hand, ROS have been shown to significantly contribute as regulators of cell signalling pathways in model organisms (Burgoyne et al., 2012), and ROS are likely to have similar roles in cardiomyocytes of other vertebrates as well. Clearly, additional well-designed experiments are needed to determine the relative importance of ROS in cell signalling and/or oxidative stress in heart tissue during dormancy.

Concluding remarks

We have shown that *C. alboguttata* heart and skeletal muscle tissue respond differently during aestivation with respect to mitochondrial respiration and ROS production. This is of particular interest, as it exemplifies *C. alboguttata's* capacity to independently regulate distinct organs throughout dormancy. The downregulation of mitochondrial respiration in gastrocnemius muscle is consistent with markedly reduced muscle contraction throughout the aestivating period, allowing significant energy savings for dormant frogs. Muscle is a highly excitable tissue and its metabolic rate can increase rapidly within a very brief period of time. Thus, it is likely that skeletal muscle mitochondrial respiration is quickly restored to normal levels to facilitate muscle contraction when aestivating *C. alboguttata* arouse. Whereas skeletal muscle essentially ceases function but can contract upon arousal, it

is imperative that the burrowing frog heart maintain its morphology and contractile activity during aestivation. Maintenance of mitochondrial respiration in *C. alboguttata* cardiac muscle would allow the slow, but sustained supply of ATP for critical heart functions. ROS production generally reflected mitochondrial respiration in the different muscles. At low mitochondrial substrate concentrations, ROS production was significantly lower in the gastrocnemius muscle fibres of aestivating burrowing frogs, which may represent a mechanism contributing to the limited muscle atrophy observed in this species despite extended hindlimb disuse. Production of ROS in cardiac muscle fibres did not change during aestivation, and further research is required to determine the roles of mitochondrial ROS in cardiomyocyte signalling and homeostasis during metabolic depression.

Chapter 4

Activity, abundance and expression of Ca^{2+}-activated proteases in skeletal muscle of the aestivating frog, *Cyclorana alboguttata*

INTRODUCTION

During extreme environmental conditions many animals enter into dormancy, a period of inactivity that prolongs the amount of time an organism may survive on endogenous fuel reserves (Storey and Storey, 1990). Many Australian terrestrial frogs such as the Green-striped burrowing frog, *Cyclorana alboguttata* inhabit arid environments and avoid desiccation by burrowing beneath the ground and entering a prolonged metabolic suppression called aestivation. Aestivating *C. alboguttata* also form a cocoon made by the accumulation of shed epidermis, which functions as a barrier to water loss. In this capacity, aestivating frogs are immobile in their burrows for months or even years at a time (Withers, 1993; Withers, 1995). Aestivating burrowing frogs do not arouse intermittently during dormancy to eat or drink, and long-term viability is likely to depend upon lipid reserves laid down prior to aestivation (Van Beurden, 1980). Like many hibernating mammals, aestivating *C. alboguttata* have been shown to be remarkably resistant to skeletal muscle atrophy despite extended periods of chronic muscle inactivity and fasting (Hudson and Franklin, 2002a; Hudson et al., 2006; Mantle et al., 2009; Symonds et al., 2007). Such resistance to muscle atrophy would be beneficial as upon heavy rainfall, frogs can arouse from aestivation with the capacity to immediately feed and breed before the highly ephemeral waters retreat.

Atrophy in skeletal muscles during conditions of prolonged disuse (e.g. cast immobilisation, extended bed rest, muscle unloading) and/or fasting, has debilitating effects in most mammalian species (Hudson and Franklin, 2002b). Disuse-induced muscle atrophy is characterised by a decrease in muscle mass and strength, which is related to an imbalance in muscle protein synthesis and degradation (Thomason et al., 1989). Although the molecular and cellular mechanisms that regulate these processes are complicated, evidence indicates that reactive oxygen species (ROS) regulate cell signalling pathways that control both protein synthesis and protein degradation in skeletal muscle (Powers et al., 2011). Specifically, ROS have been shown to increase the expression and activity of the calpain proteases in skeletal muscle. Calpains are Ca^{2+}-dependent cysteine proteases found in all vertebrate cells and are primarily regulated by intracellular Ca^{2+} concentrations and activity of the endogenous calpain inhibitor, calpastatin (Goll et al., 2003). The ubiquitous calpains, isoforms 1 and 2, or μ- and

m-type, respectively, are thought to be the initiators of myofibrillar protein degradation during muscle atrophy (Bartoli and Richard, 2005). With respect to ROS, treatment of human skeletal muscle satellite cells with hydrogen peroxide (H_2O_2) was shown to increase the expression of both calpain 1 and 2 genes (Dargelos et al., 2010), whereas exposure of mouse myoblast cells to H_2O_2 elevated calpain 1 activity and led to myotube atrophy (McClung et al., 2009).

Other studies have indicated that calpain activation might be an early, necessary stage in the development of disuse-induced muscle atrophy, but results have been mixed and controversial (Bartoli and Richard, 2005; Enns et al., 2007; Jones et al., 2004; Maes et al., 2007; Taillandier et al., 1996). However, experiments have also demonstrated that pharmacological inhibition of calpain results in prevention of skeletal muscle atrophy imposed by both hindlimb casting and hindlimb suspension (Talbert et al., 2013a; Tischler et al., 1990). It is thought that calpains might degrade several muscle structural proteins during atrophy, thus releasing actin and myosin from sarcomeres allowing them to be targeted for degradation by another major proteolytic pathway, the ubiquitin-proteasome system (UPS) (Mitch and Goldberg, 1996; Talbert et al., 2013a).

Calpain 3 (p94) is another calpain isoform which is largely expressed in skeletal muscle. Calpain 3 is found within sarcomeres where it specifically binds to the giant protein titin, which is critical for the contraction of striated muscle tissue (Duguez et al., 2006). Gene mutations in calpain 3 cause limb girdle muscular dystrophy type 2A, while calpain 3 deficiency leads to irregular sarcomeres and impairment of muscle contractile capacity (Duguez et al., 2006). In contrast to calpains 1 and 2, which can exhibit a positive correlation with tissue degradation during muscle disuse, calpain 3 mRNA has been shown to be downregulated during the atrophic phase seen in denervation and limb immobilisation models (Chen et al., 2007; Jones et al., 2004; Stockholm et al., 2001).

For dormant animals such as aestivators or hibernators, energy (or energetically) expensive processes such as proteolysis must be tightly regulated to ensure enzyme/protein concentrations are stabilised over what could be a prolonged period of metabolic suppression (Storey and Storey, 2010). In hibernating mammals there is evidence that proteolytic activity is downregulated at low temperatures during dormancy, but recommences during periodic arousals (van Breukelen and Carey, 2002; Velickovska et al., 2005; Velickovska and van Breukelen, 2007). Evidence also suggests that protein degradation is strongly suppressed in different tissues of aestivating snails (Ramnanan et al., 2009). Given that *C. albogutatta*

demonstrate appreciably little muscle wasting during extended periods of aestivation, the mechanisms of proteolytic control in skeletal muscle remain an interesting and unexplored avenue. In a recent study ROS production was found be suppressed in the disused skeletal muscle of aestivating frogs, which was suggested to possibly protect against potential oxidative damage and preserve skeletal muscle mass during aestivation (Reilly et al., 2014) (Chapter 3).

Given the mechanistic links between ROS and calpains in mammalian models of muscle disuse atrophy, the aim of the present study was to examine the biochemical activity of calpains 1 and 2 in aestivating versus control *C. alboguttata* skeletal muscle to better understand the role calpains might play in the relative preservation of aestivating skeletal muscle structure and function. Additionally, we sought to identify putative *C. alboguttata* homologs of calpains 1, 2 and 3 and measure their relative protein levels and messenger RNA (mRNA) transcript abundance in control versus aestivating frog skeletal muscle using western blotting and quantitative real-time polymerase chain reaction (qPCR), respectively. We hypothesised that calpain activity and expression are suppressed in muscle of aestivating frogs relative to awake, control frogs, which may contribute to a decrease in skeletal muscle proteolysis and preservation of muscle mass during extended periods of immobility.

MATERIALS AND METHODS

Study animals and experimental treatments

Active *C. alboguttata* were collected after heavy summer rains from the districts of Dalby and Theodore, Queensland, Australia (Scientific Purposes Permit WISP10060511). Frogs were transported in individual plastic bags to the University of Queensland. Frogs were split into two treatment groups. Control frogs were active and were fed live food (crickets and cockroaches) weekly, whereas the treatment group consisted of frogs that had been aestivating for four months. The latter group was induced into aestivation by placing them into glass jars with water and paper pellets (Breeders Choice Cat Litter) until the water slowly evaporated. During experimentation, control frogs were maintained under a 12:12 h light-dark regime, while aestivating frogs were kept in 24 h darkness. Resting rates of oxygen consumption were measured using closed-system respirometry as previously described (Reilly et al., 2013). Frogs were removed from their aestivation chambers at the end of the 4-month treatment period and were immediately sacrificed by cranial and spinal pithing. The body mass and

snout-vent length (SVL) were measured for each individual before muscle dissection. All experiments were conducted with the approval of the University of Queensland Animal Ethics Committee (permit number: SBS/238/11/ARC). In the present study the gastrocnemius muscle was selected for analysis because this muscle produces the force necessary for jumping, and in *C. alboguttata* has been shown to be less sensitive to atrophy compared with the smaller non-jumping muscles (e.g. sartorius, iliofibularis) (Mantle et al., 2009). For practical reasons, the exact same frogs were not used in the enzyme activity, protein abundance and gene expression studies. Frogs in the current experiment were used for enzyme activity and western blot studies (hereinafter Group 1), whereas frogs used in gene expression analyses were sourced from the RNA Seq experiment (Chapter 2; Reilly et al. 2013; hereinafter Group 2). Despite this, gastrocnemius muscles were dissected out and weighed using the same protocol in both experimental groups.

Enzyme activity

To test the effect of aestivation on muscle calpain activity, gastrocnemius muscle tissue was extracted from aestivating (N = 8) and control (N = 8) frogs immediately after pithing and was snap frozen in an airtight cryotube. Muscles were then stored at -80°C until analysis. Prior to analysis, frozen muscle tissue was double wrapped in industrial strength aluminium foil and pulverised with a hammer on a metal plate over dry ice. Samples were homogenised with an Ultra-turrax homogeniser (IKA T10 Basic, Labtek, Brisbane, Queensland, Australia) in ice cold Passive Lysis Buffer (E1941; Promega, Madison, WI, USA). Muscle extracts were separated from debris by centrifugation at 10,000 *g* for 10 min at 4°C (Beckman Coulter Allegra 25R bench-top centrifuge, Gladesville, NSW). Calpain 1 and calpain 2 activities was measured simultaneously using a luminogenic succinyl calpain substrate ((Suc-LLVY-aminoluciferin) Calpain-Glo; Promega). Muscle extract (50 µl) was added to a microtiter plate well, and Calpain-Glo reagent supplemented with Suc-LLVY-aminoluciferin and 2.5 mM $CaCl_2$ was added to bring the total volume to 100 µl. The plate was incubated at 25°C and the luminescence signal monitored every 5 min for 45 min using a Beckman Coulter DTX880 multimode detector (Beckman Coulter Aust. P/L, Gladesville, NSW, Australia). Control assays were performed under identical conditions, except that $CaCl_2$ was omitted and 10 mM EDTA and 10 mM EGTA was added to the assay. Calpain activity was calculated as the difference between activity measured in the presence of 2.5 mM calcium and the activity measured in the absence of $CaCl_2$ and the presence of 10 mM

EDTA/10 mM EGTA. Protein concentration was determined by the Coomassie Plus (Bradford) Assay (ThermoScientific) with BSA as a standard. All assays were performed in triplicate and calpain activity was expressed in arbitrary units (AU) per µg of protein.

Semi-quantitative western blotting

Protein abundance of calpains 1, 2 and 3 was determined in gastrocnemius muscle samples via Western blot analysis. Muscle tissue was collected from animals at the time of pithing, snap frozen in an airtight cryotube and stored at -80°C until analysis. Frozen muscle tissue was prepared as above, except that samples were homogenized in ice cold passive lysis buffer supplemented with 50 mmol l^{-1} EGTA, and centrifuged at 3,000 *g* for 10 min at 4°C. After collection of the resulting supernatant muscle protein content was determined. Protein samples (20 or 30 µg) were heated to 70°C for 10min and then loaded into 4–12% Bolt Bis-Tris Plus gels (Life Technologies, Mulgrave, VIC, Australia) and run at 155 V for approximately 45 minutes. Following electrophoresis, the proteins were transferred to PVDF membranes (Westran® Clear Signal; 25 V, 90 min). Membranes were then rinsed with distilled water, air dried and stored at -80°C until stained.

Membranes were briefly rewet in methanol and exposed at 4°C overnight to either rabbit anti-calpain 1 (N3C2), rabbit anti-calpain 2 (N2C1-2) or rabbit anti-calpain 3 (C1C3) primary antibodies (1:2000). Membranes were then incubated in a goat anti-rabbit secondary antibody (1:2000) followed by visualisation using a colourmetric horseradish peroxidase-3'3' diaminobenzidine system. All primary antibodies were purchased from Genetex, Inc., Irvine, CA, USA. Blots were converted into digital images using a Canoscan colour image scanner (Canon) and analysed using ImageJ software (National Institutes of Health, Bethesda, MD, USA). Protein abundance of calpains 1, 2 and 3 was determined by comparing the density of bands from aestivating frog muscle homogenate (N = 7) relative to those of control frogs (N = 7). The density of each calpain band was normalized by a respective ~42 kDa band present on each membrane, which was likely to represent alpha-actin. For each blot an equal amount of active human calpain 1 (Biovision, Milpitas, CA, USA) and mouse gastrocnemius muscle tissue were loaded to facilitate interpretation of antibody binding to *C. alboguttata* protein.

RNA extraction, reverse transcription and sequencing

A portion of gastrocnemius muscle was immediately excised and placed into RNA*later*® (Ambion). Muscle samples were stored at 4°C overnight and then transferred to -80°C until processed. Total RNA was extracted from frozen tissue using a commercially available kit (PureLink RNA Mini Kit, Invitrogen, Mount Waverley, VIC, Australia) as previously described (Reilly et al., 2013) (Chapter 2).

cDNA synthesis and cross-species primer design

First-strand cDNA was synthesised from 2 µg of RNA using an iScript cDNA synthesis kit (Biorad) with oligo (dT) and random primers. The samples were purified and eluted using a High Pure PCR Product Purification Kit (Roche, Castle Hill, NSW, Australia). Contaminating RNA was eliminated by incubating the samples with 0.5 µl RNase H (Invitrogen) for 20 min at 37°C. Degenerate primer pairs were designed both manually and using CODEHOP (Staheli et al., 2011) to amplify *cpn1* (calpain mu-type), *cpn2* (calpain M-type), and *cpn3* (calpain p94) genes in burrowing frog muscle (Table 4.1). Known protein sequences from other vertebrates were obtained from the National Center for Biotechnology Information database (www.ncbi.nlm.nih.gov/) using the basic local alignment search tool (BLAST). Protein sequences were aligned using the program ClustalW (www.genome.jp/tools/clustalw/) and degenerate primers were designed from highly conserved regions of amino acid sequence within the alignment.

Selecting an appropriate reference gene for normalisation of quantitative gene expression (qRT-PCR) data is crucial for obtaining biologically-meaningful results. This is particularly significant in regard to studies examining gene expression in hypometabolic organisms, which may experience dramatic physiological and/or morphological changes during experimentation. Thus, we also used primer pairs to amplify a selection of candidate reference genes, including glyceraldehyde-3-phosphate dehydrogenase (*gapdh*), histidine triad nucleotide binding protein 1 (*hint1*), methylmalonyl CoA mutase (*mut*) and SH3 and cysteine rich domain containing protein 3 (*stac3*) (Table 4.1). Normfinder software (Andersen et al., 2004) was used to determine the most stable, least variable, reference gene from our candidate set. We found *mut* to be the most stable reference gene in gastrocnemius of control and aestivating frogs (data not shown).

Table 4.1. Degenerate and specific primers used in standard and qRT-PCR experiments

Gene	Assay	Orientation	Primer Sequence (5' to 3')
Target genes			
capn1	Initial RT-PCR	Sense	AAYTWYCCWGCCACHTTYTGG*
		Antisense	HGTAKCKSRKRATGATSAGCT*
capn2	Initial RT-PCR	Sense	ATCTGCCAAGGAGCCCTGGGNGAYTGYTGG†
		Antisense	GGATCCGTTCAGTTTGGCRTANGCYTTYTC†
capn3	Initial RT-PCR	Sense	CTGGAATCTTCCATTTYCARTTYTG†
		Antisense	TCTTTCCTCCGGTYYTTYTGCATNA†
Candidate reference genes			
gapdh	Initial RT-PCR	Sense	CTGGCTCCTCTTGCAAAGGT**
		Antisense	GTGTATCCCAGGATTCCCTTC **
hint1	Initial RT-PCR	Sense	GGGAAAATTATCCGCAAAGARATHCCNGC †
		Antisense	AGGTGAAGGTGGTACACNGAYTGNCCNC †
mut	Initial RT-PCR	Sense	AACGCTGTTTGGCTGCAATC ††
		Antisense	ATCGCTGGCTTTGTGTTCAC ††
stac3	Initial RT-PCR	Sense	CCAAAACAGGAGGAAGGAAAGC ††
		Antisense	TTCTCCAGCGCTTTGAAACG ††
Target & reference genes			
capn1	qRT-PCR	Sense	GAGAGGCGGTTTGGAAAGGA
		Antisense	CACGTTTAAGGTGCACAGCC
capn2	qRT-PCR	Sense	CGGACCAGAGTTTCCAGGAG
		Antisense	AACCACGTCCACCCATTCTC
capn3	qRT-PCR	Sense	ATGATTCAGGGTGTGGGTGAC
		Antisense	AACTGTGCAGGGACAATTGC
mut	qRT-PCR	Sense	As above
		Antisense	As above

*Modified from primers presented in (Macqueen et al., 2010); **primers designed by (Kumano et al., 2008); †Primers designed using CODEHOP (Staheli et al., 2011); †† Species-specific primers used.

Gene amplification, sequencing and qRT-PCR

The *C. alboguttata* cDNAs were amplified using touchdown PCR reactions before amplicons were size-separated by agarose gel electrophoresis. Extracted amplicons were purified and concentrated using a PureLink® PCR Micro Kit (Life Technologies). The cleaned amplicons were directly sequenced by the Australian Genome Research Facility (AGRF) using capillary separation (Purified DNA service). We designed qRT-PCR primers (to amplify targets of 80-170 bp) based on the *C. alboguttata* sequences returned from AGRF using Primer3Plus (Untergasser et al., 2007); Table 4.1). qRT-PCR reactions were performed in duplicate using iTaq Universal SYBR Green Supermix (Biorad) on a MiniOpticon detection system (Biorad). Each reaction contained 4.3 µl of diluted cDNA (1:10) and 300 nmol l^{-1} of each primer in a total reaction volume of 10 µl. Cycle parameters were: 95°C for 60 s, followed by 40 cycles of 95°C for 15s, 59°C for 15s and 72°C for 30s. Each assay included a no-reverse transcriptase and a no template control, as well as melt curve analysis to verify amplification of only a single product in the reaction. All PCR efficiencies were ≥85% and the expression of each gene was quantified using the ΔCt method with *mut* as the endogenous reference gene.

Transcriptomic analysis of calpains

A *de novo C.alboguttata* muscle transcriptome assembly (Reilly et al., 2013) (Chapter 2) was used to identify different calpain isoforms. Candidate isoforms were searched against the nonredundant National Center for Biotechnology Information (NCBI) protein database (BLASTx) with an expectation value of 0.001. Identified calpain isoforms were then examined for differential gene expression using the Bioconductor package EdgeR as previously described (Reilly et al., 2013) (Chapter 2), and compared with qRT-PCR results to validate each method.

Statistics

The enzyme activity, protein abundance and qRT-PCR expression data were visualised using Q-Q plots and tested for normality using the Shapiro-Wilk Test. A one-way ANCOVA was used with SVL as the covariate to examine the effect of aestivation on muscle wet mass. Data sets with non-normal error distribution were analysed using a Wilcoxon rank-sum test whereas parametric data were analysed using ANOVA. All data were examined for constancy of variance and statistical tests were performed in R. In all tests α was set at 0.05.

RESULTS

There was no significant difference in body size (SVL) of *C. alboguttata* individuals from Group 1 (mean ± s.e.m. 54.69 ± 0.95 mm) compared with frogs from Group 2 (55.42 ± 0.91 mm; P=0.59). Consequently, muscle mass data from the two groups were combined to test the effect of aestivation on gastrocnemius wet mass. The effect of aestivation on gastrocnemius wet mass was not significant, however muscle mass was significantly related to body size (ANCOVA: full model, P=0.11; treatment, P=0.33; relationship to SVL, P<0.001; Table 4.2). Similarly, aestivating gastrocnemius muscle exhibited no significant reduction in muscle protein concentration or cross-sectional area during aestivation (P = 0.27 and 0.70, respectively, Table 4.2). However, muscles from aestivating frogs from Group 2 exhibited a much greater loss in wet mass (~ 23%) compared with Group 1 aestivators (~ 12%), despite having similar body sizes and both groups experiencing four months of dormancy (data not shown).

Table 4.2. Measurements of wet mass, total protein content and whole muscle cross-sectional area of *Cyclorana alboguttata* gastrocnemius muscles

	Control	Aestivation
Wet mass (mg) †	268.78 ± 22.08 (19)	219.14 ± 13.74 (17)
Total protein content (mg g^{-1} wet mass)	40.56 ± 3.76 (8)	45.98 ± 2.78 (8)
Muscle cross-sectional area (mm^2) ††	22.79 ± 2.06 (8)	14.83 ± 1.36 (9)

Values represent means ± s.e.m.; numbers in parentheses represent number of animals. † Muscle wet masses of frogs used in the current study (Group 1) were combined with those sourced from Chapter 2 (Group 2; Reilly et al. 2013). There was no significant effect of aestivation on body size-adjusted muscle wet mass or muscle protein content. †† Similarly, our previous study indicated aestivation had no significant effect on body size-adjusted whole muscle cross-sectional area. (Chapter 2; Reilly et al. 2013).

Calpain activity

In the present study the activity levels of calpains 1 and 2 were approximately 44% lower in gastrocnemius muscle of aestivating frogs relative to those of active *C. alboguttata* (P = 0.28, Fig. 4.1). The absence of a significant difference may be due to the high level of variation in control frogs (Fig. 4.1). When activity was normalized to tissue rather than

protein (activity/g^{-1} wet mass), the activity levels of calpains 1/2 were approximately 10% lower in muscle of aestivators compared with active *C. alboguttata* (data not shown).

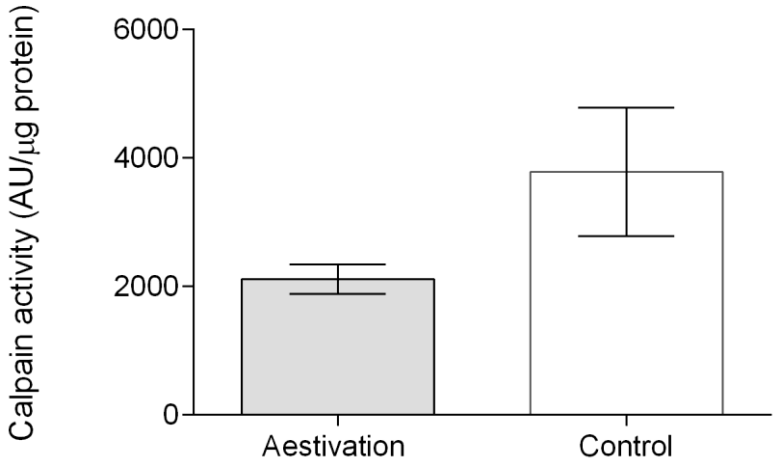

Figure 4.1. Effect of four months of aestivation on the enzyme activity levels of calpain 1 and calpain 2 in the gastrocnemius muscle of *Cyclorana alboguttata*. Calpain activity was determined by calpain cleavage of the substrate Suc-LLVY-aminoluciferin in the presence of 2.5 mM $CaCl_2$, or the absence of $CaCl_2$ and the presence of 10 mM EDTA/10 mM EGTA. Data are presented as mean ± s.e.m in arbitrary units (AU); N = 8 for both aestivating and control frogs.

Calpain protein abundance

Western blots were used to ascertain whether calpain 1, 2 and 3 were present in *C. alboguttata* muscle homogenate. Firstly, the human amino acid sequences used by Genetex to produce the calpain antibodies (amino acids (AA) 317-493 for calpain 1; AA 317-374 for calpain 2 and AA 528-741 for calpain 3) were aligned against the calpain isoform nucleotide sequences (i.e. translated using *C. alboguttata* contigs using blastx; Table 4.3) generated from the *C. alboguttata* transcriptome to determine the degree of similarity between the species. Homologies between the two species in these regions were 72%, 81% and 77% for calpains 1, 2 and 3, respectively (Fig. 4.2). However, the *C. alboguttata* calpain 2 predicted sequence was not entirely full-length, thus the exact percent similarity with the human epitope region is unknown. Secondly, the *C. alboguttata* predicted protein sequences were imported into ProtParam (http://web.expasy.org/protparam/) to obtain predicted molecular weights (MW) for the different frog calpain isoforms. The predicted MW and length of *C. alboguttata* calpain 1 was 80 kDa; 705 AA, whereas calpain 3 was 92.5 kDa and 808 AA. These results are consistent with data from other species. Because *C. alboguttata* calpain 2 was a partial

sequence, its predicted MW was 74 kDa. It is likely however, that full length *C. alboguttata* calpain 2 has a MW of 80 kDa.

Table 4.3. Log2 fold-changes of calpain genes in gastrocnemius muscle of *C. alboguttata* as determined by RNA Seq (CLC Genomics Workbench) and exact tests conducted in EdgeR

	Symbol	Top Hit Accession No.	% Similarity	*P* value	Log2 fold change
Calpain 1, large subunit	*capn1*	NP_001013631	88	0.43	0.33
Calpain 2	*capn2.2*	NP_001005446	80	0.27	-0.62
PREDICTED: calpain 3-like isoform X2	LOC100497532	XP_004917296	81	0.80	0.10
Calpastatin, putative	*cast*	CAB62094.2	63	0.94	-0.03

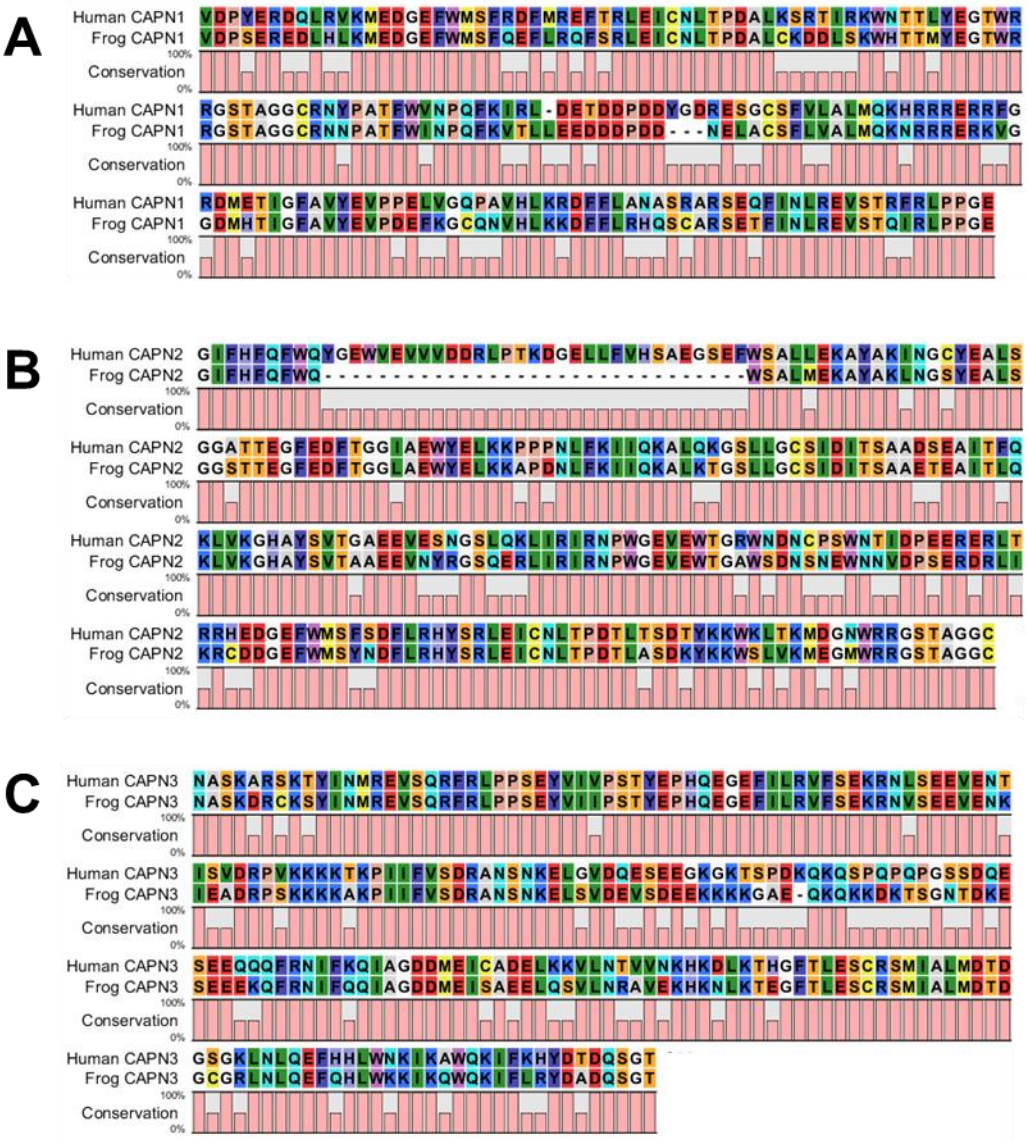

Figure 4.2. Human amino acid sequences used to produce the epitope for calpain (A) 1, (B) calpain 2 and (C) calpain 3 antibodies (AA317-493 for calpain 1; AA317-374 for calpain 2 and AA528-741 for calpain 3; Genetex, Inc.) aligned against corresponding region of *C. alboguttata* calpain proteins. Homologies between the two species in these regions were 72%, 81% and 77% for calpains 1, 2 and 3, respectively. Note that *C. alboguttata* calpain 2 is only a partial sequence whereas calpains 1 and 3 are full length in the epitope region.

As calpains have not previously been reported in burrowing frog muscle, we compared protein bands identified using the anti-calpain antibodies in both mouse and *C. alboguttata* gastrocnemius muscle (Fig. 4.3). In mammalian muscle calpain 1 (80-82 kDa) is usually an inactive proenzyme. Its activation involves autolysis to a 78-kDa and then to a 76-kDa protein, both of which are proteolytically active calpain 1 isoforms (Baki et al., 1996). Similarly, autolysis of full-length calpain 2 (80 kDa) results in a 78-kDa proteolytically active protein (Edmunds et al., 1991). Both calpain 1 and calpain 2 were detected in mouse and frog muscle samples at the expected MW (75-80 kDa), although there appeared to be a difference in mobility between the mouse/frog samples and the active human calpain 1 enzyme, with calpain 1 appearing marginally smaller in *Mus* and *Cyclorana* (Fig. 4.3A, B). Although autolysed calpains are often observed as the cleaved, shorter products during western blot experiments (Murphy et al., 2006), there was little to no evidence of autolysis of calpain 1 or calpain 2 in aestivating or active *C. alboguttata* muscle (Fig. 4.3A, B). In mouse however, autolysis of calpain 2 may be seen as the appearance of a very faint, second smaller band (Fig. 4.3B). The relative protein abundance of calpain 1 and calpain 2 was not significantly different between control and aestivating animals (P = 0.47 and 0.09, respectively; Fig. 4.4A, B).

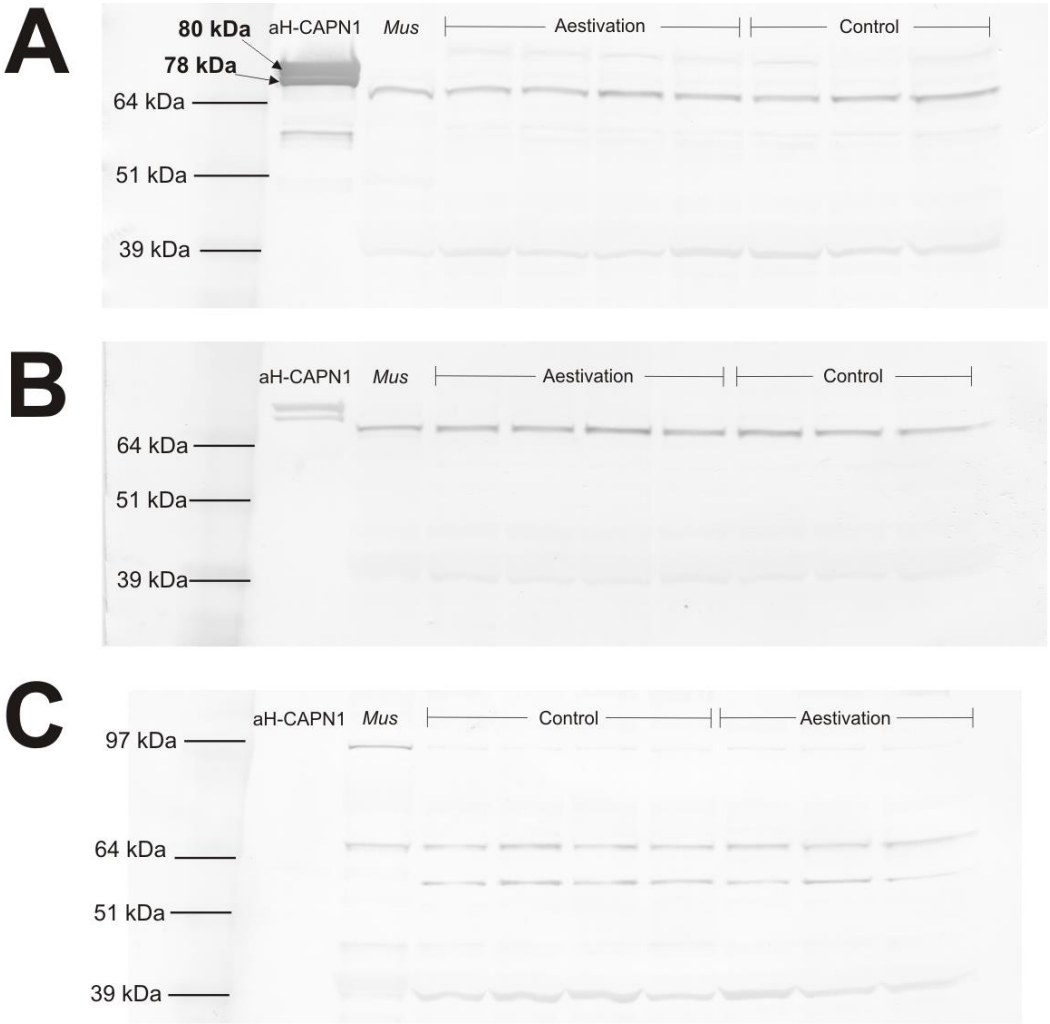

Figure 4.3. Calpain isoforms during aestivation and while active (control) in skeletal muscle of *Cyclorana alboguttata*. Representative Western blots for calpain 1 (A), calpain 2 (B) and calpain 3 (C) in mouse (*Mus*) and *C. alboguttata* gastrocnemius muscles are shown. The same samples were used in each Western blot and lanes contained equivalent amounts of protein from muscle extracts prepared from individual animals. All muscles were homogenized in lysis buffer containing 50 mM EGTA. Full-length calpain 1 (~80 kDa) is evident in mouse and burrowing frog samples; autolysed fragments (~78 and 76 kDa) are not seen. Similarly, full-length calpain 2 can be seen in mouse and frog homogenates with an absence of smaller autolysed bands. Full-length calpain-3 at ~94 kDa is clear in mouse, with only faint bands apparent in *C. alboguttata* samples. In contrast, lysed calpain-3 bands at ~60-56 kDa are strong in frog but absent in mouse. The bands at ~75-80 kDa in the lanes containing the mouse and frog homogenates have previously been observed in homogenates from rat and toad skeletal muscle (Verburg et al., 2005) (see RESULTS). Equal amounts of active human calpain 1 enzyme (aH-CAPN1) were loaded in each blot. Note the intensity of staining of aH-CAPN1 in panel A, and the lighter background and absence of staining when using calpain 2 and 3 antibodies (B, C). Molecular masses are shown at *left*.

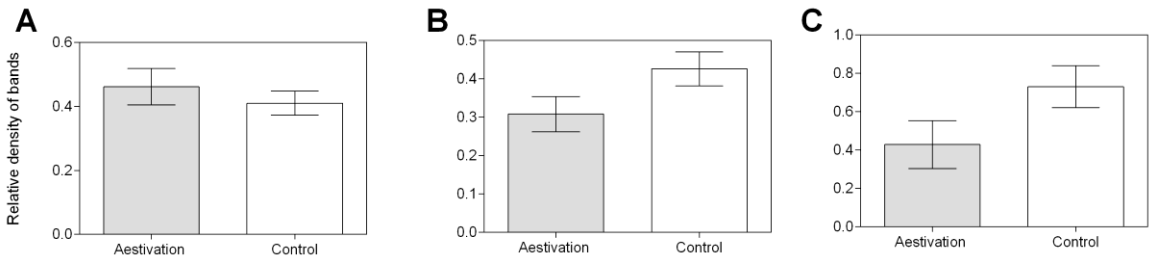

Figure 4.4. Protein abundance of (A), calpain 1, (B) calpain 2 and (C) calpain 3 during aestivation and while active (control) in gastrocnemius muscle tissue of *Cyclorana alboguttata*. Total protein was extracted from muscle of aestivators (N = 7) and while frogs were awake and active (control; N = 7). Lanes contained equivalent amounts of protein from individual animals and were analysed using Western blot analysis (see Fig. 2). The density of putative calpain bands were calculated as the density of each band normalised to relative to the density of a ~42 kDa band visible in each blot likely representing alpha-actin. Data are presented as mean ± s.e.m. In all cases one-way ANOVA indicated that the total protein abundance of calpains did not change significantly during aestivation. P = >0.05.

The autolysis of calpain 3 (94-kDa), results in the formation of 60-, 58-, and 56-kDa proteins (Taveau et al., 2003). In contrast to humans, previous characterisation of calpain 3 protein expression has shown that in addition to protein bands at ~ 94 and 58 kDa, immunoblotting of muscle from rat, mouse, hamster, chicken and toad detects a strong band at ~ 82 kDa (Anderson et al., 1998; Kramerova et al., 2004; Verburg et al., 2005). This 82 kDa protein is unlikely to be calpain 3 given that it was reported to be Ca^{2+} insensitive (Murphy et al., 2006; Verburg et al., 2005). Consistent with these studies, we also observed two bands of approximately 94 and 75-82 kDa in both mouse and frog gastrocnemius homogenate (Fig. 4.3C). However, the 94 kDa bands were relatively faint in *C. alboguttata* compared with mouse (Fig. 4.3C). A band of approximately 56-60 kDa was consistently observed in frog homogenates and may represent autolysed calpain 3 (Fig. 4.3C). The intensity of this 56-60 kDa band did not increase in aestivating animals. Like calpain 1 and 2, relative endogenous protein levels of calpain 3 (i.e. density of the 94 and 60 kDa bands combined) were not significantly different in the gastrocnemius of aestivators compared with controls (P = 0.09; Fig. 4.4C).

Calpain gene expression

The putative protein sequences of *C. alboguttata* calpain genes sequenced in the present study for qPCR experiments usually showed the highest similarity to calpain

sequences of *Xenopus* and *Silurana*, the two best annotated amphibians (Table 4.4). Calpain gene expression levels (*capn1*, *capn2* and *capn3*) were analysed relative to the expression of the reference gene *mut*. There was no effect of aestivation on the gene expression levels of *capn1*, *capn2* or *capn3* in frog gastrocnemius muscle (P = 0.99, 0.22 and 0.14, respectively; Fig. 4.5). Because the cross-species primer design, PCR and sequencing were conducted before the transcriptome assembly data (Reilly et al., 2013) was generated, we thought it interesting to examine the *C. alboguttata* muscle transcriptome for candidate calpain genes. Fourteen of the constructed contigs were related to calpain proteins in NCBI's non-redundant database with an E value of $<1e^{-3}$. These included *capn1*, *capn2*, *capn3*, *capn 5*, *capn 7*, *capn 9*, *capn 10* and the endogenous calpain inhibitor, calpastatin (*cast*). The expression patterns of the putative *capn1*, *capn2*, *capn3* and *cast* genes were compared between 4-month aestivating frogs (N = 4) with those of control animals (N = 4) using EdgeR. In agreement with results of qRT-PCR the expression levels of *capn1*, *capn2*, *capn3* were unchanged between aestivators and controls, as was the mRNA abundance of *cast* (Table 4.3).

Table 4.4. Identity and functional homology of *C.alboguttata* sequence

Gene	Putative protein sequence (Highest Annotated BLAST Hit)
gapdh	Glyceraldehyde-3-phosphate dehydrogenase, *Hoplobatrachus tigerinus*, ACN79578.1 (85%, 185, 1e-57)
hint1	Histidine triad nucleotide-binding protein 1, *Ficedula albicollis* XP_005061075.1 (78%, 128, 4e-36)
mut	Methylmalonyl CoA mutase, mitochondrial isoform X2, *Silurana tropicalis* XP_004915007.1 (91%, 1422, 0.0)
stac3	SH3 and cysteine-rich domain-containing protein 3 isoform X1, *Latimeria chalumnae* XP_005986321.1 (85%, 474, 8e-154)
capn1	Calpain-1 large subunit, *Xenopus laevis* NP_001080485.1 (85%, 462, 8e-156)
capn2	Calpain-2, *Xenopus* (*Silurana*) *tropicalis* NP001005446.1 (85%, 146, 3e-39)
capn3	Calpain-3-like isoform X2, *Xenopus* (*Silurana*) *tropicalis* XP_004917296.1 (78%, 159, 1e-152)

Numbers in parentheses represent identity (%), score (bits) and E-value, respectively.

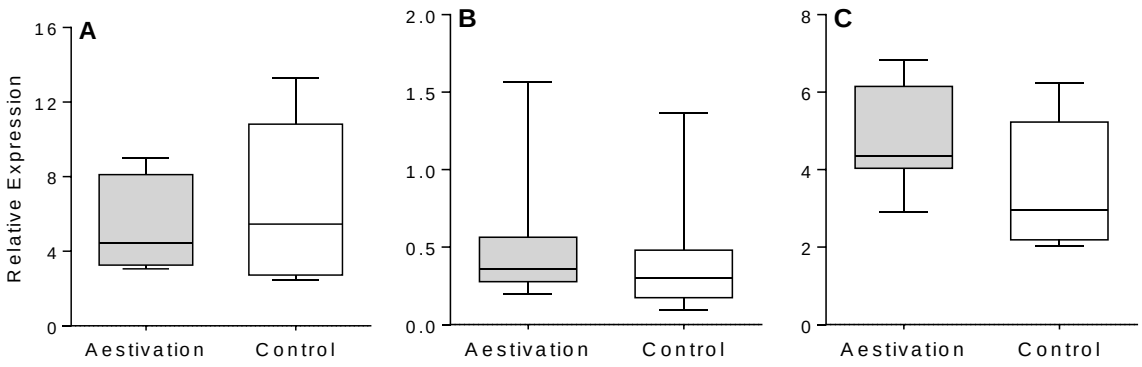

Figure 4.5. Effect of four months of aestivation on the gene expression levels of (A) calpain 1 (*capn1*), (B) calpain 2 (*capn2*) and (C) calpain 3 (*capn3*) in the gastrocnemius muscle of *Cyclorana alboguttata*. Whisker-box plots show the median value and expression variation for each gene after normalisation to the reference gene, methylmalonyl CoA mutase (*mut*); $N = 7$ for both aestivating and control frogs.

DISCUSSION

Suppression of metabolism during aestivation limits ATP use so as to extend total survival time, which can be achieved by minimising the activity of energy expensive processes. Because protein synthesis is greatly minimised during aestivation (Fuery et al., 1998; Pakay et al., 2002), protein degradation is usually suppressed to a similar level to delay entry into a state of negative protein balance (Ramnanan et al., 2009). This is particularly important in tissue such as skeletal muscle which must maintain its protein content and contractile capacity for when animals emerge from the aestivating state. Overall, aestivating *C. alboguttata* exhibited no significant loss in gastrocnemius muscle wet mass (~18% reduction). Because the water content of aestivating *C. alboguttata* gastrocnemius muscle has been reported to be unchanged from that of control animals (Hudson and Franklin, 2002a; Mantle et al. 2009, Mantle et al. 2010) muscle wet masses are reliable indicators of muscle size. Additionally, total protein content does not change appreciably in the gastrocnemius of aestivating frogs (current study; Mantle et al. 2009, Mantle et al. 2010). Together these data indicate attenuation of protein catabolism in the gastrocnemius and an absence of atrophy following four months of aestivation. However, it is interesting to note that muscles from aestivating frogs in Group 2 exhibited a greater loss in wet mass (~ 23%) compared with aestivators from Group 1 (~ 12%), despite no differences in SVL or duration of the experiment. Differences in the proportion of muscle mass lost in the two different experimental groups of frogs may be related to the fact that in amphibians, fat bodies undergo

annual or seasonal changes in size (Girish and Saidapur, 2000), and/or different diets are known to affect the lipid composition of skeletal muscle in *C. alboguttata* (Berner et al. 2009). Thus, the availability of lipids as an energy source may not have been the same between studies, and such circumstances might force some individual frogs to start using muscle protein as a fuel supply during aestivation.

Nevertheless, losses of muscle wet mass in aestivating *C. alboguttata* are modest compared with conventional experimental models. In rats, skeletal muscle disuse can result in an almost 60% loss of gastrocnemius muscle wet mass and a 50% reduction in whole-muscle cross sectional area after just 1 month of hindlimb immobilisation (Spector et al., 1982; Zarzhevsky et al., 1999). In the current study, we have shown that *C. alboguttata* muscle expresses various calpain protease isoforms, including the ubiquitous calpains 1 and 2 and the muscle-specific calpain 3. While there were no changes in calpain activity, total protein or gene expression levels, there is some evidence that calpain 3 might be autolysed (and potentially active) in *C. alboguttata* muscle.

The proteolytic activities of calpain 1 and 2 were estimated simultaneously in skeletal muscle of *C. alboguttata* using the calpain substrate Suc-LLVY-aminoluciferin. To our knowledge, our study is the first to measure calpain activity in muscle during aestivation. Contrary to our hypothesis, there was no change in enzyme activity between aestivating and control frogs despite a more than 40% reduction in aestivators. Although this may be due to the high level of variation in active frogs, it appears that the aestivating condition does not require suppression of calpain 1 and 2 proteolytic activity. It is important to note that the activity assay used in our study does not differentiate between the two calpain isoforms, and may also include contributions from other Ca^{2+}-sensitive proteases such as cathepsins. Nevertheless, our enzyme activity data are supported by the observation that the activities of calpain 1 and 2 were also maintained in the soleus muscle of hibernating Daurian ground squirrels (*Spermophilus dauricus*) (Yang et al., 2014). In contrast to aestivators and hibernators, enzyme activity levels of calpain 1 and 2 have been shown to be increased during hindlimb suspension in rodents (Enns et al., 2007; Taillandier et al., 1996; Yang et al., 2014). Calpain activation in skeletal muscle appears to occur early during hindlimb suspension and can show a progressive increase in activity over time (Enns et al., 2007; Ma et al., 2011). Such disuse-induced activation has been suggested to be due to an early rise in intracellular $[Ca^{2+}]$ (Enns et al., 2007).

In the present study three isoforms of calpain were quantified at the protein and transcript level. Immunoblots of whole muscle extracts showed that muscle calpain 1 and calpain 2 total protein levels were unaffected by aestivation. Additionally, calpains 1 and 2 appeared to be in their full-length form suggesting that autolysis does not occur in muscle following 4 months of aestivation. The absence of any increase in calpain 1 and 2 protein abundance or their autolysed forms in aestivating *C. alboguttata* muscle could represent a mechanism by which aestivating frogs limit proteolysis in skeletal muscle. In agreement with our study, Lee et al. (Lee et al., 2010) found no difference in the protein abundance of calpain 1 in pectoralis muscles of summer-active and 3-month hibernating *Murina leucogaster* bats, a species which also undergoes minimal loss in muscle mass despite inactivity during dormancy. Protein levels of both calpain 1 and 2 were also recently found to be unaffected by hibernation in squirrels (Yang et al., 2014). Cast immobilisation in typical rodent models has been shown to be associated with increased autolysis of calpain 1 and calpain 2 (Min et al., 2011; Talbert et al., 2013a; Talbert et al., 2013b; Vermaelen et al., 2007), highlighting the different response of *C. alboguttata* muscle to extended disuse.

Calpain 3 appeared to be present in its autolysed form in both control and aestivating frogs. This is an interesting result given that calpain 3 has been shown to downregulated under different atrophic scenarios and aestivating *C. alboguttata* show evidence of only minimal skeletal muscle atrophy at 6-9 months aestivation (Chen et al., 2007; Jones et al., 2004; Mantle et al., 2009). Although the physiological function(s) of calpain 3 are obscure, it has been proposed that the protease is important in the regulation of maintenance of muscle integrity, myogenesis, and apoptosis (Murphy, 2010). Additionally, calpain 3 activity has been shown to initiate cleavage of a number of cytoskeletal proteins (e.g. actin-binding proteins) and is localised in costameres and myotendinous junctions, which are known sites of muscle force transmission (Taveau et al., 2003). Thus, it has been suggested that calpain 3 likely plays a role in regulating the cytoskeleton of myocytes during force production, adaptation to exercise or stretching or protection during fibre contraction (Taveau et al., 2003). Murphy et al. (Murphy et al., 2007) demonstrated calpain 3 activation *in vivo* following eccentric exercise, whereas *in vitro* data indicate calpain 3 activation may result from a small but chronic increase in cytoplasmic [Ca^{2+}] following eccentric exercise but not due to the lengthening contractions performed (Murphy and Lamb, 2009).

It is difficult to predict the specific function of the apparent autolysed calpain 3 isoform in *C. alboguttata* gastrocnemius muscle. However, given that 1) aestivating frogs

have their hindlimbs rendered immobile and have no need to produce force until arousal from aestivation, and 2) that in most frogs the gastrocnemius is a primarily glycolytic muscle used for powerful, short bursts of activity necessary for prey capture and escape, it is plausible that *C. alboguttata* calpain 3 may play a role in adaptation to movement/exercise or cytoskeletal regulation, as it does in mammals. Four months of aestivation in *C. alboguttata* has previously been shown to lead to changes in gene expression of components of myotendinous junctions and the cytoskeleton, including actin-binding proteins (e.g. LIM domain and actin-binding protein 1, filamin-binding LIM protein 1) (Reilly et al., 2013). Clearly remodelling of cytoskeletal elements is important in aestivating muscle, but further work is required to ascertain the function of calpain 3 and the mechanisms by which it is activated in *C. alboguttata* muscle.

In the current study the gene expression levels (as measured by qRT-PCR) of calpains 1, 2 and 3 remained at control levels during aestivation in *C. alboguttata* muscle. These data were supported by results of our transcriptomic analysis which also demonstrated no changes in expression levels of calpains or the specifc endogenous calpain inhibitor, calpastatin (Table 4.3). As gene transcription represents an energy cost to an organism, one would predict that if a protein is not critical for survival during aestivation then the transcription of the encoding gene will be suppressed. Indeed, the overall rates of transcription (and translation) are downregulated in all systems of hypometabolism (Storey and Storey, 2010). Because calpain activation can lead to unregulated proteolysis of cellular proteins, calpains are highly regulated and are considered to be in an inactive state most of the time (Bartoli and Richard, 2005). Indeed, both fasting and disuse lead to an increase in calpain (1 and 2) mRNA abundance in mammalian muscle and correlate with the loss of muscle tissue (Andrianjafiniony et al., 2010; Ilian and Forsberg, 1992; Servais et al., 2007). The maintenance of pre-aestivation gene transcript levels of calpains in aestivating *C. alboguttata* muscle is consistent with the protection of muscle against unregulated proteolysis throughout aestivation.

The absence of a change in calpain 1 and 2 enzyme activity, autolysis and gene expression levels observed in the gastrocnemius muscle from aestivating frogs provides evidence that the ubiquitous calpains are inactive during aestivation, but is different to our hypothesis that their enzyme activity and protein and mRNA levels would be suppressed. The enzyme activity and gene expression levels of calpains 1 and 2 could be affected by changes in calpastatin activity, which were not measured in this study. However, calpastatin mRNA

was unaffected by 4 months of aestivation (Table 4.3) suggesting it too is inactive during this time. Yang et al. found that calpastatin protein abundance increased almost 200% in hibernating squirrels compared with control animals (Yang et al., 2014) and suggested this to be the most likely mechanism underpinning inhibition of disuse atrophy in dormant *S. dauricus*. In contrast to calpains 1 and 2, calpain 3 is apparently not inhibited endogenously by calpastatin (Murphy, 2010).

Given that *in vivo* calpain 1 and 2 activity is elevated by a sustained increase in cytosolic calcium levels and/or a reduction in calpastatin, it is likely that *C. alboguttata* are able to maintain intracellular calcium homeostasis in skeletal muscle during aestivation, which would prevent activation of calpain. Indeed, activity levels of Ca^{2+} channels from the cell membranes of hibernators tend to be suppressed relative to non-hibernating cells, helping to prevent excessive Ca^{2+} influx (Wang et al., 2002). In mammalian models of disuse atrophy, it has been suggested that excessive ROS production in cells could lead to disruption of calcium homeostasis leading to calpain activation and fibre degradation (Powers et al., 2007). The suppression of ROS production and the lack of oxidative damage previously observed in the disused skeletal muscle of aestivating frogs is consistent with this hypothesis (Reilly et al., 2014; Young et al., 2013).

In summary, we have characterised calpains in *C. alboguttata* skeletal muscle and suggest that prevention of autolysis of calpains 1 and 2 in aestivators may be important in retaining muscle integrity during prolonged dormancy. However, it is unclear as to the physiological function of calpain 3 in burrowing frogs, and whether its autolysis contributes to resistance to disuse atrophy in this species. The absence of any increase in calpains during aestivation is probably due to the maintenance of calcium balance in myocytes, although we cannot rule out any upregulation of calpastatin activity. Much more research is needed with respect to proteolysis in aestivating *C. alboguttata* muscle, starting with the determination of the relative roles of the UPS and autophagy-lysosome systems in regulation of protein degradation during the aestivating state, in addition to calpains. Based on the results of this study, it appears that aestivators can tightly regulate muscle calpains and thus exert control of this proteolytic pathway during metabolic suppression.

Chapter 5

General Discussion

The overall aim of this thesis was to enhance our understanding of the effect of extended aestivation on skeletal muscle of *C. alboguttata* by exploring the possible cellular and molecular mechanisms associated with the inhibition of muscle disuse atrophy. In chapter 2, *C. alboguttata* depressed whole-animal metabolic rate by approximately 70% following four months of aestivation and exhibited no significant changes in whole muscle cross-sectional area or wet mass. Next generation RNA sequencing (RNA-Seq) technology was used to determine the influence of aestivation on global gene expression patterns in skeletal muscle. Comparison of the transcriptional profiles of the gastrocnemius muscle from active (control) and aestivating frogs showed that the majority of genes examined were downregulated during aestivation (64%). Among the downregulated genes, those implicated in energy metabolism were found to be overrepresented, as were mRNAs involved in muscle contraction (actin, myosin). The coordinated upregulation of genes associated with nucleic acid metabolism, cell death and survival and DNA replication, recombination and repair was also a prominent feature of the transcriptome of aestivating *C. alboguttata*. In addition, the modulation of genes involved in cytoskeletal organisation (vinculin, actinin, tubulin) and the NRF2-mediated oxidative stress response is likely to be critical in the maintenance of muscle integrity in aestivating *C. alboguttata*.

In chapter 3, mitochondrial respiration and ROS (H_2O_2) production was investigated in permeabilised skeletal and cardiac muscle fibres of *C. alboguttata*. After four months of aestivation, *C. alboguttata* reduced oxygen consumption of skeletal muscle mitochondria by almost 50% when malate, succinate and pyruvate were present in concentrations likely to reflect those *in vivo*, while mitochondrial H_2O_2 production showed up to an 88% reduction in aestivating skeletal muscle during leak respiration (i.e. respiration without adenylates present). However, mitochondrial respiration and H_2O_2 production in permeabilised cardiac muscle fibres were found to be unchanged between control and aestivating *C. alboguttata*.

In chapter 4, calpain proteases were assayed in *C. alboguttata* gastrocnemius muscle to gain a better understanding of the role calpains may play in the relative maintenance of aestivating skeletal muscle mass and integrity. While there were no changes in calpain enzyme activity or gene expression levels, western blot experiments indicated that calpain 3 may be autolysed (active) in burrowing frog gastrocnemius muscle. However, the relative

protein abundance of all three calpains was unchanged during aestivation. The maintenance of total protein content in the gastrocnemius combined with the lack of any increase in expression or activity of calpains suggests that aestivators exert tight control over muscle proteolytic pathways, despite prolonged disuse and fasting.

In this final chapter, I will synthesise the findings from each experiment conducted during this thesis, and discuss the findings in the broader context of muscle disuse atrophy in clinical and non-clinical models. The discussion will focus on the potential mechanisms employed by organisms that enter seasonal dormancy that enables them to maintain basic physiological functions in muscle during an unknown period of dormancy while ensuring a rapid and successful return to normal activity upon arousal during the summer rainfall events. Based on questions that have been generated as a result of my research, I will address key areas for future investigations on the effects of prolonged aestivation in *C. alboguttata* muscles.

Hibernators vs. aestivators as natural models of disuse

Hibernating mammals and aestivating frogs are very interesting models in which to examine mechanisms of skeletal muscle atrophy because both enter a hypometabolic state that entails chronic inactivity as well as hypophagia. Prolonged hibernation (greater than six months) is usually associated with mammals which inhabit temperate, high-latitude and/or highly seasonal cold environments (Carey et al., 2003). The winter survival strategies used by these 'typical' hibernators are highly variable (e.g. regulation of *T*b, frequency of arousals, food storage vs. fat accumulation). Although hibernation is often considered to be a specific adaptation of species inhabiting highly seasonal cold environments, it is also used by many diverse species from all climate zones, including the tropics (Geiser, 2013). Known hibernators include various mammals from all three mammalian subclasses (Monotremes, Marsupials, Placentals), and also a species of bird (the common poorwill, *Phalaenoptilus nuttallii*) (Geiser, 2013).

Despite the fact that many hibernators undergo a pattern of periodic arousals in winter followed by foraging and reproduction in the warmer months, this strategy is not universal. For example, marsupial pygmy-possums (*Cercartetus* spp.) are relatively flexible with their torpor/activity patterns and are able to forage during warmer periods in winter but resume multi-day torpor when the environmental temperature drops (Geiser, 2013). In contrast,

hibernation in reproductive echidnas (*Tachyglossus aculeatus*) is often terminated in the middle of winter for breeding (Morrow and Nicol, 2009). In addition, not all hibernators rewarm periodically. Tenrecs (*Tenrec ecaudatus*) were found to undergo nine months of hibernation with no evidence of any periodic interbout arousals (T_b during hibernation never decreased below 22°C) (Lovegrove et al., 2014).

While prolonged inactivity contributes to energy conservation during dormancy, some species such as the black bear (*U. americanus*) are far from being completely immobile and instead periodically arouse and move during hibernation (Toien et al., 2011). In hibernators it has actually been hypothesised that routine neural activation of muscles (shivering) could occur and help offset the negative effects of muscle wasting (Harlow et al., 2004). Other hibernating animals often consume food during dormancy, thereby replenishing fuel reserves and abating the threat of starvation (Humphries et al., 2001). Because hibernation strategies and behaviours are extremely diverse, it is difficult to draw broad conclusions about the physiological responses of skeletal muscle in hibernating species. Consequently, hibernators are not necessarily a good model of natural muscle disuse.

Aestivating amphibians are an intriguing, alternative model for examining muscle disuse atrophy. In general, aestivators enter dormancy at relatively high environmental temperatures (Young et al., 2011), and because of the high risk of dehydration aestivators are often confined within a cocoon inside a subterranean burrow. Although the cocoon significantly hinders evaporative water loss, it also secondarily inhibits movement of the limbs and can be considered analogous to a cast or splint. As aestivators are completely restrained during their dormancy, they do not experience periodic arousals and are completely dependent on energy stores accumulated before entering aestivation (Van Beurden, 1980). Starvation is a real survival threat for aestivators and it is feasible that, should lipid reserves be exhausted, muscle protein could be used as a fuel source, potentially contributing to muscle disuse atrophy (Mantle et al., 2009). Thus, physiological and molecular studies of *C. alboguttata* skeletal muscle can reveal information about both the similarities and diversity of mechanisms potentially used to attenuate the rate of muscle disuse atrophy during dormancy.

Gene expression signatures in *C. alboguttata* skeletal muscle: evidence for inhibition of apoptosis and chromatin remodelling

A major achievement of the current research was the *de novo* construction of a *C. alboguttata* skeletal muscle transcriptome, providing for the first time a genomic resource for this unusual species. Moreover, this work has revealed novel information regarding global gene expression patterns during aestivation. To date, only a small number of studies have used gene expression profiling to identify and characterise key functional proteins and pathways involved in hypometabolism (Hampton et al., 2011; Schwartz et al., 2013; Storey et al., 1999; Yan et al., 2008). Widespread suppression of gene transcription is an essential component of metabolic depression exploited by all dormant organisms (Storey and Storey, 2010). However, it is important to note that while an array of transcripts may be suppressed during dormancy, the majority of genes show only moderate reductions in expression levels (Fedorov et al., 2014). Given that aestivators are reliant solely on their endogenous fuel supplies, it is perhaps not surprising that genes found to be strongly downregulated in *C. alboguttata* muscle were those functioning in catabolic pathways (e.g. glycolysis). The maintenance of intrinsic control of carbohydrate metabolism during aestivation is achieved not only via suppression of gene expression (current study), but also by post-translational modifications such as reversible protein phosphorylation (Cowan and Storey, 1999; Whitwam and Storey, 1990). While protein phosphorylation appears to be an important regulator of select metabolic processes during aestivation, recent work from hibernators suggests that widespread coordination of phosphorylation is not a major feature in orchestrating cellular changes throughout metabolic depression (Hindle et al., 2014).

Despite an overall downregulation of transcription and translation during hibernation and aestivation, increased expression of selected genes and the proteins that they encode does occur during metabolic depression (Storey et al., 1999; Storey and Storey, 2010). The current study has greatly contributed to our knowledge of genetic mechanisms that need to be enhanced throughout dormancy phenomena. The key gene functional groups found to be upregulated in *C. alboguttata* gastrocnemius muscle were cell death and survival, DNA replication, recombination and repair and chromatin remodelling. A multitude of extra- and intra-cellular stimuli induce apoptosis including alterations in temperature and osmolarity, ROS (i.e. H_2O_2), deprivation of nutrients, oxygen or growth factors and organ disuse (Marzetti et al., 2010; Portt et al., 2011). These are all stressful conditions which either can or do accompany the aestivating state. Upregulation of pro-apoptotic genes in aestivating *C.*

alboguttata muscle may serve to eliminate individual myocytes (and intracellular macromolecules) that are defective, damaged or otherwise a potential threat to the integrity of the whole animal. However, in response to potential apoptotic signals aestivating cells would need to avoid triggering premature or excessive apoptosis, which can be accomplished by balancing the ratio of pro- and anti-apoptotic mechanisms. This was reflected in our transcriptomic data by the enhanced expression of genes with reported anti-apoptotic functions (e.g. the IAP survivin, or BIRC5). Like *C. alboguttata*, members of the IAP protein family also appear to be regulated during hibernation (Rouble et al., 2013), with an increase in xIAP (a.k.a BIRC4) protein levels reported in muscle of hibernating *S. tridecemlineatus*. This indicates the possibility that inhibition of caspase activity via increased IAP expression may be a critical regulatory mechanism which enhances survival of myocytes in dormant species that are resistant to disuse atrophy.

Other cell protective mechanisms that were upregulated in aestivating *C. alboguttata* muscle included genes functioning in cell-cycle control (growth arrest through checkpoint control), DNA and chromatin stabilisation and repair, and expression of heat shock proteins to fold/refold and stabilise proteins. These are all important mechanisms that are part of the broadly conserved cell stress response (Kultz, 2005), and likely contribute to the preservation of muscle tissue during aestivation.

The modulation of myogenesis/muscle growth might also contribute to the lack of muscle atrophy in aestivating frogs. Although not detected by IPA, myostatin mRNA was markedly suppressed in aestivating frog gastrocnemius muscle, which is consistent with the reduction in myostatin gene expression in soleus and diaphragm muscles of hibernating ground squirrels, two muscle types also known to be resistant to disuse atrophy (Nowell et al., 2011). Myostatin signalling can activate MAFbx/atrogin-1 and MuRF1 (Elliot et al., 2012), the two genes known to be consistently upregulated in different muscle atrophy models (Gomes-Marcondes and Tisdale, 2002; Li et al., 2003). Furthermore, binding of myostatin to its receptor can activate the common SMAD signalling pathway leading to inhibition of MyoD production, which plays a key role in regulating muscle differentiation (Elliot et al., 2012). Alternatively, myostatin inhibits activation of the Akt/mTOR protein synthesis pathway (Trendelenburg et al., 2009), therefore decreased myostatin gene expression may facilitate mTOR signalling by reducing this inhibition.

Gene expression profiling of aestivating *C. albogutatta* muscle also revealed new information about specific mechanisms that control transcription during aestivation, in

particular ATP-dependent chromatin remodelling (*smarca4*, *smarca5* and RBBP4). The main characteristic of ATP-dependent chromatin remodelling enzymes is their capacity to remodel chromatin by modifying the DNA-histone contacts within an individual nucleosome, resulting in either localised interruption of the histone–DNA contacts or shifting of the nucleosomes on the chromatin fibre. Importantly, these enzyme complexes exhibit striking specificity in selecting their genomic targets and may positively or negatively regulate transcription to modulate numerous cellular processes, such as skeletal muscle differentiation (Albini and Puri, 2010). Interestingly, *smarca4* (also known as *brg1*) was shown to have a vital role in modulating cardiac muscle growth, differentiation and gene expression (Hang et al., 2010). *Smarca4* is normally switched off in adult cardiomyocytes, but is activated during cardiac stress such as hypertrophic cardiomyopathy, and induces a shift in myosin heavy chain isoforms (Hang et al., 2010). Inhibition of *smarca4* expression reduces cardiac hypertrophy and reverses the isoform switch (Hang et al., 2010). SMARCA gene family members and their encoded proteins appear to be a fundamental component of the transcriptional reprogramming (enforced expression of key transcription factors and co-regulatory proteins) that occurs in aestivating *C. alboguttata* muscle, and are likely be involved in regulating myocyte growth, differentiation and perhaps muscle protein isoforms.

Rbbp4 is a histone-binding subunit and a core component of complexes that control chromatin metabolic processes, such as chromatin assembly following DNA replication and repair and transcriptional suppression. Surprisingly, a previous study found no change in gene expression levels of cruralis muscle *rbbp4* between aestivating and control *C. alboguttata* (Hudson et al., 2008). However, in support of the current study, other genes with established roles in gene silencing (SIN3A co-repressor and DNA cytosine-5-methyltransferase 1) were upregulated 160 and 350%, respectively. Morin and Storey (Morin and Storey, 2006) showed that hibernating *S. tridecemlineatus* muscle exhibited almost 2-fold higher histone deacetylase activity than control animals, indicating that mammalian hibernation and amphibian aestivation share common mechanisms of epigenetic modification related to histone deacetylation. Given the widespread suppression of gene expression during dormancy, the upregulation of *rbbp4*, *smarca4* and *smarca5* in *C. alboguttata* muscle is noteworthy. Moreover, this is the first time SMARCA genes have been linked to dormancy and thus provides novel information about specific epigenetic modifications at play during metabolic depression.

Effect of aestivation on ROS production and calpains in *C. alboguttata* muscle

As metabolic depression involves all levels of biological organisation it is likely that multiple systems must interact to control a coordinated and reversible cessation of both ATP-producing and consuming processes. Consequently, mitochondrial function was also studied in aestivating gastrocnemius muscle by investigating mitochondrial oxygen consumption and associated ROS production. The study of mitochondrial ROS production is relevant to hypometabolic systems for at least two reasons. As discussed, disuse-induced skeletal muscle atrophy has been linked to increased ROS production in muscle fibres, leading to oxidative stress and muscle tissue damage (Powers et al., 2011). Secondly, because the rate of mitochondrial superoxide production in many biological systems is proportional to oxygen tension, it is thought that physiological oxidative stress occurs in animals that arouse from dormancy due to a rapid return to the active state and a 'normal' rate of oxygen consumption, in a manner similar to that which occurs during reperfusion injury (Ferreira-Cravo et al., 2010).

In the present study, gastrocnemius muscle mitochondrial oxygen consumption decreased by approximately 50% during four months of aestivation in *C. alboguttata,* which was accompanied by a decrease in mitochondrial H_2O_2 production. The reduction in gastrocnemius mitochondrial respiration is consistent with previous work on *C. alboguttata* (Kayes et al., 2009b) and correlates well with the ~70% reduction in whole animal oxygen consumption measured in the current study. The reduction in skeletal muscle mitochondrial H_2O_2 production is important given the paucity of information about rates of free radical production during metabolic depression. The reduction in H_2O_2 production observed in aestivators compared with controls may be a consequence of the ETC operating at a slower rate, simply resulting in less electrons being mismanaged or lost during electron transfer. Alternatively, ROS production may be attenuated by mild uncoupling of mitochondria (i.e. H^+ re-enter the mitochondrial matrix without contributing to ATP synthesis), as H^+ leak has been shown to decrease ROS generation (Brookes, 2005). Though this would be energetically costly during hypometabolism, it is conceivable that such a strategy could be protective throughout dormancy and upon arousal. However, evidence obtained from both aestivating and hibernating animals do not support the hypothesis that increased rates of proton leak occur during metabolic depression (Bishop and Brand, 2000; Bishop et al., 2002; Boutilier and St Pierre, 2002).

The decrease in ROS production recorded in aestivating *C. alboguttata* muscle mitochondria may be due to enhanced antioxidant capacities relative to control animals (potentially a combination of both enzymatic and endogenous, non-enzymatic). Indeed, the gene expression of ferritin (*fth1*), glutamate cysteine ligase (*gclm*), glutathione S-transferase (*gsto2*) and sulfiredoxin 1 (*srxn1*), all of which have antioxidant properties, were significantly increased in *C. alboguttata* muscle (Chapter 2). These expression data are supported by previous studies of *C. alboguttata* which have shown that transcription of antioxidant enzymes and total antioxidant capacity are maintained at control levels in skeletal muscle during aestivation (Hudson et al., 2006; Mantle et al., 2009). In addition, levels of lipid and protein oxidation (indices of ROS-induced oxidative damage) were unchanged in the gastrocnemius muscle of *C. alboguttata* following 6 months aestivation (Young et al., 2013). Similar to aestivating *C. alboguttata*, total antioxidant capacity was found to be elevated in the gastrocnemius muscle of torpid thirteen-lined ground squirrels relative to active animals (James et al., 2013). These results demonstrate that increases in skeletal muscle antioxidants occur during metabolic depression, which could explain decreased rates of mitochondrial ROS production. Thus, elevated levels of antioxidants are likely to contribute to cytoprotection during dormancy by providing greater protection of macromolecules and reducing the susceptibility of muscle tissue to the effects of oxidative damage.

It is still unknown as to why prolonged skeletal muscle inactivity results in increased mitochondrial ROS production in human and rodent models of muscle disuse atrophy. However, there are four potential pathways through which increases in mitochondrial ROS production may occur: 1) disturbed calcium handling and elevated levels of cytosolic and mitochondrial calcium within the disused muscle fibres, 2) an increase in mitochondrial levels of fatty acid hydroperoxides, 3) hindrance of protein transport into mitochondria leading to impairment of mitochondrial function and 4) an increase in mitochondrial fission in inactive skeletal muscles (Powers et al., 2012). The modulation of these potential processes and mechanisms remains an interesting and unexplored avenue in aestivators and hibernators, and could represent ways by which they reduce mitochondrial ROS production in their inactive skeletal muscles.

Elevated ROS production during chronic muscle inactivity can lead to accelerated protein degradation, atrophy and reductions in contractile performance (Powers et al., 2007). Recently, Talbert et al. demonstrated that mitochondrial ROS production is necessary for activation of key proteolytic pathways in inactive muscle fibres, including the calpains

(Talbert et al., 2013b). With respect to the role of calpains in muscle disuse atrophy, it is known that extended inactivity of skeletal muscle fibres is associated with higher levels of cytosolic calcium and calpain activity (Powers et al., 2007). Impairment of calcium balance has been suggested to promote mitochondrial ROS production (see above). However, the production of ROS themselves could also exacerbate disturbances in calcium homeostasis leading to calcium overload (Powers et al., 2007). To this end, reactive aldehydes formed as a result of oxidative stress have been shown to inhibit Ca^{2+} -ATPase, which in turn would suppress Ca^{2+} removal from the cell (Siems et al., 2003). Thus, it has been hypothesised that an intracellular Ca^{2+} overload produced *via* this mechanism could induce calpain activation (Powers et al., 2007).

Results from the final experimental chapter showed that there was no significant decrease in the enzyme activity levels or the relative protein abundances of calpain 1 and calpain 2 in aestivating *C. alboguttata* muscle. Similarly, gene expression assays demonstrated that transcription of calpains was unaffected by aestivation. Western blotting of 'muscle-specific' calpain 3, which is consistently downregulated during atrophic conditions, indicated that this isoform is present in burrowing frog muscle where it appears to be in its autolysed state. The absence of any increase in enzyme activity, protein and mRNA abundance of calpains in aestivators is consistent with the protection of gastrocnemius muscle against uncontrolled proteolysis throughout aestivation.

At this time, it is unknown which specific mechanisms might prevent accelerated calpain 1 and 2 activation in aestivating muscle, but it is reasonable to suggest that the endogenous calpain inhibitor, calpastatin, may play a role. Overexpression of calpastatin can decrease skeletal muscle atrophy by 30% during just 10 days of hindlimb unloading in mice (Tidball and Spencer, 2002). Moreover, calpastatin protein expression was almost 200% higher in muscle of hibernating *S. dauricus* compared with control squirrels (Yang et al., 2014), indicating that this could be an important mechanism contributing to inhibition of disuse atrophy throughout dormancy. Aestivating *C. alboguttata* are also likely to have the capacity to tightly regulate cellular calcium homeostasis, which would prevent unwanted calpain proteolytic activity. Considering the data from biomedical disuse models, this idea is consistent with both the very low H_2O_2 production observed in aestivating gastrocnemius muscle, and the lack of any increase in calpain 1 and 2.

Future directions

There are several important questions that have arisen as a result of this research. Despite the scale and novelty of information generated using RNA-Seq, hypothesis-driven studies that test predictions at the whole animal, tissue, cellular and molecular level, will be critical for future investigations of the mechanisms of aestivation in *C. alboguttata*.

The most important trait that makes *C. alboguttata* an excellent model for studying muscle disuse atrophy during aestivation is the formation of the waterproof cocoon because it acts like a cast and immobilises the frog. Furthermore, the hardened clay soil burrow prevents the frog from being able to make significant movements throughout aestivation. While we can be confident that *C. alboguttata* is inactive and immobile once the cocoon of shed skin has been formed during deep aestivation, it cannot be ruled out that regular neural activation of muscles might be utilised to protect the musculoskeletal system against disuse-induced atrophy. However, hibernating bears were reported to be unusually resistant to the atrophic effects of denervation, indicating that neural activation and/or neural-associated trophic factors may not play a significant role in maintaining muscle architecture during hibernation (Lin et al., 2012). A similar type of response to loss of neuromuscular communication might be envisioned for aestivating frogs, given that the quantity of acetylcholine neurotransmitter 'packages' (i.e. quanta) released per synapse was reduced in six-month aestivating *C. alboguttata* (Hudson et al., 2005).

Among the possible factors predicted to prevent muscle disuse atrophy, muscle stretch may be an important player. Limb immobilisation experiments in mammals, such as rats and rabbits, have shown that immobilisation of a muscle in a stretched (or lengthened) position can increase muscle mass, RNA content and IGF-1 gene expression, thus reducing the extent of atrophy (Loughna et al., 1986; Yang et al., 1997). The water-conserving pose adopted by *C. alboguttata* throughout aestivation may place vital locomotory muscles (e.g. cruralis and gastrocnemius) in a stretched position that could delay the onset of fibre atrophy. Unfortunately there are no current data to suggest this may be the case. If true however, this may also explain the preferential atrophy of smaller, non-jumping muscles in this species during prolonged aestivation bouts (Mantle et al., 2009). Following on from this idea, it is important that future investigations examine the effect of experimental immobilisation on skeletal muscles of both non-aestivating and aestivating *C. alboguttata*. If the ability to enter dormancy is a vital mechanism in protecting muscle against disuse atrophy, artificially-

immobilised muscles of aestivators should be less prone to atrophy than immobilised muscles from non-aestivating frogs.

Comparisons of muscle disuse atrophy data from different species are somewhat confounded by factors such as age, different time periods of muscle disuse, different limb immobilisation methods and different muscle (and fibre) types. This can make it difficult to compare data from natural disuse models (e.g. aestivating *Cyclorana alboguttata* in a water conserving posture) with skeletal muscle atrophy models such as hindlimb unloading or prolonged human bed rest. Although skeletal muscles are roughly similar among vertebrates, specific differences between frog and mammalian skeletal muscle may affect the responses of their myofibres to disuse. For example, differential expression of myosin heavy chain isoforms drastically influences the mechanical and energetic properties of skeletal muscle fibre types. A comparison of myosin heavy chain isoforms between mammals, amphibians and birds showed that the specific myosin molecular isoforms evolved separately among these groups and that their variants are not evolutionarily homologous (Lutz et al., 1998). These differences alone might alter the susceptibility of frog vs. mammalian fibres to atrophic signals. Indeed, mammalian skeletal muscle slow oxidative (Type I) fibres seem more prone to atrophy induced by denervation, microgravity, and limb immobilisation, whereas fast glycolytic fibre (Type II)-specific atrophy is typically observed during sarcopenia and disease states (e.g. cachexia) (Wang and Pessin, 2013). In contrast, the proportions of fibre types do not change following extended fasting and disuse in aestivating *C. alboguttata* (Symonds, et al., 2007). Data regarding the rates of muscle atrophy from artificially-immobilised *C. alboguttata* would still be useful to compare with those of the usual mammalian disuse models.

It is interesting to note that frog skeletal muscle possesses two isoforms (α and β) of the ryanodine receptor (i.e. calcium channel in muscle) in equal proportions, with each exhibiting distinct intracellular calcium signals in muscle tissue (Kashiyama et al., 2010). In contrast, mammals primarily express the RyR1 (α) in muscle with only small amount of RyR3 (β) in the diaphragm and soleus. While it is completely unknown how α and β ryanodine receptors might respond to inactivity and fasting in aestivating frogs, it is interesting to contemplate given that RyR1 and RyR3 receptor expression was shown to be altered following muscle disuse in rats and humans (Bastide et al., 2000; Chopard et al., 2009).

The current study helped to greatly advance our knowledge regarding the transcriptional changes that occur during deep aestivation. While it is beyond the scope of this

thesis to discuss the potential functions of all of the differentially-expressed genes in *C. alboguttata* muscle, the transcriptome analysis has provided an array of candidate genes for future gene or protein expression studies of dormant animals. The interpretation of the gene expression data thus far is based on the assumption that observed mRNA levels correlate with protein abundance and carry over to a phenotypic response. However, it is probably true that in aestivating *C. alboguttata* muscle mRNA and protein abundances do not correlate that well all of the time, due to regulation at different levels (e.g. post-transcriptional, post-translational). Other high-throughput or 'omics' methods, such as proteomic and metabolomic measurements would be useful in providing a more comprehensive assessment of the sub-cellular changes that occur in aestivating *C. alboguttata* muscle. For example, although expression of the *birc5* gene (survivin) was significantly increased during aestivation, it is known that survivin protein expression is regulated by a number of distinct posttranscriptional mechanisms (Zhang et al., 2006). Importantly, mammalian cell studies have demonstrated that phosphorylation of survivin at threonine sites is critical for its functions in both mitosis and cell survival (Barrett et al., 2011; O Connor et al., 2000). Given the importance of reversible protein phosphorylation in controlling energy metabolism during aestivation, it would be interesting to examine the extent of protein phosphorylation in frog gastrocnemius muscle, particularly in those proteins implicated in cell death and survival. Future use of high-throughput techniques would also be invaluable for determining the molecular changes that occur during the both transition from the active state into aestivation, and during arousal.

Given the paucity of studies verifying the use of the saponin-permeabilisation technique for studying mitochondrial metabolism, the data presented in experimental chapter 3 are important. To deliver electrons to the mitochondrial ETC in aestivating muscle, pyruvate, succinate and malate were used together at low concentrations likely to reflect those *in vivo*. However, it is currently unknown exactly what those concentrations are in active and aestivating *C. alboguttata*. Data of such metabolites are scanty in the literature, but the concentration of pyruvate in the gastrocnemius of *Rana temporaria* was reported to be 0.12 µmol/g (Beis and Newsholme, 1975). Given that aestivating *C. alboguttata* are deprived of food for so long, it is highly likely that fatty acids serve as a key substrate throughout dormancy (Van Beurden, 1980). However, other metabolic pathways, such as ketone body metabolism, may also contribute to the overall energy budget during aestivation (Frick et al., 2008b). In any case, future studies of mitochondrial function in dormant animals would benefit by measuring tissue metabolite concentrations, and by using substrates such as

palmitic acid or palmitoylcarnitine to fuel mitochondrial respiration. This would lead to a better understanding of the relationship between fatty acid degradation and mitochondrial function during metabolic depression. In a similar vein, it is difficult to ascertain the *in vivo* levels of ATP/ADP in *C. alboguttata* muscle, but it is likely they are seldom zero or fully saturating (the conditions measured in the current study). To gain further insight into the effect of aestivation on mitochondrial ROS production, it would be valuable to use an oxygraph titration protocol to gradually increase ADP levels into permeabilised *C. albuguttata* myocytes.

The gastrocnemius muscle was selected for analyses in the current experiments because in frogs this (glycolytic) muscle contributes to the power necessary for jumping. In contrast, muscle such as the iliofibularis and sartorius are not involved in producing power during locomotion, and are considered to be more oxidative than the gastrocnemius. There is some evidence that smaller, non-jumping hindlimb muscles of *C. alboguttata* could be preferentially used as a protein source during aestivation over larger muscles like the gastrocnemius (Mantle et al., 2009). Consequently, there are several important questions that remain unanswered and should to be explored in aestivating muscle. For example, how do the gene expression changes observed in *C. alboguttata* gastrocnemius muscle differ in a muscle that is more susceptible to atrophy, such as the iliofibularis? Are pro-apoptotic pathways expressed earlier on during aestivation and do their effects result in atrophy of fibres in 'susceptible' muscle types? Similarly, are Nrf2-mediated oxidative defences impaired, or show a different response in smaller non-jumping muscles? Young et al. (Young et al., 2013) found that protein oxidation increases in the iliofibularis during aestivation (and is higher than in the gastrocnemius), which is consistent with the greater level of atrophy of this muscle type in *C. alboguttata*. It is also unknown how mitochondrial respiration and ROS production might differ in alternative muscle types, such as forearm, rib or sartorius muscles. Given the different mitochondrial responses between *C. alboguttata* cardiac and gastrocnemius muscle, it is possible that other muscle types might exhibit increased rates of mitochondrial ROS production relative to the gastrocnemius. Similar questions may be asked in regard to activation of key proteolytic pathways (i.e calpain, UPS, autophagy, caspases) in distinct *C. alboguttata* muscle types.

Finally, there are a number of recent findings from mammalian hibernator muscle disuse models that deserve comparative attention in the *C. alboguttata* disuse model. Recent work from hibernating *S. tridecemlineatus* suggests that the serum and glucocorticoid-

regulated kinase, SGK1, plays a key role in regulating muscle mass throughout hibernation (Andres-Mateos et al., 2013). SGK1, like protein kinase-B/Akt, is a downstream target of IGF-1/phosphatidylinositol 3-kinase signalling. Although the active form of Akt was found to be suppressed in skeletal muscle of hibernating *S. tridecemlineatus*, SGK1 was increased in quadriceps of hibernating squirrels relative to active animals, where it appears to play a role in inhibition of muscle disuse atrophy *via* concomitant suppression of proteolysis and autophagy and elevated protein synthesis (Andres-Mateos et al., 2013). In that same study, SGK1-null mice exhibited a loss in the mass of tibialis anterior muscles without a reduction in whole-body mass, as well as decreased muscle fibre size in tibialis anterior, gastrocnemius and soleus muscles (Andres-Mateos et al., 2013). The muscle atrophic response in SGK1-null mice was exacerbated following both limb immobilisation and fasting.

In another study on hibernating *S. tridecemlineatus* squirrels, PGC-1*α* and its associated upstream and downstream signalling molecules were examined to determine their importance in retention of muscle mass during dormancy (Xu et al., 2013). PGC-1α was chosen for examination because it is a transcriptional coactivator involved in the regulation of a variety of biological processes including fat metabolism, mitochondrial biogenesis, angiogenesis, formation of muscle fibre types and antioxidant defences. Xu et al. found a significant increase in the percentage of slow type muscle fibres in skeletal muscle of hibernating squirrels as well as increases in PGC-1α mRNA and protein. There was also an increase in mitochondrial biogenesis, oxidative capacity, and antioxidant capacity in hibernating animals. Although PGC-1*α* requires further study in *C. alboguttata*, the fact that its gene expression was downregulated in aestivating gastrocnemius (Chapter 2), and that *C. alboguttata* does not undergo torpor-arousal cycles like hibernating squirrels, suggests that modulation of PGC-1*α* and/or its targets may be different between aestivating and hibernating tissues.

Could *C. alboguttata* be developed into a novel model organism for biomedical research?

To further the understanding of human pathophysiologies, and for the development and authentication of new therapies, the use of suitable animal models continues to be of utmost importance. While aestivating *C. alboguttata* may provide insights into the mechanisms underpinning inhibition of muscle disuse atrophy, they could also be studied to facilitate our understanding of the cellular pathways associated with other disordered

physiological processes, such as disuse-induced osteoporosis, ischaemia/reperfusion injury or even dormancy in cancer cells.

Disuse-induced osteoporosis

Like skeletal muscle, bone is a highly plastic tissue that undergoes remodelling in response to increased or decreased usage. Whereas an increase in bone usage tends to result in bigger, stronger bones, bone disuse following limb immobilisation, hindlimb unloading or microgravity may result in bone demineralisation, compromised bone architecture and a loss of strength, increasing the risk of bone fracture. Interestingly, *C. alboguttata* appears resistant to osteoporosis induced by disuse (Hudson et al., 2004). Frogs aestivated for both three and nine months exhibited no significant changes in long bone size, anatomy or bending strength when compared with active, control animals. It is feasible that the metabolic depression and associated metabolic recycling that is fundamental to dormancy may help defend skeletal tissues from the effects of disuse. Early studies suggested that small hibernating mammals such as bats, ground squirrels and hamsters might experience bone loss during hibernation (Kayser and Frank, 1963; Mayer and Bernick, 1959; Whalen et al., 1972). However, more recent data from hibernating *S. lateralis* squirrels indicate that bone strength and stiffness are unaffected by winter inactivity (Utz et al., 2009). Interestingly, summer (i.e. awake) squirrels that experienced restricted mobility exhibited reduced flexural modulus (stiffness) of the femur when compared with active summer squirrels (Utz et al., 2009).

Because many hypometabolic organisms are still relatively quiescent when not dormant, it is conceivable that prior to chronic inactivity during dormancy their bones have only a moderate loading history. If the extent of bone remodelling is dependent on the degree of unloading, bone of relatively inactive animals, like amphibians, should be intrinsically more resilient to disuse-induced osteoporosis than more metabolically-active animals (such as mammals) as the change in stimulus is much less. Thus, it could be argued that *C. alboguttata* are set to withstand prolonged periods of disuse without losing bone mass, and their value as a model system for biomedical studies of disuse-induced osteoporosis is decreased. However, periods of disuse in mammals produce a rather rapid response involving bone loss, and there could be compensatory molecular mechanisms at play in aestivating frogs to maintain bone architecture, as has been demonstrated in their skeletal muscle tissue.

Ischaemia/reperfusion injury

Aestivating burrowing frogs may represent an interesting natural model for potential adaptive responses to the harmful effects of low tissue perfusion and the restoration of blood supply following ischaemia. ROS generation increases during both ischaemia and reperfusion in most mammals, and plays a fundamental role in subsequent deleterious events like myocardial injury. In aestivating amphibians, rates of lung ventilation completely cease and heart rate can decrease by 30-50% (Gehlbach et al., 1973; Glass et al., 1997; Seymour, 1973b; Word, 2007). In addition, mean arterial blood pressure decreases from ~25 mmHg to ~ 15mmHg in aestivating lungfish after one month of aestivation (Delaney et al., 1974). Thus, aestivation could increase the potential for ischaemia in some organs (e.g. the intestine) as presumably blood flow is preferentially delivered to critical organs such as the brain and heart.

Upon arousal from aestivation, metabolic activity in cells is restored to normal rates, and oxygenated blood reperfuses the tissues. Examinations of intracellular antioxidant enzyme activities throughout aestivation suggest a widespread upregulation in numerous tissues, which may provide protection against ischemia–reperfusion events associated with aestivation to arousal transitions (Ferreira-Cravo et al., 2010). Results from the current study showed that rates of ROS generation from cardiac muscle of aestivating *C. alboguttata* were not significantly different from control animals. Thus, it is conceivable that *C. alboguttata* could experience a 'burst' of ROS in cardiomyocytes as they return to normal rates of oxygen consumption during the transition from the aestivating to the awakened state. There is recent evidence that aestivators increase antioxidant enzyme levels and/or activities in heart and brain during aestivation and arousal (Page et al., 2010; Salway et al., 2010). These tissues are highly sensitive to oxidative damage in most animal species, therefore it appears that upregulation of intracellular antioxidant capacity could function in oxidative stress resistance during arousal in aestivators. Although it is still not clear whether tissues of aestivators undergo true ischaemia and/or reperfusion during aestivation and arousal, continued study of ROS, antioxidants and other potential cytoprotective mechanisms during dormancy may help define ischaemia and reperfusion in more susceptible species.

Dormancy in cancer cells

In cancer biology it has been established that residual tumour cells can enter a state of dormancy and elude conventional therapies (Sosa et al., 2014). This is an important, active area of research because it appears that the biology of residual disseminated (i.e. spread throughout the organ of body) tumour cells is highly divergent from that of primary tumours (Klein, 2013), such as their capacity to remain clinically asymptomatic. Because dormant tumour cells are hypothesised to be a significant source of tumour recurrence, understanding the molecular mechanisms of disseminated cancer cell dormancy is critical.

Althought this field is in its infancy, it has been established that stress signalling pathways stimulated by exogenous stressors, intrinsic damage or microenvironmental cues can trigger tumour cell dormancy. Specifically, the balance between extracellular-signal-regulated kinase (ERK) and p38 mitogen-activated protein kinase signalling has been shown to regulate dormancy versus proliferation decisions in distinct cancer models (Sosa et al., 2014). At this point, it could be asked how cancer dormancy is related to aestivation. Although ERKs are involved in many different cell functions, activation of the ERK cascade was shown in different tissues of aestivating *X. laevis*, where it is likely to be involved in coordinating the appropriate responses to ameliorate cell stress, for example dehydration (Malik and Storey, 2009). Additonally, there was a large increase in gene expression of an MLT-like mitogen-activated protein kinase kinase kinase in aestivating frog muscle (Reilly et al., 2013) (Chapter 2). MLT (a.k.a. MLK7 or MLTK; *zak* gene) is a stress-activated protein functioning in signal transduction and has been shown to regulate the p38 and c-Jun N-terminal kinase (JNK) pathways (Gotoh et al., 2001). Interestingly, overexpression of MLT was shown to suppress lung cancer cell proliferation concomitant with elevated phosphorylated levels of ERK and JNK (Yang et al., 2010). Moreover, MLT significantly supressed tumor growth *in vivo*. It has also been shown that other mitogen-activated signalling kinases such as MKK4 (also known as MAPKK4) can also activate JNKs and induce dormancy in other cancer cell models (Griend et al., 2005; Hickson et al., 2006).

Consequently, the pathways that induce dormancy in natural systems (aestivators, hibernators) appear not unlike those in tumour cells, and future in-depth examinations of both the similarities and differences between specific mechanisms that induce cell dormancy in aestivators and cancer cell lines could provide unexpected insights for biomedicine. However, to develop the burrowing frog into a novel model organism for biomedical research, a greater understanding of the *C. alboguttata* biological 'toolbox' is required. This includes the

construction of a *C. alboguttata* genome, an extensive catalogue of the genes and genetic variation in burrowing frogs, characterisation of *C. alboguttata* proteomes and transcriptomes, as well as the development of tissue cell lines.

Aestivating frogs are a fascinating study system that can provide useful insights into the regulation of muscle disuse, starvation and possibly other pathphysiologies, by furthering our understanding of both their basic underlying controls and their responses to specific challenges. The common molecular features and variety of pathways at play during aestivation in *C. alboguttata* will hopefully provide new directions for future studies of metabolic suppression and, more broadly, metabolic regulation.

REFERENCES

Adams, G. R., Caiozzo, V. J. and Baldwin, K. M. (2003). Skeletal muscle unweighting: spaceflight and ground-based models. *J. Appl. Physiol.* **95**, 2185-2201.

Adelman, R., Saul, R. L. and Ames, B. N. (1988). Oxidative damage to DNA - relation to species metabolic rate and life span. *Proc. Natl. Acad. Sci. U. S. A.* **85**, 2706-2708.

Albini, S. and Puri, P. L. (2010). SWI/SNF complexes, chromatin remodeling and skeletal myogenesis: It's time to exchange! *Exp. Cell Res.* **316**, 3073-3080.

Alford, E. K., Roy, R. R., Hodgson, J. A. and Edgerton, V. R. (1987). Electromyography of rat soleus, medial gastrocnemius, and tibialis anterior during hindlimb suspension. *Exp. Neurol.* **96**, 635-649.

Alkner, B. A. and Tesch, P. A. (2004). Knee extensor and plantar flexor muscle size and function following 90 days of bed rest with or without resistance exercise. *Eur. J. Appl. Physiol.* **93**, 294-305.

Allan, M. E. and Storey, K. B. (2012). Expression of NF-kB and downstream antioxidant genes in skeletal muscle of hibernating ground squirrels, *Spermophilus tridecemlineatus*. *Cell Biochem. Funct.* **30**, 166-174.

Amelio, D., Garofalo, F., Wong, W. P., Chew, S. F., Ip, Y. K., Cerra, M. C. and Tota, B. (2013). Nitric oxide synthase-dependent ‘‘On/Off’’ switch and apoptosis in freshwater and aestivating lungfish, *Protopterus annectens*: Skeletal muscle versus cardiac muscle. *Nitric Oxide – Biol. Ch.* **32**, 1-12.

Andersen, C. L., Jensen, J. L. and Orntoft, T. F. (2004). Normalization of real-time quantitative reverse transcription-PCR data: A model-based variance estimation approach to identify genes suited for normalization, applied to bladder and colon cancer data sets. *Cancer Res.* **64**, 5245-5250.

Anderson, L. V. B., Davison, K., Moss, J. A., Richard, I., Fardeau, M., Tome, F. M. S., Hubner, C., Lasa, A., Colomer, J. and Beckmann, J. S. (1998). Characterization of monoclonal antibodies to calpain 3 and protein expression in muscle from patients with limb-girdle muscular dystrophy type 2A. *Am. J. Pathol.* **153**, 1169-1179.

Andres-Mateos, E., Brinkmeier, H., Burks, T. N., Mejias, R., Files, D. C., Steinberger, M., Soleimani, A., Marx, R., Simmers, J. L., Lin, B. et al. (2013). Activation

of serum/glucocorticoid-induced kinase 1 (SGK1) is important to maintain skeletal muscle homeostasis and prevent atrophy. *EMBO Mol. Med.* **5**, 80-91.

Andrianjafiniony, T., Dupre-Aucouturier, S., Letexier, D., Couchoux, H. and Desplanches, D. (2010). Oxidative stress, apoptosis, and proteolysis in skeletal muscle repair after unloading. *Am. J. Physiol. Cell Physiol.* **299**, C307-C315.

Armstrong, C. and Staples, J. F. (2010). The role of succinate dehydrogenase and oxaloacetate in metabolic suppression during hibernation and arousal. *J. Comp. Physiol. B Biochem. Syst. Environ. Physiol.* **180**, 775-783.

Awede, B., Thissen, J. P., Gailly, P. and Lebacq, J. (1999). Regulation of IGF-I, IGFBP-4 and IGFBP-5 gene expression by loading in mouse skeletal muscle. *FEBS Lett.* **461**, 263-267.

Baki, A., Tompa, P., Alexa, A., Molnar, O. and Friedrich, P. (1996). Autolysis parallels activation of mu-calpain. *Biochem. J.* **318**, 897-901.

Baras, A. and Moskaluk, C. A. (2010). Intracellular localization of GASP/ECOP/VOPP1. *J. Mol. Hist.* **41**, 153-164.

Baras, A. S., Solomon, A., Davidson, R. and Moskaluk, C. A. (2011). Loss of VOPP1 overexpression in squamous carcinoma cells induces apoptosis through oxidative cellular injury. *Lab. Investig.* **91**, 1170-1180.

Barbieri, E. and Sestili, P. (2012). Reactive oxygen species in skeletal muscle signaling. *J. Signal Transduct.* **2012**, Article ID 982794.

Barrett, R. M. A., Colnaghi, R. and Wheatley, S. P. (2011). Threonine 48 in the BIR domain of survivin is critical to its mitotic and anti-apoptotic activities and can be phosphorylated by CK2 in *vitro*. *Cell Cycle* **10**, 538-548.

Bartoli, M. and Richard, I. (2005). Calpains in muscle wasting. *Int. J. Biochem. Cell Biol.* **37**, 2115-2133.

Bastide, B., Conti, A., Sorrentino, V. and Mounier, Y. (2000). Properties of ryanodine receptor in rat muscles submitted to unloaded conditions. *Biochem. Biophys. Res. Commun.* **270**, 442-447.

Beis, I. and Newsholme, E. A. (1975). Contents of adenine-nucleotides, phosphagens and some glycolytic intermediates in resting muscles from vertebrates and invertebrates. *Biochem. J.* **152**, 23-32.

Benjamini, Y. and Hochberg, Y. (1995). Controlling the false discovery rate - a practical and powerful approach to multiple testing. *J. R. Stat. Soc. Ser. B Stat. Methodol.* **57**, 289-300.

Berner, N.J., Else, P.L., Hulbert, A.J., Mantle, B.L., Cramp, R.L., Franklin, C.E. (2009). Metabolic depression during aestivation does not involve remodelling of membrane fatty acids in two Australian frogs. *J. Comp. Physiol. B Biochem. Syst. Environ. Physiol.* **179**, 857-866.

Bishop, T. and Brand, M. D. (2000). Processes contributing to metabolic depression in hepatopancreas cells from the snail *Helix aspersa*. *J. Exp. Biol.* **203**, 3603-3612.

Bishop, T., St-Pierre, J. and Brand, M. D. (2002). Primary causes of decreased mitochondrial oxygen consumption during metabolic depression in snail cells. *Am. J. Physiol. Regul. Integr. Comp. Physiol.* **282**, R372-R382.

Bloomfield, S. A. (1997). Changes in musculoskeletal structure and function with prolonged bed rest. *Med. Sci. Sports Exerc.* **29**, 197-206.

Blumenthal, S., Morgan-Boyd, R., Nelson, R., Garshelis, D. L., Turyk, M. E. and Unterman, T. (2011). Seasonal regulation of the growth hormone-insulin-like growth factor-I axis in the American black bear (*Ursus americanus*). *Am. J. Physiol. Endocrinol. Metab.* **301**, E628-E636.

Bodine, S. C. (2013a). Disuse-induced muscle wasting. *Int. J. Biochem. Cell Biol.* **45**, 2200-2208.

Bodine, S. C. (2013b). Hibernation: The search for treatments to prevent disuse-induced skeletal muscle atrophy. *Exp. Neurol.* **248**, 129-135.

Booth, F. W. and Seider, M. J. (1979). Recovery of skeletal muscle after 3 months of hindlimb immobilization in rats. *J. Appl. Physiol.* **47**, 435-439.

Boutilier, R. G. and St Pierre, J. (2002). Adaptive plasticity of skeletal muscle energetics in hibernating frogs: mitochondrial proton leak during metabolic depression. *J. Exp. Biol.* **205**, 2287-2296.

Brenner, F. J. and Lyle, P. D. (1975). Effect of previous photoperiodic conditions and visual stimulation on food storage and hibernation in eastern chipmunk (*Tamias striatus*). *Am. Midl. Nat.* **93**, 227-234.

Brocca, L., Cannavino, J., Coletto, L., Biolo, G., Sandri, M., Bottinelli, R. and Pellegrino, M. A. (2012). The time course of the adaptations of human muscle proteome to bed rest and the underlying mechanisms. *J. Physiol. (Lond.)* **590**, 5211-5230.

Brookes, P. S. (2005). Mitochondrial H^+ leak and ROS generation: An odd couple. *Free Radic. Biol. Med.* **38**, 12-23.

Brooks, N. E., Myburgh, K. H. and Storey, K. B. (2011). Myostatin levels in skeletal muscle of hibernating ground squirrels. *J. Exp. Biol.* **214**, 2522-2527.

Brown, J. C. L., Chung, D. J., Belgrave, K. R. and Staples, J. F. (2012). Mitochondrial metabolic suppression and reactive oxygen species production in liver and skeletal muscle of hibernating thirteen-lined ground squirrels. *Am. J. Physiol. Regul. Integr. Comp. Physiol.* **302**, R15-R28.

Brown, J. C. L., Chung, D. J., Cooper, A. N. and Staples, J. F. (2013). Regulation of succinate-fuelled mitochondrial respiration in liver and skeletal muscle of hibernating thirteen-lined ground squirrels. *J. Exp. Biol.* **216**, 1736-1743.

Bruce, S. A., Phillips, S. K. and Woledge, R. C. (1997). Interpreting the relation between force and cross-sectional area in human muscle. *Med. Sci. Sports Exerc.* **29**, 677-683.

Buck, C. L. and Barnes, B. M. (1999). Annual cycle of body composition and hibernation in free-living arctic ground squirrels. *J. Mammal.* **80**, 430-442.

Burgoyne, J. R., Mongue-Din, H., Eaton, P. and Shah, A. M. (2012). Redox signaling in cardiac physiology and pathology. *Circ. Res.* **111**, 1091-1106.

Cannon, B. and Nedergaard, J. (2004). Brown adipose tissue: Function and physiological significance. *Physiol. Rev.* **84**, 277-359.

Cao, G., Clark, R. S., Pei, W., Yin, W., Zhang, F., Sun, F. Y., Graham, S. H. and Chen, J. (2003). Translocation of apoptosis-inducing factor in vulnerable neurons after transient cerebral ischemia and in neuronal cultures after oxygen-glucose deprivation. *J. Cereb. Blood Flow Metab.* **23**, 1137-1150.

Carey, H. V., Andrews, M. T. and Martin, S. L. (2003). Mammalian hibernation: cellular and molecular responses to depressed metabolism and low temperature. *Physiol. Rev.* **83**, 1153-1181.

Chen, Y.-W., Gregory, C. M., Scarborough, M. T., Shi, R., Walter, G. A. and Vandenborne, K. (2007). Transcriptional pathways associated with skeletal muscle disuse atrophy in humans. *Physiol. Genomics* **31**, 510-520.

Chopard, A., Lecunff, M., Danger, R., Lamirault, G., Bihouee, A., Teusan, R., Jasmin, B. J., Marini, J. F. and Leger, **J. J.** (2009). Large-scale mRNA analysis of female skeletal muscles during 60 days of bed rest with and without exercise or dietary protein supplementation as countermeasures. *Physiol. Genomics*. **38**, 291-302.

Conesa, A., Gotz, S., Garcia-Gomez, J. M., Terol, J., Talon, M. and Robles, M. (2005). Blast2GO: a universal tool for annotation, visualization and analysis in functional genomics research. *Bioinformatics* **21**, 3674-3676.

Cotton, C. J. and Harlow, H. J. (2010). Avoidance of skeletal muscle atrophy in spontaneous and facultative hibernators. *Physiol. Biochem. Zool.* **83**, 551-560.

Cowan, K. J., MacDonald, J. A., Storey, J. M. and Storey, K. B. (2000). Metabolic reorganization and signal transduction during estivation in the spadefoot toad. *Exp. Biol. Online* **5**, 1-27.

Cowan, K. J. and Storey, K. B. (1999). Reversible phosphorylation control of skeletal muscle pyruvate kinase and phosphofructokinase during estivation in the spadefoot toad, *Scaphiopus couchii*. *Mol. Cell. Biochem.* **195**, 173-181.

Crockett, C. J. and Peters, S. E. (2008). Hindlimb muscle fiber types in two frogs (*Rana catesbeiana* and *Litoria caerulea*) with different locomotor behaviors: histochemical and enzymatic comparison. *J. Morphol.* **269**, 365-374.

Dalla Libera, L., Ravara, B., Gobbo, V., Tarricone, E., Vitadello, M., Biolo, G., Vescovo, G. and Gorza, L. (2009). A transient antioxidant stress response accompanies the onset of disuse atrophy in human skeletal muscle. *J. Appl. Physiol.* **107**, 549-557.

Dargelos, E., Brule, C., Stuelsatz, P., Mouly, V., Veschambre, P., Cottin, P. and Poussard, S. (2010). Up-regulation of calcium-dependent proteolysis in human myoblasts under acute oxidative stress. *Exp. Cell Res.* **316**, 115-125.

Datta, S. R., Katsov, A., Hu, L., Petros, A., Fesik, S. W., Yaffe, M. B. and Greenberg, M. E. (2000)**.** 14-3-3 proteins and survival kinases cooperate to inactivate BAD by BH3 domain phosphorylation. *Mol. Cell.* **6**, 41-51.

Delaney, R. G., Lahiri, S. and Fishman, A. P. (1974). Aestivation of African lungfish *Protopterus aethiopicus*: cardiovascular and respiratory functions. *J. Exp. Biol.* **61**, 111-128.

Derbre, F., Ferrando, B., Gomez-Cabrera, M. C., Sanchis-Gomar, F., Martinez-Bello, V. E., Olaso-Gonzalez, G., Diaz, A., Gratas-Delamarche, A., Cerda, M. and Vina, J. (2012). Inhibition of xanthine oxidase by allopurinol prevents skeletal muscle atrophy: role of p38 MAPKinase and E3 ubiquitin ligases. *PLoS ONE* **7**.

Devol, D. L., Rotwein, P., Sadow, J. L., Novakofski, J. and Bechtel, P. J. (1990). Activation of insulin-like growth-factor gene expression during work-induced skeletal muscle growth. *Am. J. Physiol.* **259**, E89-E95.

Duguez, S., Bartoli, M. and Richard, I. (2006). Calpain 3: a key regulator of the sarcomere? *FEBS J.* **273**, 3427-3436.

Dupont-Versteegden, E. E., Strotman, B. A., Gurley, C. M., Gaddy, D., Knox, M., Fluckey, J. D. and Peterson, C. A. (2006). Nuclear translocation of EndoG at the initiation of disuse muscle atrophy and apoptosis is specific to myonuclei. *Am. J. Physiol. Regul. Integr. Comp. Physiol.* **291**, R1730–R1740.

Edmunds, T., Nagainis, P. A., Sathe, S. K., Thompson, V. F. and Goll, D. E. (1991). Comparison of the autolyzed and unautolyzed forms of mu- and m-calpain from bovine skeletal muscle. *Biochim. Biophys. Acta* **1077**, 197-208.

Ekblom, R. and Galindo, J. (2011). Applications of next generation sequencing in molecular ecology of non-model organisms. *Heredity* **107**, 1-15.

Elliott, B., Renshaw, D., Getting, S. and Mackenzie, R. (2012). The central role of myostatin in skeletal muscle and whole body homeostasis. *Acta Physiol.* **205**, 324-340.

Enns, D. L., Raastad, T., Ugelstad, I. and Belcastro, A. N. (2007). Calpain/calpastatin activities and substrate depletion patterns during hindlimb unweighting and reweighting in skeletal muscle. *Eur. J. Appl. Physiol.* **100**, 445-455.

Fedorov, V. B., Goropashnaya, A. V., Stewart, N. C., Toien, O., Chang, C., Wang, H., Yan, J., Showe, L. C., Showe, M. K. and Barnes, B. M. (2014). Comparative functional genomics of adaptation to muscular disuse in hibernating mammals. *Mol. Ecol.* **23**, 5524-5537.

Fedorov, V. B., Goropashnaya, A. V., Toien, O., Stewart, N. C., Gracey, A. Y., Chang, C. L., Qin, S. Z., Pertea, G., Quackenbush, J., Showe, L. C. et al. (2009). Elevated expression of protein biosynthesis genes in liver and muscle of hibernating black bears (*Ursus americanus*). *Physiol. Genomics* **37**, 108-118.

Ferreira-Cravo, M., Welker, A. F. and Hermes-Lima, M. (2010). The connection between oxidative stress and estivation in gastropods and anurans. In *Aestivation: molecular and physiological aspects,* (eds. C. A. Navas and J. E. Carvalho), pp. 47-61. Berlin: Springer-Verlag.

Ferreira, R., Neuparth, M. J., Vitorino, R., Appell, H. J., Amado, F. and Duarte, J. A. (2008). Evidences of apoptosis during the early phases of soleus muscle atrophy in hindlimb suspended mice. *Physiol. Res.* **57**, 601-611.

Flanigan, J. E. and Guppy, M. (1997). Metabolic depression and sodium-potassium ATPase in the aestivating frog, *Neobatrachus kunapalari*. *J. Comp. Physiol. B Biochem. Syst. Environ. Physiol.* **167**, 135-145.

Flanigan, J. E., Withers, P. C., Fuery, C.J. and Guppy, M. (1993). Metabolic depression and Na^+/K^+ gradients in the Australian goldfields frog, *Neobatrachus wilsmorei*. *J. Comp. Physiol. B Biochem. Syst. Environ. Physiol.* **163**, 587-593.

Flanigan, J. E., Withers, P. C. and Guppy, M. (1991). *In vitro* metabolic depression of tissues from the estivating frog *Neobatrachus pelobatoides*. *J. Exp. Biol.* **161**, 273-283.

Foksinski, M., Rozalski, R., Guz, J., Ruszkowska, B., Sztukowska, P., Piwowarski, M., Klungland, A. and Olinski, R. (2004). Urinary excretion of DNA repair products correlates with metabolic rates as well as with maximum life spans of different mammalian species. *Free Radic. Biol. Med.* **37**, 1449-1454.

Frick, N. T., Bystriansky, J. S., Ip, Y. K., Chew, S. F. and Ballantyne, J. S. (2008a). Carbohydrate and amino acid metabolism in fasting and aestivating African lungfish (*Protopterus dolloi*). *Comp. Biochem. Physiol. Part A Mol. Integr. Physiol.* **151**, 85-92.

Frick, N. T., Bystriansky, J. S., Ip, Y. K., Chew, S. F. and Ballantyne, J. S. (2008b). Lipid, ketone body and oxidative metabolism in the African lungfish, *Protopterus dolloi* following 60 days of fasting and aestivation. *Comp. Biochem. Physiol. Part A Mol. Integr. Physiol.* **151**, 93-101.

Fuery, C. J., Withers, P. C., Hobbs, A. A. and Guppy, M. (1998). The role of protein synthesis during metabolic depression in the Australian desert frog *Neobatrachus centralis*. *Comp. Biochem. Physiol. Part A Mol. Integr. Physiol.* **119**, 469-476.

Gallagher, K. and Staples, J. F. (2013). Metabolism of brain cortex and cardiac muscle mitochondria in hibernating 13-lined ground squirrels *Ictidomys tridecemlineatus*. *Physiol. Biochem. Zool.* **86**, 1-8.

Gans, C. and De Gueldre, G. (1992). Striated muscle physiology and functional morphology. In *Environmental physiology of the amphibians*, (eds. M. E. Feder and W. W. Burggren), pp 275–313. Chicago: University of Chicago Press.

Gehlbach, F. R., Gordon, R. and Jordan, J. B. (1973). Aestivation of salamander, *Siren intermedia*. *Am. Midl. Nat.* **89**, 455-463.

Geiser, F. (2013). Hibernation. *Curr. Biol.* **23**, R188-193.

Geiser, F. and Ruf, T. (1995). Hibernation versus daily torpor in mammals and birds - physiological variables and classification of torpor patterns. *Physiol. Zool.* **68**, 935-966.

Girish, S. and Saidapur, S.K. (2000). Interrelationship between food availability, fat body, and ovarian cycles in the frog, *Rana tigrina*, with a discussion on the role of fat body in anuran reproduction. *J. Exp. Zool.* **286,** 487-493.

Glass, M. L., Fernandes, M. S., Soncini, R., Glass, H. and Wasser, J. S. (1997). Effects of dry season dormancy on oxygen uptake, heart rate, and blood pressures in the toad, *Bufo paracnemis*. *J. Exp. Zool.* **279**, 330-336.

Goldberg, A. L. (1967). Work-induced growth of skeletal muscle in normal and hypophysectomized rats. *Am. J. Physiol.* **213**, 1193-1198.

Goldspink, D. F., Morton, A. J., Loughna, P. and Goldspink, G. (1986). The effect of hypokinesia and hypodynamia on protein turnover and the growth of four skeletal muscles of the rat. *Pflugers Arch.* **407**, 333-340.

Goll, D. E., Thompson, V. F., Li, H. Q., Wei, W. and Cong, J. Y. (2003). The calpain system. *Physiol. Rev.* **83**, 731-801.

Gomes-Marcondes, M. C. C. and Tisdale, M. J. (2002). Induction of protein catabolism and the ubiquitin-proteasome pathway by mild oxidative stress. *Cancer Lett.* **180**, 69-74.

Gotoh, I., Adachi, M. and Nishida, E. (2001). Identification and characterization of a novel MAP kinase kinase kinase, MLTK. *J. Biol. Chem.* **276**, 4276-4286.

Griend, D. J. V., Kocherginsky, M., Hickson, J. A., Stadler, W. M., Lin, A. N. and Rinker-Schaeffer, C. W. (2005). Suppression of metastatic colonization by the context-dependent activation of the c-jun NH2-terminal kinase kinases JNKK1/MKK4 and MKK7. *Cancer Res.* **65**, 10984-10991.

Grundy, J. E. and Storey, K. B. (1998). Antioxidant defenses and lipid peroxidation damage in estivating toads, *Scaphiopus couchii*. *J. Comp. Physiol. B Biochem. Syst. Environ. Physiol.* **168**, 132-142.

Guppy, M. and Withers, P. (1999). Metabolic depression in animals: physiological perspectives and biochemical generalizations. *Biol. Rev. Camb. Philos. Soc.* **74**, 1-40.

Haddad, F., Roy, R. R., Zhong, H., Edgerton, V. R. and Baldwin, K. M. (2003). Atrophy responses to muscle inactivity. II. Molecular markers of protein deficits. *J. Appl. Physiol.* **95**, 791-802.

Hampton, M., Melvin, R. G., Kendall, A. H., Kirkpatrick, B. R., Peterson, N. and Andrews, M. T. (2011). Deep sequencing the transcriptome reveals seasonal adaptive mechanisms in a hibernating mammal. *PLoS ONE* **6**.

Hang, C. T., Yang, J., Han, P., Cheng, H. L., Shang, C., Ashley, E., Zhou, B. and Chang, C. P. (2010). Chromatin regulation by Brg1 underlies heart muscle development and disease. *Nature* **466**, 62-U74.

Harlow, H. J., Lohuis, T., Anderson-Sprecher, R. C. and Beck, T. D. I. (2004). Body surface temperature of hibernating black bears may be related to periodic muscle activity. *J. Mammal.* **85**, 414-419.

Harlow, H. J., Lohuis, T., Beck, T. D. I. and Iaizzo, P. A. (2001). Muscle strength in overwintering bears - Unlike humans, bears retain their muscle tone when moribund for long periods. *Nature* **409**, 997-997.

Harlow, H. J. and Menkens, G. E. (1986). A comparison of hibernation in the black-tailed prairie dog, white-tailed prairie dog, and Wyoming ground squirrel. *Can. J. Zool.* **64**, 793-796.

Hather, B. M., Adams, G. R., Tesch, P. A. and Dudley, G. A. (1992). Skeletal muscle responses to lower-limb suspension in humans. *J. Appl. Physiol.* **72**, 1493-1498.

Hershey, J. D., Robbins, C. T., Nelson, O. L. and Lin, D. C. (2008). Minimal seasonal alterations in the skeletal muscle of captive brown bears. *Physiol. Biochem. Zool.* **81**, 138-147.

Hickey, A. J. R., Renshaw, G. M. C., Speers-Roesch, B., Richards, J. G., Wang, Y. X., Farrell, A. P. and Brauner, C. J. (2012). A radical approach to beating hypoxia: depressed free radical release from heart fibres of the hypoxia-tolerant epaulette shark (*Hemiscyllum ocellatum*). *J. Comp. Physiol. B Biochem. Syst. Environ. Physiol.* **182**, 91-100.

Hickson, J. A., Huo, D. Z., Vander Griend, D. J., Lin, A. N., Rinker-Schaeffer, C. W. and Yamada, S. D. (2006). The p38 kinases MKK4 and MKK6 suppress metastatic colonization in human ovarian carcinoma. *Cancer Res.* **66**, 2264-2270.

Hindle, A. G., Grabek, K. R., Epperson, L. E., Karimpour-Fard, A., Martin, S. L. (2014). Metabolic changes associated with the long winter fast dominate the liver proteome in 13-lined ground squirrels. *Physiol. Genomics*. **46**, 348-361.

Hindle, A. G., Karimpour-Fard, A., Epperson, L. E., Hunter, L. E. and Martin, S. L. (2011). Skeletal muscle proteomics: carbohydrate metabolism oscillates with seasonal and torpor-arousal physiology of hibernation. *Am. J. Physiol. Regul. Integr. Comp. Physiol.* **301**, R1440-R1452.

Hudson, N. J., Bennett, M. B. and Franklin, C. E. (2004). Effect of aestivation on long bone mechanical properties in the green-striped burrowing frog, *Cyclorana alboguttata*. *J. Exp. Biol.* **207**, 475-482.

Hudson, N. J. and Franklin, C. E. (2002a). Effect of aestivation on muscle characteristics and locomotor performance in the Green-striped burrowing frog, *Cyclorana alboguttata*. *J. Comp. Physiol. B Biochem. Syst. Environ. Physiol.* **172**, 177-182.

Hudson, N. J. and Franklin, C. E. (2002b). Maintaining muscle mass during extended disuse: Aestivating frogs as a model species. *J. Exp. Biol.* **205**, 2297-2303.

Hudson, N. J. and Franklin, C. E. (2003). Preservation of three-dimensional capillary structure in frog muscle during aestivation. *J. Anat.* **202**, 471-474.

Hudson, N. J., Lavidis, N. A., Choy, P. T. and Franklin, C. E. (2005). Effect of prolonged inactivity on skeletal motor nerve terminals during aestivation in the burrowing frog, *Cyclorana alboguttata*. *J. Comp. Physiol. A Sens. Neural Behav. Physiol.* **191**, 373-379.

Hudson, N. J., Lehnert, S. A., Ingham, A. B., Symonds, B., Franklin, C. E. and Harper, G. S. (2006). Lessons from an estivating frog: sparing muscle protein despite starvation and disuse. *Am. J. Physiol. Regul. Integr. Comp. Physiol.* **290**, R836-R843.

Hudson, N. J., Lonhienne, T. G. A., Franklin, C. E., Harper, G. S. and Lehnert, S. A. (2008). Epigenetic silencers are enriched in dormant desert frog muscle. *J. Comp. Physiol. B Biochem. Syst. Environ. Physiol.* **178**, 729-734.

Humphries, M. M., Thomas, D. W. and Kramer, D. L. (2001). Torpor and digestion in food-storing hibernators. *Physiol. Biochem. Zool.* **74**, 283-292.

Hur, W. and Gray, N. S. (2011). Small molecule modulators of antioxidant response pathway. *Curr. Opin. Chem. Biol.* **15**, 162-173.

Ilian, M. A. and Forsberg, N. E. (1992). Gene expression of calpains and their specific endogenous inhibitor, calpastatin, in skeletal-muscle of fed and fasted rabbits. *Biochem. J.* **287**, 163-171.

Jackman, R. W. and Kandarian, S. C. (2004). The molecular basis of skeletal muscle atrophy. *Am. J. Physiol. Cell Physiol.* **287**, C834-C843.

James, R. S., Staples, J. F., Brown, J. C. L., Tessier, S. N. and Storey, K. B. (2013). The effects of hibernation on the contractile and biochemical properties of skeletal muscles in the thirteen-lined ground squirrel, *Ictidomys tridecemlineatus*. *J. Exp. Biol.* **216**, 2587-94.

Jones, D. (2004). Structure of the muscle fibre. In *Skeletal muscle from molecules to movement*, (eds. D. Jones J. Round and A. de Haan), pp. 1-8. London: Churchill Livingstone.

Jones, R. M. (1980). Metabolic consequences of accelerated urea synthesis during seasonal dormancy of spadefoot toads, *Scaphiopus couchii* and *Scaphiopus multiplicatus*. *J. Exp. Zool.* **212**, 255-267.

Jones, S. W., Hill, R. J., Krasney, P. A., O'Conner, B., Peirce, N. and Greenhaff, P. L. (2004). Disuse atrophy and exercise rehabilitation in humans profoundly affects the expression of genes associated with the regulation of skeletal muscle mass. *FASEB J.* **18**, 1025-1027.

Kashiyama, T., Murayama, T., Suzuki, E., Allen, P. D. and Ogawa, Y. (2010). Frog α- and β-ryanodine receptors provide distinct intracellular Ca^{2+} signals in a myogenic cell line. *PLoS ONE.* **5**, e11526.

Kayes, S. M., Cramp, R. L. and Franklin, C. E. (2009a). Metabolic depression during aestivation in *Cyclorana alboguttata*. *Comp. Biochem. Physiol. Part A Mol. Integr. Physiol.* **154**, 557-563.

Kayes, S. M., Cramp, R. L., Hudson, N. J. and Franklin, C. E. (2009b). Surviving the drought: burrowing frogs save energy by increasing mitochondrial coupling. *J. Exp. Biol.* **212**, 2248-2253.

Kayser, C. and Frank, R. M. (1963). Comportement des tissus calcifies du hamster d'Europe *Cricetus cricetus* au cours de l' hibernation. *Arch. Oral Biol.* **8**, 703-710.

Klein, C. A. (2013). Selection and adaptation during metastatic cancer progression. *Nature* **501**, 365-372.

Kondo, H., Miura, M. and Itokawa, Y. (1991). Oxidative stress in skeletal muscle atrophied by immobilization. *Acta Physiol. Scand.* **142**, 527-528.

Kramerova, I., Kudryashova, E. and Spencer, M. J. (2004). Null mutation of calpain 3 (p94) in mice causes abnormal sarcomere formation *in vivo* and *in vitro*. *Hum. Mol. Genet.* **13**, 1373-1388.

Kultz, D. (2005). Molecular and evolutionary basis of the cellular stress response. *Annu. Rev. Physiol.* **67**, 225-257.

Kumano, T., Konno, N., Wakasugi, T., Matsuda, K., Yoshizawa, H. and Uchiyama, M. (2008). Cellular localization of a putative Na^+/H^+ exchanger 3 during ontogeny in the pronephros and mesonephros of the Japanese black salamander (*Hynobius nigrescens* Stejneger). *Cell Tissue Res.* **331**, 675-685.

Kutschke, M., Grimpo, K., Kastl, A., Schneider, S., Heldmaier, G., Exner, C. and Jastroch, M. (2013). Depression of mitochondrial respiration during daily torpor of the Djungarian hamster, *Phodopus sungorus*, is specific for liver and correlates with body temperature. *Comp. Biochem. Physiol. Part A Mol. Integr. Physiol.* **164**, 584-589.

Kuznetsov, A. V., Veksler, V., Gellerich, F. N., Saks, V., Margreiter, R. and Kunz, W. S. (2008). Analysis of mitochondrial function in situ in permeabilized muscle fibers, tissues and cells. *Nat. Protoc.* **3**, 965-976.

Lans, H., Marteijn, J. A. and Vermeulen, W. (2012). ATP-dependent chromatin remodeling in the DNA-damage response. *Epigenetics Chromatin* **5**.

Lawler, J. M., Song, W. and Demaree, S. R. (2003). Hindlimb unloading increases oxidative stress and disrupts antioxidant capacity in skeletal muscle. *Free Radic. Biol. Med.* **35**, 9-16.

Lawler, J. M., Song, W. and Kwak, H. B. (2006). Differential response of heat shock proteins to hindlimb unloading and reloading in the soleus. *Muscle Nerve* **33**, 200-207.

Leblanc, A. D., Schneider, V. S., Evans, H. J., Pientok, C., Rowe, R. and Spector, E. (1992). Regional changes in muscle mass following 17 weeks of bed rest. *J. Appl. Physiol.* **73**, 2172-2178.

Lee, K., So, H., Gwag, T., Ju, H., Lee, J. W., Yamashita, M. and Choi, I. (2010). Molecular mechanism underlying muscle mass retention in hibernating bats: role of periodic arousal. *J. Cell. Physiol.* **222**, 313-319.

Lee, P. D. K., Giudice, L. C., Conover, C. A. and Powell, D. R. (1997). Insulin-like growth factor binding protein-1: Recent findings and new directions. *Proc. Soc. Exp. Biol. Med.* **216**, 319-357.

Lee, K., Park, J. Y., Yoo, W., Gwag, T., Lee, J.-W., Byun, M.-W. and Choi, I. (2008). Overcoming muscle atrophy in a hibernating mammal despite prolonged disuse in dormancy: proteomic and molecular assessment. *J. Cell. Biochem.* **104**, 642-656.

Leeuwenburgh, C., Gurley, C. M., Strotman, B. A. and Dupont-Versteegden, E. E. (2005). Age-related differences in apoptosis with disuse atrophy in soleus muscle. *Am. J. Physiol. Regul. Integr. Comp. Physiol.* **288**, R1288-R1296.

Li, Y. P., Chen, Y. L., Li, A. S. and Reid, M. B. (2003). Hydrogen peroxide stimulates ubiquitin-conjugating activity and expression of genes for specific E2 and E3 proteins in skeletal muscle myotubes. *Am. J. Physiol. Cell Physiol.* **285**, C806-C812.

Lieber, R. L. (2010). Skeletal muscle structure, function, and plasticity: the physiological basis of rehabilitation. Baltimore: Lippincott Williams & Wilkins.

Lieber, R. L., Friden, J. O., Hargens, A. R., Danzig, L. A. and Gershuni, D. H. (1988). Differential response of the dog quadriceps muscle to external skeletal fixation of the knee. *Muscle Nerve* **11**, 193-201.

Lin, D. C., Hershey, J. D., Mattoon, J. S. and Robbins, C. T. (2012). Skeletal muscles of hibernating brown bears are unusually resistant to effects of denervation. *J. Exp. Biol.* **215**, 2081-2087.

Lohuis, T. D., Harlow, H. J. and Beck, T. D. I. (2007a). Hibernating black bears (*Ursus americanus*) experience skeletal muscle protein balance during winter anorexia. *Comp. Biochem. Physiol. Part B Biochem. Mol. Biol.* **147**, 20-28.

Lohuis, T. D., Harlow, H. J., Beck, T. D. I. and Iaizzo, P. A. (2007b). Hibernating bears conserve muscle strength and maintain fatigue resistance. *Physiol. Biochem. Zool.* **80**, 257-269.

Lopez-Torres, M., Perez-Campo, R., Rojas, C., Cadenas, S. and Barja, G. (1993). Maximum life-span in vertebrates - relationship with liver antioxidant enzymes, glutathione system, ascorbate, urate, sensitivity to peroxidation, true malondialdehyde, *in vivo* H_2O_2, and basal and maximum aerobic capacity. *Mech. Ageing Dev.* **70**, 177-199.

Loughna, P., Goldspink, G. and Goldspink, D. F. (1986). Effect of inactivity and passive stretch on protein turnover in phasic and postural rat muscles. *J. Appl. Physiol.* **61**, 173-179.

Lovegrove, B. G., Lobban, K. D. and Levesque, D. L. (2014). Mammal survival at the Cretaceous-Palaeogene boundary: metabolic homeostasis in prolonged tropical hibernation in tenrecs. *Proc. R. Soc. B.* **281**, 20141304.

Loveridge, J. P. and Withers, P. C. (1981). Metabolism and water balance of active and cocooned African bullfrogs *Pyxicephalus adspersus*. *Physiol. Zool.* **54**, 203-214.

Lutz, G. J., Cuizon, D. B., Ryan, A. F and Lieber, R. L. (1998). Four novel myosin heavy chain transcripts in *Rana pipiens* define a molecular basis for muscle fibre types in *Rana pipiens*. *J. Physiol.* **508**, 667–680.

Ma, X. W., Li, Q., Xu, P. T., Zhang, L., Li, H. and Yu, Z. B. (2011). Tetanic contractions impair sarcomeric Z-disk of atrophic soleus muscle via calpain pathway. *Mol. Cell. Biochem.* **354**, 171-180.

Macqueen, D. J., Meischke, L., Manthri, S., Anwar, A., Solberg, C. and Johnston, I. A. (2010). Characterisation of *capn1*, *capn2*-like, *capn3* and *capn11* genes in Atlantic halibut (*Hippoglossus hippoglossus* L.): Transcriptional regulation across tissues and in skeletal muscle at distinct nutritional states. *Gene* **453**, 45-58.

Maes, K., Testelmans, D., Powers, S., Decramer, M. and Gayan-Ramirez, G. (2007). Leupeptin inhibits ventilator-induced diaphragm dysfunction in rats. *Am. J. Respir. Crit. Care. Med.* **175**, 1134-1138.

Malhotra, J. D. and Kaufman, R. J. (2007). The endoplasmic reticulum and the unfolded protein response. *Semin. Cell Dev. Biol.* **18**, 716-731.

Malik, A. I. and Storey, K. B. (2009). Activation of extracellular signal-regulated kinases during dehydration in the African clawed frog, *Xenopus laevis*. *J. Exp. Biol.* **212**, 2595-2603.

Mantle, B. L. (2007). Effect of prolonged aestivation on muscle morphology and biochemistry in the Green-striped burrowing frog, *Cyclorana alboguttata*. PhD Thesis, The University of Queensland.

Mantle, B. L., Guderley, H., Hudson, N. J. and Franklin, C. E. (2010). Enzyme activity in the aestivating Green-striped burrowing frog (*Cyclorana alboguttata*). *J. Comp. Physiol. B Biochem. Syst. Environ. Physiol.* **180**, 1033-1043.

Mantle, B. L., Hudson, N. J., Harper, G. S., Cramp, R. L. and Franklin, C. E. (2009). Skeletal muscle atrophy occurs slowly and selectively during prolonged aestivation in *Cyclorana alboguttata* (Gunther 1867). *J. Exp. Biol.* **212**, 3664-3672.

Marzetti, E., Hwang, J. C. Y., Lees, H. A., Wohlgemuth, S. E., Dupont-Versteegden, E. E., Carter, C. S., Bernabei, R. and Leeuwenburgh, C. (2010). Mitochondrial death effectors: Relevance to sarcopenia and disuse muscle atrophy. *Biochim. Biophys. Acta* **1800**, 235-244.

Matsushima, Y., Nanri, H., Nara, S., Okufuji, T., Ohta, M., Hachisuka, K. and Ikeda, M. (2006). Hindlimb unloading decreases thioredoxin-related antioxidant proteins and increases thioredoxin-binding protein-2 in rat skeletal muscle. *Free Radic. Res.* **40**, 715-722.

Mayer, W. V. and Bernick, S. (1959). Dental caries in hibernating arctic ground squirrels, *Spermophilus undulatus*. *Anat. Rec.* **134**, 606-607.

McClung, J. M., Judge, A. R., Talbert, E. E. and Powers, S. K. (2009). Calpain-1 is required for hydrogen peroxide-induced myotube atrophy. *Am. J. Physiol. Cell Physiol.* **296**, C363-C371.

McPherron, A. C., Lawler, A. M. and Lee, S. J. (1997). Regulation of skeletal muscle mass in mice by a new TGF-beta superfamily member. *Nature* **387**, 83-90.

Min, K., Smuder, A. J., Kwon, O. S., Kavazis, A. N., Szeto, H. H. and Powers, S. K. (2011). Mitochondrial-targeted antioxidants protect skeletal muscle against immobilization-induced muscle atrophy. *J. Appl. Physiol.* **111**, 1459-1466.

Mitch, W. E. and Goldberg, A. L. (1996). Mechanisms of disease - Mechanisms of muscle wasting - The role of the ubiquitin-proteasome pathway. *N. Engl. J. Med.* **335**, 1897-1905.

Miyabara, E. H., Nascimento, T. L., Rodrigues, D. C., Moriscot, A. S., Davila, W. F., AitMou, Y., deTombe, P. P. and Mestril, R. (2012). Overexpression of inducible 70-kDa heat shock protein in mouse improves structural and functional recovery of skeletal muscles from atrophy. *Pflueg. Arch. Eur. J. Physiol.* **463**, 733-741.

Morin, P. J. and Storey, K. B. (2006). Evidence for a reduced transcriptional state during hibernation in ground squirrels. *Cryobiology* **53**, 310-318.

Morrow, G. and Nicol, S. C. (2009). Cool sex? Hibernation and reproduction overlap in the Echidna. *PLoS ONE*. **4**, e6070.

Murphy, K. T., Cobani, V., Ryall, J. G., Ibebunjo, C. and Lynch, G. S. (2011). Acute antibody-directed myostatin inhibition attenuates disuse muscle atrophy and weakness in mice. *J. Appl. Physiol.* **110**, 1065-1072.

Murphy, R. M. (2010). Calpains, skeletal muscle function and exercise. *Clin. Exp. Pharmacol. Physiol.* **37**, 385-391.

Murphy, R. M., Goodman, C. A., McKenna, M. J., Bennie, J., Leikis, M. and Lamb, G. D. (2007). Calpain-3 is autolyzed and hence activated in human skeletal muscle 24 h following a single bout of eccentric exercise. *J. Appl. Physiol.* **103**, 926-931.

Murphy, R. M. and Lamb, G. D. (2009). Endogenous calpain-3 activation is primarily governed by small increases in resting cytoplasmic Ca^{2+} and is not dependent on stretch. *J. Biol. Chem.* **284**, 7811-7819.

Murphy, R. M., Snow, R. J. and Lamb, G. D. (2006). mu-calpain and calpain-3 are not autolyzed with exhaustive exercise in humans. *Am. J. Physiol. Cell Physiol.* **290**, C116-C122.

Musacchia, X. J., Steffen, J. M. and Fell, R. D. (1988). Disuse atrophy of skeletal muscle: animal models. *Exerc. Sport Sci. Rev.* **16**, 61-87.

Myung, J., Kim, K. B. and Crews, C. M. (2001). The ubiquitin-proteasome pathway and proteasome inhibitors. *Med. Res. Rev.* **21**, 245-273.

Nicks, D. K., Beneke, W. M., Key, R. M. and Timson, B. F. (1989). Muscle fiber size and number following immobilization atrophy. *J. Anat.* **163**, 1-5.

Nowell, M. M., Choi, H. and Rourke, B. C. (2011). Muscle plasticity in hibernating ground squirrels (*Spermophilus lateralis*) is induced by seasonal, but not low-temperature, mechanisms. *J. Comp. Physiol. B Biochem. Syst. Environ. Physiol.* **181**, 147-164.

O Connor, D. S., Grossman, D., Plescia, J., Li, F. Z., Zhang, H., Villa, A., Tognin, S., Marchisio, P. C. and Altieri, D. C. (2000). Regulation of apoptosis at cell division by p34 (cdc2) phosphorylation of survivin. *Proc. Natl. Acad. Sci. U. S. A.* **97**, 13103-13107.

Oki, S., Desaki, J., Matsuda, Y., Okumura, H. and Shibata, T. (1995). Capillaries with fenestrae in the rat soleus muscle after experimental limb immobilization. *J. Electron Microsc.* **44**, 307-310.

Page, M. M., Salway, K. D., Ip, Y. K., Chew, S. F., Warren, S. A., Ballantyne, J. S. and Stuart, J. A. (2010). Upregulation of intracellular antioxidant enzymes in brain and heart during estivation in the African lungfish *Protopterus dolloi*. *J. Comp. Physiol. B Biochem. Syst. Environ. Physiol.* **180**, 361-369.

Pakay, J. L., Withers, P. C., Hobbs, A. A. and Guppy, M. (2002). *In vivo* downregulation of protein synthesis in the snail *Helix apersa* during estivation. *Am. J. Physiol. Regul. Integr. Comp. Physiol.* **283**, R197-R204.

Pedler, S., Fuery, C. J., Withers, P. C., Flanigan, J. and Guppy, M. (1996). Effectors of metabolic depression in an estivating pulmonate snail (*Helix aspersa*): Whole animal and *in vitro* tissue studies. *J. Comp. Physiol. B Biochem. Syst. Environ. Physiol.* **166**, 375-381.

Pellegrino, M. A., Desaphy, J. F., Brocca, L., Pierno, S., Camerino, D. C. and Bottinelli, R. (2011). Redox homeostasis, oxidative stress and disuse muscle atrophy. *J. Physiol. (Lond.)* **589**, 2147-2160.

Phillips, S. M., Glover, E. I. and Rennie, M. J. (2009). Alterations of protein turnover underlying disuse atrophy in human skeletal muscle. *J. Appl. Physiol.* **107**, 645-654.

Picard, M., Taivassalo, T., Ritchie, D., Wright, K. J., Thomas, M. M., Romestaing, C. and Hepple, R. T. (2011). Mitochondrial structure and function are disrupted by standard isolation methods. *PLoS ONE* **6**.

Pilegaard, H., Saltin, B. and Neufer, P. D. (2003). Exercise induces transient transcriptional activation of the PGC-1 alpha gene in human skeletal muscle. *J. Physiol. (Lond.)* **546**, 851-858.

Portt, L., Norman, G., Clapp, C., Greenwood, M. and Greenwood, M. T. (2011). Anti-apoptosis and cell survival: A review. *Biochim. Biophys. Acta* **1813**, 238-259.

Powers, S. K., Kavazis, A. N. and McClung, J. M. (2007). Oxidative stress and disuse muscle atrophy. *J. Appl. Physiol.* **102**, 2389-2397.

Powers, S. K., Smuder, A. J. and Criswell, D. S. (2011). Mechanistic links between oxidative stress and disuse muscle atrophy. *Antioxid. Redox Signal.* **15**, 2519-2528.

Powers, S. K., Wiggs, M. P., Duarte, J. A., Zergeroglu, A. M. and Demirel, H. A. (2012). Mitochondrial signaling contributes to disuse muscle atrophy. *Am. J. Physiol. Endocrinol. Metab.* **303**, E31-E39.

Price, S. R. (2003). Increased transcription of ubiquitin-proteasome system components: molecular responses associated with muscle atrophy. *Int. J. Biochem. Cell Biol.* **35**, 617-628.

Ramnanan, C. J., Allan, M. E., Groom, A. G. and Storey, K. B. (2009). Regulation of global protein translation and protein degradation in aerobic dormancy. *Mol. Cell. Biochem.* **323**, 9-20.

Ramnanan, C. J., Groom, A. G. and Storey, K. B. (2007). Akt and its downstream targets play key roles in mediating dormancy in land snails. *Comp. Biochem. Physiol. Part B Biochem. Mol. Biol.* **148**, 245-255.

Ramnanan, C. J. and Storey, K. B. (2006). Suppression of Na^+/K^+-ATPase activity during estivation in the land snail *Otala lactea*. *J. Exp. Biol.* **209**, 677-688.

Ramos-Vasconcelos, G. R. and Hermes-Lima, M. (2003). Hypometabolism, antioxidant defenses and free radical metabolism in the pulmonate land snail *Helix aspersa*. *J. Exp. Biol.* **206**, 675-685.

Reardon, K. A., Davis, J., Kapsa, R. M. I., Choong, P. and Byrne, E. (2001). Myostatin, insulin-like growth factor-1, and leukemia inhibitory factor mRNAs are upregulated in chronic human disuse muscle atrophy. *Muscle Nerve* **24**, 893-899.

Reilly, B. D., Hickey, A. J. R., Cramp, R. L. and Franklin, C. E. (2014). Decreased hydrogen peroxide production and mitochondrial respiration in skeletal muscle but not cardiac muscle of the green-striped burrowing frog, a natural model of muscle disuse. *J. Exp. Biol.* **217**, 1087-1093.

Reilly, B. D., Schlipalius, D. I., Cramp, R. L., Ebert, P. R. and Franklin, C. E. (2013). Frogs and estivation: transcriptional insights into metabolism and cell survival in a natural model of extended muscle disuse. *Physiol. Genomics* **45**, 377-388.

Rizzatti, A. C. S. and Romero, S. M. B. (2001). Heart rate and body weight alterations in juvenile specimens of the tropical land snail *Megalobulimus sanctipauli* during dormancy. *Braz. J. Med. Biol. Res.* **34**, 959-967.

Robinson, M. D., McCarthy, D. J. and Smyth, G. K. (2010). edgeR: a Bioconductor package for differential expression analysis of digital gene expression data. *Bioinformatics* **26**, 139-140.

Robinson, M. D. and Oshlack, A. (2010). A scaling normalization method for differential expression analysis of RNA-seq data. *Genome Biol.* **11**, R25.

Rommel, C., Bodine, S. C., Clarke, B. A., Rossman, R., Nunez, L., Stitt, T. N., Yancopoulos, G. D. and Glass, D. J. (2001). Mediation of IGF-1-induced skeletal myotube hypertrophy by PI(3)K/Akt/mTOR and PI(3)K/Akt/GSK3 pathways. *Nat. Cell Biol.* **3**, 1009-1013.

Rossi, D. and Gaidano, G. (2003). Messengers of cell death: apoptotic signaling in health and disease. *Haematologica* **88**, 212-218.

Rouble, A. N., Hefler, J., Mamady, H., Storey, K. B. and Tessier, S. N. (2013). Anti-apoptotic signaling as a cytoprotective mechanism in mammalian hibernation. *Peer J.* **1**, e29.

Rourke, B. C., Cotton, C. J., Harlow, H. J. and Caiozzo, V. J. (2006). Maintenance of slow type I myosin protein and mRNA expression in overwintering prairie dogs (*Cynomys leucurus* and *ludovicianus*) and black bears (*Ursus americanus*). *J. Comp. Physiol. B Biochem. Syst. Environ. Physiol.* **176**, 709-720.

Rourke, B. C., Yokoyama, Y., Milsom, W. K. and Caiozzo, V. J. (2004). Myosin isoform expression and MAFbx mRNA levels in hibernating golden-mantled ground squirrels (*Spermophilus lateralis*). *Physiol. Biochem. Zool.* **77**, 582-593.

Sah, N. K., Khan, Z., Khan, G. J. and Bisen, P. S. (2006). Structural, functional and therapeutic biology of survivin. *Cancer Lett.* **244**, 164-171.

Sakakima, H., Yoshida, Y., Sakae, K. and Morimoto, N. (2004). Different frequency treadmill running in immobilization-induced muscle atrophy and ankle joint contracture of rats. *Scand. J. Med. Sci. Sports* **14**, 186-192.

Sakurai, T., Fujita, Y., Ohto, E., Oguro, A. and Atomi, Y. (2005). The decrease of the cytoskeleton tubulin follows the decrease of the associating molecular chaperone alpha B-crystallin in unloaded soleus muscle atrophy without stretch. *FASEB J.* **19**, 1199-1201.

Salway, K. D., Tattersall, G. J. and Stuart, J. A. (2010). Rapid upregulation of heart antioxidant enzymes during arousal from estivation in the Giant African snail (*Achatina fulica*). *Comp. Biochem. Physiol. Part A Mol. Integr. Physiol.* **157**, 229-236.

Schmidt, K. E. and Kelley, K. M. (2001). Down-regulation in the insulin-like growth factor (IGP) axis during hibernation in the golden-mantled ground squirrel, *Spermophilus lateralis*: IGF-I and the IGF-binding proteins (IGFBPs). *J. Exp. Zool.* **289**, 66-73.

Schwartz, C., Hampton, M. and Andrews, M. T. (2013). Seasonal and regional differences in gene expression in the brain of a hibernating mammal. *PLoS ONE* **8**.

Secor, S. M. and Lignot, J-H. (2010). Morphological plasticity of vertebrate aestivation. In *Aestivation: molecular and physiological aspects*, (eds. C. A. Navas and J. E. Carvalho), pp. 183-208. Berlin: Springer-Verlag.

Seddon, M., Looi, Y. H. and Shah, A. M. (2007). Oxidative stress and redox signalling in cardiac hypertrophy and heart failure. *Heart* **93**, 903-907.

Servais, S., Letexier, D., Favier, R., Duchamp, C. and Desplanches, D. (2007). Prevention of unloading-induced atrophy by vitamin E supplementation: Links between oxidative stress and soleus muscle proteolysis? *Free Radic. Biol. Med.* **42**, 627-635.

Seymour, R. S. (1973a). Energy metabolism of dormant spadefoot toads (*Scaphiopus*). *Copeia*, 435-445.

Seymour, R. S. (1973b). Gas exchange in spadefoot toads beneath ground. *Copeia*, 452-460.

Shavlakadze, T. and Grounds, M. (2006). Of bears, frogs, meat, mice and men: complexity of factors affecting skeletal muscle mass and fat. *BioEssays* **28**, 994-1009.

Siems, W., Capuozzo, E., Lucano, A., Salerno, C. and Crifo, C. (2003). High sensitivity of plasma membrane ion transport ATPases from human neutrophils towards 4-hydroxy-2,3-trans-nonenal. *Life Sci.* **73**, 2583-2590.

Siu, P. M., Pistilli, E. E. and Alway, S. E. (2005). Apoptotic responses to hindlimb suspension in gastrocnemius muscles from young adult and aged rats. *Am. J. Physiol. Regul. Integr. Comp. Physiol.* **289**, R1015-R1026.

Smuder, A. J., Kavazis, A. N., Hudson, M. B., Nelson, W. B. and Powers, S. K. (2010). Oxidation enhances myofibrillar protein degradation via calpain and caspase-3. *Free Radic. Biol. Med.* **49**, 1152-1160.

Solomon, V. and Goldberg, A. L. (1996). Importance of the ATP-ubiquitin-proteasome pathway in the degradation of soluble and myofibrillar proteins in rabbit muscle extracts. *J. Biol. Chem.* **271**, 26690-26697.

Song, K. H., Kim, T. M., Kim, H. J., Kim, J. W., Kim, H. H., Kwon, H. B., Kim, W. S. and Choi, H. S. (2003). Molecular cloning and characterization of a novel inhibitor of apoptosis protein from *Xenopus laevis*. *Biochem. Biophys. Res. Commun.* **301**, 236-242.

Sosa, M. S., Bragado, P. and Aguirre-Ghiso, J. A. (2014). Mechanisms of disseminated cancer cell dormancy: an awakening field. *Nat. Rev. Cancer* **14**, 611-622.

Spector, S. A., Simard, C. P., Fournier, M., Sternlicht, E. and Edgerton, V. R. (1982). Architectural alterations of rat hind-limb skeletal muscles immobilized at different lengths. *Exp. Neurol.* **76**, 94-110.

St-Pierre, J., Brand, M. D. and Boutilier, R. G. (2000). The effect of metabolic depression on proton leak rate in mitochondria from hibernating frogs. *J. Exp. Biol.* **203**, 1469-1476.

Staheli, J. R., Boyce, R., Kovarik, D. and Rose, T. M. (2011). CODEHOP PCR and CODEHOP PCR Primer Design. In *PCR Protocols, Third Edition*, vol. 687 (ed. D. J. Park), pp. 57-73. Totowa: Humana Press Inc.

Starkov, A. A. (2008). The role of mitochondria in reactive oxygen species metabolism and signaling. In *Mitochondria and oxidative stress in neurodegenerative disorders*, vol. 1147 (eds. G. E. Gibson R. R. Ratan and M. F. Beal), pp. 37-52.

Stein, T. P. and Wade, C. E. (2005). Metabolic consequences of muscle disuse atrophy. *J. Nutr.* **135**, 1824S-1828S.

Stevenson, E. J., Giresi, P. G., Koncarevic, A. and Kandarian, S. C. (2003). Global analysis of gene expression patterns during disuse atrophy in rat skeletal muscle. *J. Physiol. (Lond.)* **551**, 33-48.

Stockholm, D., Herasse, M., Marchand, S., Praud, C., Roudaut, C., Richard, I., Sebille, A. and Beckmann, J. S. (2001). Calpain 3 mRNA expression in mice after denervation and during muscle regeneration. *Am. J. Physiol. Cell Physiol.* **280**, C1561-C1569.

Storey, K. B., Dent, M. E. and Storey, J. M. (1999). Gene expression during estivation in spadefoot toads, *Scaphiopus couchii:* Upregulation of riboflavin binding protein in liver. *J. Exp. Zool.* **284**, 325-333.

Storey, K. B. and Storey, J. M. (1990). Metabolic rate depression and biochemical adaptation in anaerobiosis, hibernation and estivation. *Q. Rev. Biol.* **65**, 145-174.

Storey, K. B. and Storey, J. M. (2010). Metabolic regulation and gene expression during aestivation. In *Aestivation: molecular and physiological aspects*, (eds. C. A. Navas and J. E. Carvalho), pp. 25-45. Berlin: Springer-Verlag.

Storey, K. R., Heldmaier, G. and Rider, M. H. (2010). Mammalian hibernation: physiology, cell signaling, and gene controls on metabolic rate depression. In *Dormancy and Resistance in Harsh Environments*, vol. 21 (eds. E. Lubzens J. Cerda and M. Clark), pp. 227-252. Berlin: Springer-Verlag Berlin.

Susin, S. A., Lorenzo, H. K., Zamzami, N., Marzo, I., Snow, B. E., Brothers, G. M., Mangion, J., Jacotot, E., Costantini, P., Loeffler, M. et al. (1999). Molecular characterization of mitochondrial apoptosis-inducing factor. *Nature* **397**, 441-446.

Suzuki, Y. J. and Ford, G. D. (1999). Redox regulation of signal transduction in cardiac and smooth muscle. *J. Mol. Cell. Cardiol.* **31**, 345-353.

Symonds, B. L., James, R. S. and Franklin, C. E. (2007). Getting the jump on skeletal muscle disuse atrophy: preservation of contractile performance in aestivating *Cyclorana alboguttata* (Gunther 1867). *J. Exp. Biol.* **210**, 825-835.

Taillandier, D., Aurousseau, E., MeynialDenis, D., Bechet, D., Ferrara, M., Cottin, P., Ducastaing, A., Bigard, X., Guezennec, C. Y., Schmid, H. P. et al. (1996). Coordinate activation of lysosomal, Ca^{2+}-activated and ATP-ubiquitin-dependent proteinases in the unweighted rat soleus muscle. *Biochem. J.* **316**, 65-72.

Talbert, E. E., Smuder, A. J., Min, K., Kwon, O. S. and Powers, S. K. (2013a). Calpain and caspase-3 play required roles in immobilization-induced limb muscle atrophy. *J. Appl. Physiol.* **114**, 1482-1489.

Talbert, E. E., Smuder, A. J., Min, K., Kwon, O. S., Szeto, H. H. and Powers, S. K. (2013b). Immobilization-induced activation of key proteolytic systems in skeletal muscles is prevented by a mitochondria-targeted antioxidant. *J. Appl. Physiol.* **115**, 529-538.

Taveau, M., Bourg, N., Sillon, G., Roudaut, C., Bartoli, M. and Richard, I. (2003). Calpain 3 is activated through autolysis within the active site and lyses sarcomeric and sarcolemmal components. *Mol. Cell. Biol.* **23**, 9127-9135.

Thomason, D. B., Biggs, R. B. and Booth, F. W. (1989). Protein metabolism and beta-myosin heavy-chain mRNA in unweighted soleus muscle. *Am. J. Physiol.* **257**, R300-R305.

Tidball, J. G. and Spencer, M. J. (2002). Expression of a calpastatin transgene slows muscle wasting and obviates changes in myosin isoform expression during murine muscle disuse. *J. Physiol. (Lond.)* **545**, 819-828.

Tinker, D. B., Harlow, H. J. and Beck, T. D. I. (1998). Protein use and muscle fiber changes in free-ranging, hibernating black bears. *Physiol. Zool.* **71**, 414-424.

Tischler, M. E., Rosenberg, S., Satarug, S., Henriksen, E. J., Kirby, C. R., Tome, M. and Chase, P. (1990). Different mechanisms of increased proteolysis in atrophy induced by denervation or unweighting of rat soleus muscle. *Metab. Clin. Exp.* **39**, 756-763.

Toien, O., Blake, J., Edgar, D. M., Grahn, D. A., Heller, H. C. and Barnes, B. M. (2011). Hibernation in black bears: Independence of metabolic suppression from body temperature. *Science* **331**, 906-909.

Tracy, C. R., Reynolds, S. J., McArthur, L. and Christian, K. A. (2007). Ecology of aestivation in a cocoon-forming frog, *Cyclorana australis* (Hylidae). *Copeia*, 901-912.

Trendelenburg, A. U., Meyer, A., Rohner, D., Boyle, J., Hatakeyama, S. and Glass, D.J. (2009). Myostatin reduces Akt/TORC1/p70S6K signaling, inhibiting myoblast differentiation and myotube size. *Am. J. Physiol. Cell Physiol.* **296**, C1258-C1270.

Turrens, J. F. (2003). Mitochondrial formation of reactive oxygen species. *J. Physiol. (Lond.)* **552**, 335-344.

Untergasser, A., Nijveen, H., Rao, X., Bisseling, T., Geurts, R. and Leunissen, J. A. M. (2007). Primer3Plus, an enhanced web interface to Primer3. *Nucleic Acids Res.* **35**, W71-W74.

Utz, J. C., Nelson, S., O'Toole, B. J. and van Breukelen, F. (2009). Bone strength is maintained after 8 months of inactivity in hibernating golden-mantled ground squirrels, *Spermophilus lateralis*. *J. Exp. Biol.* **212**, 2746-2752.

Van Beurden, E. K. (1980). Energy metabolism of dormant Australian water-holding frogs (*Cyclorana platycephalus*). *Copeia*, 787-799.

van Breukelen, F. and Carey, H. V. (2002). Ubiquitin conjugate dynamics in the gut and liver of hibernating ground squirrels. *J. Comp. Physiol. B Biochem. Syst. Environ. Physiol.* **172**, 269-273.

van Breukelen, F., Krumschnabel, G. and Podrabsky, J. E. (2010). Vertebrate cell death in energy-limited conditions and how to avoid it: what we might learn from mammalian hibernators and other stress-tolerant vertebrates. *Apoptosis* **15**, 386-399.

Vazeille, E., Codran, A., Claustre, A., Averous, J., Listrat, A., Bechet, D., Taillandier, D., Dardevet, D., Attaix, D. and Combaret, L. (2008). The ubiquitin-proteasome and the mitochondria-associated apoptotic pathways are sequentially downregulated during recovery after immobilization-induced muscle atrophy. *Am. J. Physiol. Endocrinol. Metab.* **295**, E1181-E1190.

Velickovska, V., Lloyd, B. P., Qureshi, S. and van Breukelen, F. (2005). Proteolysis is depressed during torpor in hibernators at the level of the 20S core protease. *J. Comp. Physiol. B Biochem. Syst. Environ. Physiol.* **175**, 329-335.

Velickovska, V. and van Breukelen, F. (2007). Ubiquitylation of proteins in livers of hibernating golden-mantled ground squirrels, *Spermophilus lateralis*. *Cryobiology* **55**, 230-235.

Verburg, E., Murphy, R. M., Stephenson, D. G. and Lamb, G. D. (2005). Disruption of excitation-contraction coupling and titin by endogenous Ca^{2+}-activated proteases in toad muscle fibres. *J. Physiol. (Lond.)* **564**, 775-789.

Vermaelen, M., Sirvent, P., Raynaud, F., Astier, C., Mercier, J., Lacampagne, A. and Cazorla, O. (2007). Differential localization of autolyzed calpains 1 and 2 in slow and fast skeletal muscles in the early phase of atrophy. *Am. J. Physiol. Cell Physiol.* **292**, C1723-C1731.

Vleck, D. (1987). Measurement of O_2 consumption, CO_2 production, and water vapor production in a closed system. *J. Appl. Physiol.* **62**, 2103-2106.

Wang, L. C. H. (1979). Time patterns and metabolic rates of natural torpor in the Richardsons ground squirrel. *Can. J. Zool.* **57**, 149-155.

Wang, S. Q., Lakatta, E. G., Cheng, H. and Zhou, Z. Q. (2002). Adaptive mechanisms of intracellular calcium homeostasis in mammalian hibernators. *J. Exp. Biol.* **205**, 2957-2962.

Wang, X. D., Kawano, F., Matsuoka, Y., Fukunaga, K., Terada, M., Sudoh, M., Ishihara, A. and Ohira, Y. (2006). Mechanical load-dependent regulation of satellite cell and fiber size in rat soleus muscle. *Am. J. Physiol. Cell Physiol.* **290**, C981–C989.

Wang, Y. and Pessin, J. E. (2013). Mechanisms for fiber-type specificity of skeletal muscle atrophy. *Curr. Opin. Clin. Nutr. Metab. Care*. **16**, 243-250.

Wehling, M., Cai, B. Y. and Tidball, J. G. (2000). Modulation of myostatin expression during modified muscle use. *FASEB J.* **14**, 103-110.

Whalen, J. P., Nunez, E. A. and Krook, L. (1972). Radiographic and histologic study of bone in active and hibernating bat (*Myotis lucifugus*). *Anat. Rec.* **172**, 97-&.

Whitwam, R. E. and Storey, K. B. (1990). Pyruvate kinase from the land snail *Otala lactea* - regulation by reversible phosphorylation during estivation and anoxia. *J. Exp. Biol.* **154**, 321-337.

Wickler, S. J., Horwitz, B. A. and Kott, K. S. (1987). Muscle function in hibernating hamsters - a natural analog to bed rest. *J. Therm. Biol.* **12**, 163-166.

Wickler, S. J., Hoyt, D. F. and Vanbreukelen, F. (1991). Disuse atrophy in the hibernating golden-mantled ground squirrel, *Spermophilus lateralis*. *Am. J. Physiol.* **261**, R1214-R1217.

Williams, D. R., Epperson, L. E., Li, W. Z., Hughes, M. A., Taylor, R., Rogers, J., Martin, S. L., Cossins, A. R. and Gracey, A. Y. (2005). Seasonally hibernating phenotype assessed through transcript screening. *Physiol. Genomics* **24**, 13-22.

Withers, P. C. (1993). Metabolic depression during aestivation in the Australian frogs, *Neobatrachus* and *Cyclorana*. *Aust. J. Zool.* **41**, 467-473.

Withers, P. C. (1995). Cocoon formation and structure in the estivating Australian desert frogs, *Neobatrachus* and *Cyclorana*. *Aust. J. Zool.* **43**, 429-441.

Word, J. M. (2007). Physiological adjustments to aestivation and activity in the cocoon-forming frogs *Cyclorana platycephala* and *Cyclorana maini*. PhD Thesis, The University of Western Australia.

Wu, M., Xu, L. G., Li, X. Y., Zhai, Z. H. and Shu, H. B. (2002). AMID, an apoptosis-inducing factor-homologous mitochondrion-associated protein, induces caspase-independent apoptosis. *J. Biol. Chem.* **277**, 25617-25623.

Xie, Q., Lin, T. X., Zhang, Y., Zheng, J. P. and Bonanno, J. A. (2005). Molecular cloning and characterization of a human AIF-like gene with ability to induce apoptosis. *J. Biol. Chem.* **280**, 19673-19681.

Xu, R., Andres-Mateos, E., Mejias, R., MacDonald, E. M., Leinwand, L. A., Merriman, D. K., Fink, R. H. A. and Cohn, R. D. (2013). Hibernating squirrel muscle activates the endurance exercise pathway despite prolonged immobilization. *Exp. Neurol.* **247**, 392-401.

Xu, X., Chen, C. N., Arriaga, E. A. and Thompson, L. V. (2010). Asymmetric superoxide release inside and outside the mitochondria in skeletal muscle under conditions of aging and disuse. *J. Appl. Physiol.* **109**, 1133-1139.

Yacoe, M. E. (1983). Protein metabolism in the pectoralis muscle and liver of hibernating bats, *Eptesicus fuscus*. *J. Comp. Physiol.* **152**, 137-144.

Yan, J., Barnes, B. M., Kohl, F. and Marr, T. G. (2008). Modulation of gene expression in hibernating arctic ground squirrels. *Physiol. Genomics* **32**, 170-181.

Yang, C. X., He, Y., Gao, Y. F., Wang, H. P. and Goswami, N. (2014). Changes in calpains and calpastatin in the soleus muscle of Daurian ground squirrels during hibernation. *Comp. Biochem. Physiol. Part A Mol. Integr. Physiol.* **176**, 26-31.

Yang, J. J., Lee, Y. J., Hung, H. H., Tseng, W. P., Tu, C. C., Lee, H. and Wu, W. J. (2010). ZAK inhibits human lung cancer cell growth via ERK and JNK activation in an AP-1-dependent manner. *Cancer Sci.* **101**, 1374-1381.

Yang, S. Y., Alnaqeeb, M., Simpson, H. and Goldspink, G. (1997). Changes in muscle fibre type, muscle mass and IGF-I gene expression in rabbit skeletal muscle subjected to stretch. *J. Anat.* **190**, 613-622.

Young, K. M., Cramp, R. L. and Franklin, C. E. (2013). Each to their own: skeletal muscles of different function use different biochemical strategies during aestivation at high temperature. *J. Exp. Biol.* **216**, 1012-1024.

Young, K. M., Cramp, R. L., White, C. R. and Franklin, C. E. (2011). Influence of elevated temperature on metabolism during aestivation: implications for muscle disuse atrophy. *J. Exp. Biol.* **214**, 3782-3789.

Zarzhevsky, N., Coleman, R., Volpin, G., Fuchs, D., Stein, H. and Reznick, A. Z. (1999). Muscle recovery after immobilisation by external fixation. *J. Bone Joint Surg. Br.* **81B**, 896-901.

Zatzman, M. L. (1984). Renal and cardiovascular effects of hibernation and hypothermia. *Cryobiology* **21**, 593-614.

Zhang, M., Yang, J. and Li, F. (2006). Transcriptional and post-transcriptional controls of survivin in cancer cells: novel approaches for cancer treatment. *J. Exp. Clin. Cancer Res.* **25**, 391-402.

Zhang, X., Chen, J., Du Graham, S. H. L., Kochanek, P. M., Draviam, R., Guo, F., Nathaniel, P. D., Szabo, C., Watkins, S. C. and Clark, R. S. (2002). Intranuclear localization of apoptosis-inducing factor (AIF) and large scale DNA fragmentation after traumatic brain injury in rats and in neuronal cultures exposed to peroxynitrite. *J. Neurochem.* **82**, 181-191.

Zhu, X. L., Hadhazy, M., Wehling, M., Tidball, J. G. and McNally, E. M. (2000). Dominant negative myostatin produces hypertrophy without hyperplasia in muscle. *FEBS Lett.* **474**, 71-75.

Zoccarato, F., Cavallini, L. and Alexandre, A. (2009). Succinate is the controller of $O2^{-}/H_2O_2$ release at mitochondrial complex I: negative modulation by malate, positive by cyanide. *J. Bioenerg. Biomembr.* **41**, 387-393.